





UNIVERSITÀ  
DI SIENA  
1240

UNIVERSITY OF SIENA  
Doctorate in Medical Biotechnology  
Department of Pathological Anatomy  
Coordinator: Professor Lorenzo Leoncini

**THE LYMPHOMA MICROENVIRONMENT**

Supervisor :

Professor: Lorenzo Leoncini

Candidate:

Virginia Mancini

Academic Year: 2018/2021

## ***Index***

### ***Part I***

1. Tumor microenvironment
  - 1.1 Components of lymphoma microenvironment: Tumor-associated macrophage (TAM)
  - 1.2 Components of lymphoma microenvironment: Cytotoxic T cells (CTLs)
  - 1.3 Components of lymphoma microenvironment: Regulatory T cells (Tregs)
2. Primary Testicular Diffuse Large B-cell Lymphoma (PT-DLBCL)
  - 2.1 The immunophenotype and cell-of-origin of PT-DLBCL resembles nodal ABC-DLBCL
  - 2.2 Mutational profiles reveal distinct deregulated cellular signaling cascades
  - 2.3 Clinical implications and future directions
  - 2.4 Immune-escape is a prominent hallmark of PT-DLBCL pathogenesis

### ***Part II***

3. Aim of our study
4. Materials and Methods.
  - 4.1 Patients
  - 4.2 Immunohistochemistry and In Situ Hybridization
  - 4.3 Fluorescent in situ hybridization (FISH)
  - 4.4 Statistical analysis
  - 4.5 Detection of antigen by single/multiplex immunofluorescence (IF) using Opal staining method
5. Results
  - 5.1 Patient characteristics
  - 5.2 PD-L1 expression in neoplastic cells
  - 5.3 Tumour Associated Macrophages (TAM): PD-1/PD-L1 pathway activation and M2 polarization
  - 5.4 Tumor-Infiltrating Lymphocytes (Tils)
6. Discussion
7. Conclusion
8. Bibliography

## ***Part I***

### ***1. The tumour microenvironment***

The cellular milieu in which lymphoma cells thrive has solely recently become a relevant focus of investigation in order to explore potential targets for immunotherapy. Albeit our comprehension of cytogenetic abnormalities and molecular pathways in lymphoma are in advance of solid organ tumors, the same cannot be asserted of the tumor microenvironment. In B cell lymphomas, the cellular inflammatory infiltrate is intimately associated with the malignant lymphocytes, and the molecules that can be released or trapped therein, may enhance tumor cell proliferation and survival as well as evasion from immunosurveillance (1). Along with somatic mutations and inflammation, the responsibility of tumor microenvironment (TME) in achievement of key characteristics of cancer pathogenesis and progression, like sustained tumor proliferative signaling, resistance to apoptosis, avoidance of growth suppressors, and immune evasion pathway is becoming relevant in the study of lymphomagenesis. The lymphoma microenvironment is progressively being regarded as an active and mutual sustaining network of stromal cells, immune cells, blood vessels, cytokines and extracellular matrix components, comprising sclerosis, whose constitution is driven by the neoplastic cells and which in exchange, alter tumor initiation, progression, and drug resistance (2). The key agents influencing the constitution of microenvironment comprise lymphoma subtypes and signaling interplay between lymphoma cells and microenvironment cells.

#### ***1.1 Components of lymphoma microenvironment: Tumour-associated macrophages (TAMs)***

TAMs are the macrophage/circulating monocyte lineage cells detected in strict relationship with lymphoma. Their function seems to differ according to tumor type. High number of TAMs have been linked with adverse outcome in certain tumors. In individual studies of advanced stage classic Hodgkin lymphoma (CHL) as well as in meta-analyses, a high-density of TAMs is a strong predictor of poor prognosis in adult patients (3). TAMs seem to exhibit dual predictive functions in follicular lymphoma. Prominent levels of CD68+ or CD163+ TAMs are correlated with adverse prognosis in follicular lymphoma treated with conventional chemotherapy prior to the rituximab era, on the other hand, this impact was lowered or even inverted if rituximab is used in combined therapy. In mouse models, anti-CD20 monoclonal antibody (mAb) mediated depletion of B cells depend on the macrophage expression of Fc-gamma receptors (FcγR). In terms of therapy, it has also been demonstrated that novel immunomodulatory drugs such as pomalidomide convert the polarization status of macrophages from M2 to M1 in mouse models of central nervous system (CNS) lymphoma (4). Apparently, this seems to be attained by reducing signal transducer and

activator of transcription (STAT) 6 signaling while enhancing STAT1 signaling and therefore pomalidomide improves the phagocytic activity of macrophages. This discovery debated for the therapeutic activity of pomalidomide against CNS lymphomas. In a streamlined view of macrophage activation, macrophages may have two functional roles, which represent the extremes of a cascade of activation steps, the first with a pro-inflammatory phenotype, the ability to induce T helper 1 (Th1) immune responses and tumoricidal tasks (M1 macrophages) and the second with regulatory functions in tissue reconstruction, reshape and induction of Th2 immune response (M2 macrophages) (5). A key role of a subset of M2 macrophages is the production IL10. Two transcription factors are diversely expressed by polarized 170 macrophages; STAT1 is expressed in M1 macrophages, it is upregulated in response to types I, II or III interferon and its phosphorylated form (pSTAT1) binds to the promoter region of interferon stimulated genes. CMAF, a crucial transcription factor for interleukin (IL) -10 production, is expressed in M2 macrophages dedicated to IL-10 production. CD163 has been considered a M2- specific marker in macrophages (6). Investigators have showed that the combined use of a macrophage marker, such as CD68 or CD163, alongside with pSTAT1 or CMAF can be used to identify M1- or M2-polarized macrophages, respectively. The results of the analysis of various immunologically mediated diseases indicated that CD163 should not be regarded as a specific M2- marker (7)

### 1.2 Components of lymphoma microenvironment: Cytotoxic T cells (CTLs)

Significative levels of infiltrating CD8 positive T cells, especially expressing cytotoxic markers such as TIA-1, as measured by both immunohistochemistry and flow cytometric analysis have been 173 correlated with a favourable prognosis in B-cell lymphomas (8). Prominent levels of cytotoxic lymphocytes positive for programmed cell death-1 (PD-1) were also reported to be correlated with a good outcome in the context of follicular lymphoma (9). The cytotoxic effect of T cells is fostered by the targeting of the PD-1 pathway, which can drive to tumor cell lysis. Tumor specific activated T cells as well as regulatory T cells express cytotoxic T lymphocyte-associated antigen 4 (CTLA-4), which binds to CD80/CD86 receptor on antigen presenting cells (APCs) and induces T cell anergy by competing with CD28 as a costimulatory molecule. Immune checkpoint blockade can augment antitumor immunity (10). In the setting of chronic antigen stimulation, a protein by the name of lymphocyte activation gene 3 (LAG-3) is upregulated on T cells, inhibiting CD4+ T cell proliferation in reaction to antigen as well as CD8+ T cell function. In particular, LAG-3 has been demonstrated to sustain tolerance to tumor antigens via its action on CD8+ T cells. In mouse models, LAG-3 blockade fosters proliferation and effector activity of antigen-specific CD8+ T cells inside organs and tumors that express their cognate antigen (11). These murine models indicate that

LAG-3 can be a potential target for enhancing the effectiveness of cytotoxic T-cell immunity against tumor.

### 1.3 Components of lymphoma microenvironment: Regulatory T cells (Tregs)

Tregs comprise subsets of immune suppressive cells that regulate self-tolerance and immune homeostasis. Thymic derived Tregs are implied in impeding autoimmunity while peripheral Tregs sustain tolerance in mucosal sites. Both these naturally occurring CD25+CD4+ Treg populations express FoxP3, which is a more specific marker for regulatory T cells than CD25, CD45RB, or CTLA-4 (11). Tregs inhibit the activity of bystander T cells, natural killer cells and B cells via CTLA-4, IL-10, and TGF- $\beta$ 1. FoxP3+ Tregs, especially in inflamed tissues, have been demonstrated to express T cell immunoglobulin and mucin-domain containing-3 (TIM-3), which improves their regulatory activity. Blockade of TIM-3 signaling seems to demonstrate therapeutic advantage in in vitro studies. TIM-3 acts as a co-inhibitory receptor that is also expressed on IFN- $\gamma$  producing T cells as well as macrophages and dendritic cells, where it drives to suppression of normal Th1 responses. 174 Studies in murine models have demonstrated that Tregs are present in the peripheral blood of animals and that these circulating cells can regulate humoral immune responses in vivo. In addition, it was described that the PD-1 pathway can inhibit blood Treg function. Thus, there is a rationale to consider that the PD-1: PD-L1 pathway can restrict the differentiation and normal function of Tregs, indicating that manipulation of this pathway can support protective immunity (12). On the grounds of their role in lymphomagenesis, Wang et al divided Tregs into 4 groups: suppressor Tregs (suppress CD8+ CTLs), malignant FoxP3+ Tregs, direct tumor-killing Tregs, and incompetent Tregs. The link between level of Tregs and lymphoma outcome would vary according to the type of Tregs therein. Inter alia, in angioimmunoblastic T-cell lymphoma, where more of incompetent Tregs or direct tumor-killing Tregs are present, the anti-tumor cytotoxicity is conserved and thus, favourable prognosis is associated with increase in Tregs (13). In certain NHL where Tregs are overrepresented in biopsy specimens compared to normal lymphoid tissue; these cells seemed to be recruited by malignant B cells (14). Nonetheless, the fact is not straightforward. In a study of 280 CHL patients, greater levels of intratumoral Tregs were correlated with better prognosis. Likewise, in follicular lymphoma and germinal center subtype diffuse large B-cell lymphomas, there was a positive correlation between disease specific survival and numbers of intratumoral FoxP3 positive cells (15). From these studies, it has been speculated that the prominent level of Tregs enhance immune surveillance in lymphomas by reducing overall inflammation and lymphoma cell proliferation.

## ***2. Primary Testicular Lymphoma***

Primary testicular lymphoma (PTL) is a cancer which occurs in an immune-privileged site as with primary central nervous system and primary vitreoretinal lymphomas. Such immune-privileged sites are physically partitioned from peripheral immune surveillance. This feature is thought to facilitate lymphoma pathogenesis and complicate disease management with high rate of relapse in the central nervous system (CNS) and contralateral testis (16), despite the improvement of the overall prognosis due to the addition of rituximab to systemic chemotherapy (17).

PTL accounts for <2% of all nonHodgkin lymphomas (NHL), it is the most common type of testicular cancer in men older than 60 years of age. PTLs are mainly DLBCLs (80%–90%) and a minority of other histological subtypes such as plasmablastic, Burkitt's or mantle cell lymphoma and, rarely low-grade follicular lymphomas (FLs more common in young patients) or T-cell lymphomas. Testicular DLBCL, NOS, can spread to the CNS and the contralateral testis. Most cases are of the ABC subtype (18).

Clinically, the PTL presents as painless uni- or bilateral testicular masses with infrequent constitutional symptoms (19). The term primary testicular diffuse large B-cell lymphoma (PT-DLBCL) is used in order to distinguish this histologically defined lymphoma from the broader collection of entities that constitute PTL. Notably, although most patients present with localized disease (stage 1 or 2), approximately 20% have already advanced stage disease at the time of diagnosis. The introduction of anthracycline-containing regimens (CHOP) and contralateral scrotal radiation has improved patient outcomes. Rituximab has had a more modest impact on PT-DLBCL outcome compared to nodal DLBCL. This reflects the heightened risk of central nervous system (CNS) relapse in PT-DLBCL, which has not improved. Recent studies have focused on characterizing the phenotypic profile and mutational underpinnings of PT-DLBCL to refine prognosis and inform on novel treatment avenues. Early immunohistochemistry (IHC) work and subsequent gene expression profiling (GEP) defined phenotypic similarities between nodal DLBCL of activated B-cell-like (ABC) origin and PT-DLBCL. This finding helped explain the clinical course of PT-DLBCL, which parallels nodal ABC-DLBCL outcomes, and has also provided strong rationale for integrating cell-of-origin (COO) specific treatments that have been evaluated in nodal ABC-DLBCL trials (19-22). Despite the pathogenic overlap between PT-DLBCL and nodal ABC DLBCL, notable differences emerge using high-throughput sequencing to evaluate the composition and frequency of mutated genes that contribute to sustained signalling pathways in PT-DLBCL (23, 24).

Moreover, studies investigating broad-scale chromosomal rearrangements using capture-based sequencing techniques and comparative genomic hybridization (CGH) have revealed another key pathological feature of PT-DLBCL: deregulation of intercellular immune signalling mechanisms (25-28).

### 2.1 The immunophenotype and cell-of-origin of PT-DLBCL resembles nodal ABC-DLBCL

Classic histomorphology coupled with immunohistochemical analysis is commonly used to establish the PT-DLBCL diagnosis. The published literature on PT-DLBCL phenotypes can be consolidated into categories to facilitate comprehensive evaluation of PT-DLBCL antigens that include: (a) markers of antigen presentation, (b) cell lineage antigens, (c) transcription factors, (d) cell signalling and related kinase components, (e) virology status, and (f) transport channels, among other features. The presence of highly expressed B-cell markers, such as CD19, CD20, CD79A, and PAX5, with the absence of T-cell (e.g. CD3) and natural killer cell (e.g. CD56) markers robustly establishes a derivation from B-cell lineage. Most cases (80%) express both pSTAT3 and JAK2 along with components of B-cell receptor (BCR) signalling cascades, highlighting the activity of JAK-STAT and NF- $\kappa$ B signalling within PT-DLBCL. In addition to these findings, studies have demonstrated that there is variable infiltration of reactive T-cells, with helper T-cells outnumbering cytotoxic T-cells 4.5:1 within the deranged architecture of the testis (29). Initial reports interrogating the differential expression of human leukocyte antigens (HLA) and surface immunoglobulins (Ig) among nodal and extra nodal DLBCL revealed distinct clustering patterns. Specifically, enrichment for IgM expression (versus IgG) and depletion of HLA-DR versus MHC class I molecules was observed, leading to the hypothesis that PT-DLBCLs were related to nodal ABC-DLBCL (30, 31). Additional immunological features that are prevalent in PT-DLBCL include a high proliferative index and elevated expression levels of activation-induced cytidine deaminase (AID) (23).

Indeed, subsequent evaluation of COO using both IHC and gene expression-based algorithms, trained on nodal and extra nodal non-testicular DLBCL cohorts, demonstrated that PT-DLBCLs express an ABC or non-GCB profile in > 75% of cases. The Hans algorithm, which evaluates expression of CD10, BCL6, and MUM1, has been employed most frequently in PT-DLBCL studies (the non-GCB profile is CD10 negative and BCL6 negative or MUM1 positive if BCL6 is positive) (32). However, there is the possibility that such algorithms, which were designed to evaluate nodal DLBCL, do not accurately represent the biology and COO in extra- nodal entities. For example, in one study, 10% of PT-DLBCLs were classified as phenotypically ambiguous due to co-expression of CD10 and MUM1. To resolve this ambiguity and address substantial interlaboratory and



interrater variability, subsequent studies have used GEP and sequencing-based methods. The successful COO classification in these studies suggests that GEP- based methods can add critical context in these phenotypically ambiguous cases (24, 33). CGH studies have also demonstrated that a significant number of copy number variations (CNV) in PT-DLBCL overlies the nodal ABC-DLBCL CNV landscape. Although IHC work has systematically demonstrated a clear phenotypic overlap between PT-DLBCL and nodal ABC-DLBCL, notable differences in protein expression are also observed (24).

## 2.2 Mutational profiles reveal distinct deregulated cellular signaling cascades

In addition to serving as a tool for COO classification, GEP studies have revealed distinctly enriched signalling pathways in PT-DLBCLs. Specifically, PT-DLBCLs feature prominent BCR and NF- $\kappa$ B signalling as is observed within nodal ABC-DLBCL and underscores a post-germinal center B-cell origin. In comparison to nodal ABC-DLBCL, BTK, CARD11, CD72, LYN, MYD88, and TANK expression levels are elevated among PT-DLBCL while TRAF1 expression is reduced (34). Studies interrogating the CNV and single nucleotide variant (SNV) profile of PT-DLBCL provide evidence for discrepancies of BCR and NF- $\kappa$ B gene signatures when compared to nodal ABC-DLBCL. The most frequently mutated gene in PT-DLBCL is MYD88 for which L265P gain of-function mutations were observed in 68 –82% of cases (34). Although MYD88 mutations are also observed in other entities, including nodal ABC-DLBCL, marginal zone lymphoma, primary central nervous system lymphoma, and mucosa-associated lymphoid tissue lymphoma, only lymphoplasmacytic lymphoma harboured a higher frequency of MYD88 mutations (35). Other components contributing to NF- $\kappa$ B deregulation include CD79B SNVs at Y196 (comparable in frequency to nodal ABC-DLBCL), structural genomic rearrangements of BCL10 and MALT1 and copy-number gains of 3q12.3, which have recently been associated with increased NFKBIZ expression in approximately 40% of cases (23). Viral analysis suggests PT-DLBCLs are universally negative for HIV, Epstein-Barr, and Kaposi's sarcoma-associated viruses and thus, do not contribute to NF- $\kappa$ B deregulation as has been described in other lymphomas (35-37).

Elevated protein and transcript levels are also observed for genes contributing to the PI3K signalling cascade in PT-DLBCL. Elevated TCL1A in addition to increased AKT1, AKT2, and PI3KCB are specifically increased among PT-DLBCL in comparison to nodal ABC-DLBCL (33). Studies profiling the microRNA landscape support PI3K signalling as a central element of PT-DLBCL pathogenesis. In particular, increased miR-21, which is elevated in PT-DLBCL, has been observed to suppress FOXO1 and PTEN expression, thereby deregulating feedback mechanisms affecting PI3K signalling (38-40). Other pathways and factors perturbed by CNVs have also been

reported in genes involved in suppressing apoptosis (BCL2) and cell-cycle checkpoint regulation (CCND1 and MDM2) as well as in prominent lymphoid transcription factors (BCL6, MYC, and SPIB) (23, 34, 41). While the frequency of BCL2 (~10%) and MYC (~15%) rearrangements is comparable to nodal ABC-DLBCL, BCL6 genomic translocations appear less frequently in PT-DLBCL (~60% in nodal ABC-DLBCL versus ~40% in PT-DLBCL) (23, 41). Furthermore, an over two-fold increase in the frequency of CDKN2A locus deletions has been described in PTDLBCL (71%) compared to nodal ABC-DLBCL (35%) (25).

### 2.3 Clinical implications and future directions

The standard treatment for testicular DLBCL is R-CHOP and with a heightened risk of contralateral relapse, prophylactic scrotal radiotherapy is recommended (20). Given the increased risk of CNS relapse, staging investigations should include CT or MRI head, as well as a lumbar puncture with cerebrospinal fluid evaluation by both cytology and flow cytometry. Similar to nodal-DLBCL, most studies support that rituximab has improved outcome in PT-DLBCL, most notably in those with advanced stage disease. However, CNS relapse rates have not been reduced, which reflects the poor penetration of rituximab into the CNS coupled with predominantly parenchymal relapses (41). Most prophylaxis strategies therefore favour highly CNS penetrating agents, in particular, high-dose methotrexate. However, given that patients are often older, methotrexate-associated renal toxicity is problematic and thus, intrathecal chemotherapy is often used. As such, CNS-directed prophylactic strategies are needed. Profiling the mutational landscape of PT-DLBCLs reveals numerous potential drug targets that encompass deregulated BCR, NF- $\kappa$ B and PI3K signalling, in addition to the immune-escape phenotype. Given that most PT-DLBCL, if not all, have an ABC-like phenotype, studies evaluating novel therapies in this subtype are most relevant. Ibrutinib is the first in-kind oral BTK inhibitor which shows selectivity in nodal ABC-DLBCL, in keeping with in vitro studies demonstrating tonic BCR pathway signalling. Specifically, preferential efficacy has been observed among patients who harboured either non-mutated BCR components or MYD88 mutations, whereas concurrent MYD88 and CD79B, or CARD11 coiled-coil domain mutations appear to confer resistance (42, 43). Further, recent evidence supporting penetration of the blood-brain-barrier (BBB) by Ibrutinib has led to studies evaluating Ibrutinib in primary CNS lymphoma with promising early results and CSF studies showing therapeutic drug levels (43, 44). A phase III study comparing R-CHOP and Ibrutinib to R-CHOP in non-GCB DLBCL has been completed and may provide insight into whether Ibrutinib has a CNS protective effect which may be relevant to PT-DLBCL (45). Lenalidomide is also selectively active in non-GCB DLBCL and penetrates the BBB, leading to trials combining R-CHOP and lenalidomide (46, 47). A recent pooled analysis of two

phase II studies of R-CHOP and lenalidomide, suggests a protective effect against CNS relapse. Of 136 patients, 18.4% were high risk by the recently described CNS-IPI but only one patient in the whole cohort (0.7%) developed a CNS recurrence (48).

The frequency of PDL SGR and CNVs (approaching 50%) suggests PT-DLBCLs may be prime candidates for checkpoint therapies. Further, given evidence of CNS penetration in solid tumours, this may also have a CNS protective effect. Ongoing studies evaluating PD-1 and PDL inhibitors in DLBCL and specifically in PT-DLBCL include those targeting CD274 (atezolizumab and durvalumab; NCT02220842 and NCT02549651, respectively) and PDCD1 (pembrolizumab; NCT02362997) with monoclonal antibodies. With strong pre-clinical rationale to explore PD-1 inhibitors in PT-DLBCL and in primary CNS lymphoma, nivolumab was tested in five patients with responses documented in all cases including three with durable remissions over one year. The principal mechanism of action of these checkpoint inhibitors is likely to block the interaction between PDLs and cognate receptors for PDLs (PDCD1, CD80). However, antibodies with G1 Fc regions also elicit complement-mediated cytotoxicity. Although the precise mechanism of action of these agents remains unknown, it is likely that anti-PDCD1 antibodies inhibit systemic interactions between malignant cells and T-cells, while the few antibodies that do manage to pass across blood-brain and blood-testis barriers might solicit complement-mediated anti-tumoral activity. In addition to the above, a number of phase I/II clinical trials are either ongoing or enrolling NHL patients in trials that aim to disrupt NF- $\kappa$ B and PI3K signalling with inhibitors of SYK (TAK-659; NCT02000934), PI3K (copanlisib; NCT02391116), AKT (ONC201; NCT02420795), and BTK (ACP-196; NCT02112526). As NF- $\kappa$ B signalling is also deregulated through constitutive TLR signalling, inhibitors upstream of PI3K may not adequately quench signalling. For cases with MYD88 mutations, therapeutic targets of TLR signalling may be more appropriate; IMO-8400 (NCT02252146) is active against lymphomas that harbor L265P MYD88 mutations. By integrating clinical context with the mutational underpinnings and phenotypic profile, we believe the unique aspects of PT-DLBCL pathogenesis warrant future considerations to classify this entity separately from nodal ABC-DLBCL. We hope this review will further elicit an interest in developing improved therapeutic strategies and molecularly precise therapies for PT-DLBCL.

#### 2.4 Immune-escape is a prominent hallmark of PT-DLBCL pathogenesis.

In addition to sustained intracellular signalling, capture-based sequencing and CGH studies have demonstrated that mutations within genes mediating immune surveillance are central to PT-DLBCL pathogenesis. The most frequent mutations are copy number losses of the HLA class I and II loci, which are associated with reduced expression of major histocompatibility complexes (MHC); for

example, Riemersma et al. found that 66% and 76% of PT-DLBCLs expressed no MHC I or MHC II, respectively.

The transcript and protein expression such as evasion from an anti-tumour immune response are increased by gains and amplifications of the programmed death ligand (PD-L) 1 (CD274) and 2 (PDCD1LG2) locus (9p24.1) (26, 27).

It is still difficult to explain the nature of the selective pressures for these mutations also if the basis of the immune-escape phenotype in PT-DLBCL are well described, also because the PT-DLBCL exists in an anatomic immune-privilege site that is not normally subject to immune surveillance. Considering these selective pressures, there are two putative mechanisms by which PT-DLBCL may develop, the “*in loco*” and the “*migratory*” ones (Fig. 1) (45). The “*in loco*” putative

mechanism supposes that PT-DLBCL evolves from lymphocytes that naturally exist within the cytokine-rich microenvironment of the testis, based on the physiological decrease of Sertoli cells, an important part of the blood-testis barrier and with the function to protect the spermatogenesis regions, controlling the infiltrating T-cells and presumably barring other innate immune cells (such as natural killer cells). This theory is supported by the observation that PT-DLBCL is more frequently seen in elderly patients in which the count of Sertoli cells physiologically decreased so that an increasing number of immune cells could pass beyond the blood-testis barrier that would represent a protective niche to facilitate the accumulation of mutations that will support malignant cell migration and survival outside the testis (45).

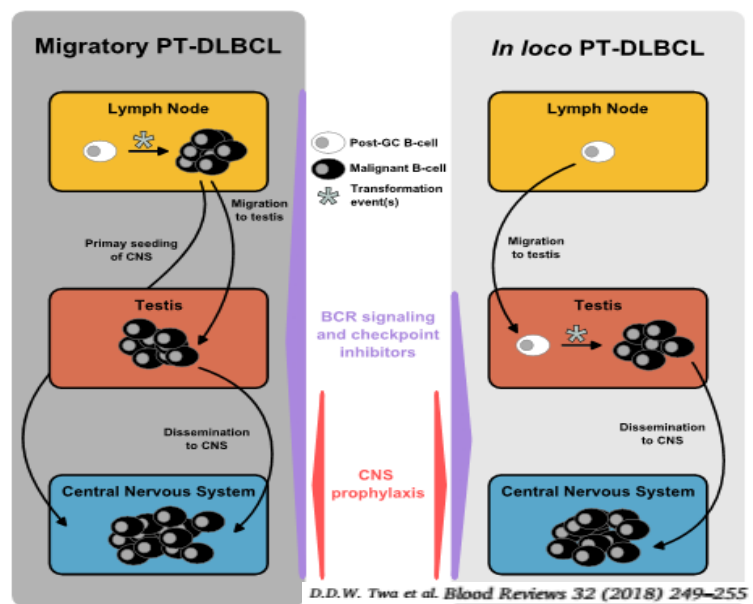


Fig. 1 The mutation-migration paradigm of primary testicular diffuse large B-cell lymphoma (PT-DLBCL). B-cells (white cells) have the potential to acquire transformative mutations with consequent result in a PT-DLBCL manifestation. Two models have been proposed: migratory PT-DLBCL and the *in-loco* PT-DLBCL. The first one is characterized by the possibility that mutations may be acquired during the process of affinity maturation (black cells) in the lymph node, predisposing to migration and seeding of anatomically immune privileged sites. Instead, for the *in-loco* PT-DLBCL, mutations may be acquired by B-cells after trafficking across the blood-testis barrier. In this instance, the blood-testis barrier serves as a protective niche to facilitate the accumulation of mutations that will support malignant cell migration and survival outside the testis (CNS dissemination).

A hybrid model might exist where a stepwise acquisition of mutations occurs in both the lymph node and testis.

Alternatively, for the “*migratory*” putative mechanism, PT-DLBCL may result from a post-germinal center malignant B-cell which has evolved in a nodal environment and subsequently

migrated to the testis. In this mechanism, the role of the blood-testis barrier would be to protect the developing PT-DLBCL from reactive immune cell detection until the full malignant genotypes and phenotypes have emerged. This theory, assuming malignant B-cell mobility, is supported by the observation that PT-DLBCLs often relapse in sites outside of the testis (45).

## ***Part II***

### ***3 Aims of our study***

Therefore, there is the need of a greater understanding of the pathophysiologic process underlying the development of PT-DLBCL and its peculiar tropism to facilitate novel therapeutic strategies.

Recent years have brought innovative insights into the network of interaction between lymphoma cells and host immune defense demonstrating that tumour cells undertake considerable efforts to keep the host immune system at bay. This involves both the tumour cells themselves, which express immuno-suppressive surface proteins such as PD-L1, as well as the tumour microenvironment (TME) which is influenced and manipulated by the tumour cells. The TME of B-cell lymphoma consists of immune cells (i.e T-cells, macrophages, and natural killer cells), stromal cells, blood vessels and extra-cellular matrix.

Several studies have focused on the characterization of immune-escape mechanism acting in Hodgkin lymphoma (HL) and DLBCL. Instead, a complete assessment in PT-DLBCL is lacking only few studies have been published identifying T-cell influenced the tumour microenvironment (TME), PD-L1 tumour-associated macrophages (TAM) and PD-1 positive tumour-infiltrating lymphocytes (Tils) as prognostic factors and suggesting the PD-1/PD-L1-2 axis as a targetable genetic feature in PTL due to the frequent 9p24.1/PD-L1/PD-L2 copy number alterations.

Notably, with the broad introduction of immuno-therapy, it has become obvious that not all the patients respond in the same way, which is both due to tumour heterogeneity as well as individual (immuno) genetic polymorphisms.

With the aim of resolving this issue, we examined the PT-DLBCL TME and checkpoint molecules by multiplex immunohistochemistry (IHC), immunofluorescence (IF) and fluorescent in situ hybridization (FISH).

Our findings were compared with those in the non-neoplastic testis and associated with clinical parameters and survival.

Collectively, our data emphasize the importance of tumour immune-evasion as a mechanism regulating therapy resistance in PT-DLBCL patients and bring new insight to the targeted treatments of this rare but aggressive disease that may translate into improved outcomes for patients with PT-DLBCL.

## ***4 Materials and Methods***

### ***4.1 Patients***

Formalin-fixed paraffin embedded (FFPE) tumor samples and clinical data from 104 patients with PTL were collected from the Section of Pathology and the Oncology Unit of Siena University Hospital, the University Hospital of Florence, the University Hospital of Basel, the Institute of Pathology of University Hospital of Berlin and the University Hospital of Bologna. The pathology

of all cases (already collected) had been reviewed and diagnosed according to the updated WHO classification of tumors of hematopoietic and lymphoid tissue (revised 4<sup>th</sup> edition, 2017) by morphology, immunophenotype and cytogenetic (when necessary). Long-term follow up (median 5 years) and detailed clinical information are available for many patients.

Moreover, we studied the normal testicular microenvironment in six samples of non-neoplastic testis, including four orchiectomies for testicular necrosis and two for infertility.

#### 4.2 Immunohistochemistry and In Situ Hybridization

The immunohistochemistry staining was performed by an automated staining system (Ventana BenchMark ULTRA, Roche diagnostic, Monza-Italy) with appropriate positive and negative controls included in each staining run. To classify lymphomas as germinal center or activated B-cell, CD10, BCL-6 and MUM-1 staining were employed. The double expressor status was assessed by means of MYC and BCL-2. To study the neoplastic background, the following antibodies were tested by single and/or multiple stainings: CD20, PAX-5, CD3, CD4, CD25, CD8, LAG-3, CD15, MPO, CD68, CD163, CMAF, CD206 and FOXP3. In this way, we were able to analyze both B and T lymphocytes, mainly by focusing on regulatory T-cell (co-expressing CD25/CD4/FOXP3) and activated/exhausted T-cells (co-expressing CD8/PD-1 plus LAG-3 in the exhausted phenotype). We also analyzed the myeloid lineage by means of CD15 and MPO as the activation of macrophages and their switch to a M2 phenotype by CD68, CD163, CMAF and CD206. Stained slides were scored separately by two pathologists. For the staining score, 10 consecutive high-power fields were examined in each sample. The discrepancies in scoring were resolved by consensus between the two pathologists. PD-1, PD-L1, PD-L2 (courtesy of Professor Freeman, Harvard University) expression was evaluated both on neoplastic and non-neoplastic cells accordingly to Kiyasu et al, 2015.

*In situ* hybridization for EBV-encoded small RNA (EBER) was carried out in each sample as previously described (De Falco, BMC Cancer 2015).

#### 4.3 Fluorescent in situ hybridization (FISH)

Dual-color FISH analysis was performed on 3-4 µm sections from formalin-fixed paraffin-embedded tissue. For *in situ* hybridization, the SPEC CD274, PDCD1LG2/CEN9 Dual Color Probe containing a mixture of fluorochrome direct labelled SPEC CD274, PDCD1LG2 probe specific for the CDC274/PD-L1 and PDCD1LG2/PD-L2 genes located at 9p24.1 and an orange fluorochrome labeled CEN 9 probe specific for the classical satellite III region of chromosome 9 (D9Z3) at 9q12

(Zytovision, Bremerhaven, Germany) was used according to the manufacturer's instructions. (Zytovision, Bio- Optica, Germany Germany). For each specimen, at least 100 intact non-overlapping cells with good signals were analyzed. In a normal interphase nucleus, two orange and two green signals are expected. *PD-L1* amplification was defined as *PD-L1/CEP9* ratio  $\geq 2.0$ , with high level amplification defined as  $\geq 4.0$  and low level amplification defined as  $\geq 2.0$  and  $\leq 4.0$ . Polysomy 9 was defined as average *PD-L1* copy number  $> 3$  signals/cell.

To detect translocations involving the chromosomal region 8q24.21 harbouring the *MYC* gene, we used ZytoLight SPEC *MYC* Dual Colour Break Apart Probe Zytovision, (Bio- Optica, Germany). In an interphase nucleus lacking a translocation involving the 8q24.21 band, two orange/green fusion signals are expected representing two normal (non-rearranged) 8q24.21 loci. A single pattern, consisting of one orange/green fusion signal, one orange signal and a separate green signal indicates one normal 8q24.21 locus and one 8q24.21 locus affected by an 8q24.21 translocation.

FISH images were acquired at 63x magnification utilizing Leica DM 6000B fluorescence microscope (Leica Microsystems, Switzerland) equipped with DAPI, SpectrumGreen™, SpectrumOrange™ filters. Images were processed by Leica LAS V3.8 Software (Leica Microsystems, Switzerland) to obtain a quantitative analysis of genes.

#### 4.4 Statistical analysis

Statistical analysis was performed using a statistical software package (SYSTAT-7). Clinical characteristics of the patients were assessed by using descriptive statistics. Associations between variables were evaluated with Fisher exact test for categorical data and Kruskal-Wallis rank sum test for continuous data. The Kaplan-Meier method was used to compare the survival curves by using the log-rank test. Multivariable Cox proportional hazards regression models were used to evaluate the proposed prognostic factors. All P values were 2-sided with  $P < .05$  statistically significant. Specifically, we assessed the correlation of PD-1<sub>t</sub>, PD-L1<sub>t</sub>, PD-L2<sub>t</sub>, PD-1<sub>TILS</sub>, PD-L1<sub>TILS</sub>, PD-L2<sub>TILS</sub>, FOXP3, EBV status, 9p chromosomal aberrations, with the main clinical features of PTL [i.e. age, Eastern Cooperative Oncology Group performance status, B symptoms, serum LDH, Ann Arbor stage, overall survival (from the day of diagnosis to the day of death), progression free survival (from the date of diagnosis until the date of relapse or death or last contact)]. We compared the immunohistochemical expression of each marker with that of the others and with EBV status and 9p chromosomal aberrations. Germinal center/Activated B-cell phenotype as well as *MYC* protein pattern expression were compared with PD-1<sub>t</sub>, PD-L1<sub>t</sub>, PD-L2<sub>t</sub>, PD-1<sub>TILS</sub>, PD-L1<sub>TILS</sub>, PD-L2<sub>TILS</sub>, FOXP3 staining, EBV status, 9p chromosomal aberrations, patients' prognosis.



#### 4.5 Detection of antigen by single/multiplex immunofluorescence (IF) using Opal staining method

Opal™ immunostaining, enables multi-labelling in-situ in formalin-fixed, paraffin-embedded (FFPE) tissue using fluorescent dyes and CD163 (clone 58965, Santa Cruz) and CD68 (clone ab53444, Abcam) antibodies. The initial simple multi-labelling method using the tyramide signal amplification (TSA) as was described before (Toth and Mezey, 2007). The newer Opal method uses labelling by fluorophores that bind in a covalent bond to the antigen. After labelling with the dye, removal of the marker by heating process will not affect the TSA signal. This facilitates next sequential binding of second or third antibody to be visualized and labelled and avoiding the issue of the overlapping (PerkinElmer Assay development guide booklet). The Opal kit by PerkinElmer was used according to manufacturer's protocol.

## **5. Results**

### 5.1 Patient characteristics

Patients and treatment characteristics of the study cohort are shown in Table 2. The mean age of our patients was 71.4 years. Altogether, 6 deaths and 10 relapses occurred during the median follow up of 67 months (range from 6.7 to 120 months). Five-year OS and PFS rates were 56%. All patients were treated by chemotherapy (CHOP or R-CHOP treatment) and surgery. The majority of the patients represented low stage and had low/intermediate International Prognostic Index (IPI).

N° of Patients	104
Median Age	71.4 (43-98)
Age	
<60, years	84
>60, years	20
Stage	
I-II	13/74
III-IV	5/28
NA	2

All samples were EBER-ISH negative and most of them (84/104; 87%) of non GCB phenotype. Interestingly 15 out of 104 cases expressed both MYC and BCL-2 (DE PT-DLBCL) according to the revised 4<sup>th</sup> edition WHO classification of tumors of hematopoietic and lymphoid tissue. We identified only 2 cases with MYC and BCL-2 rearrangement (DH PT-DLBCL) which present the worst prognosis.

### 5.2 PD-L1 expression in neoplastic cells

About 15% (16/104) of cases expressed the PD-L1 on neoplastic cells (Fig. 2).

Of these cases about 31% (5/16) presented an amplification in the neoplastic cells (Fig. 3).

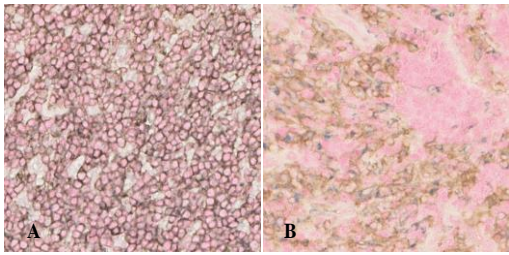


Fig. 2. Representative immunohistochemical analysis of PD-L1 expression in PT-DLBCL using multi-staining technique.

(A) PD-L1<sup>+</sup> PT-DLBCL. Tumour cells were double positive for PD-L1 (brown) and PAX5 (red).

(B) PD-L1<sup>-</sup> PT-DLBCL. In these case, tumour cells were PAX5<sup>+</sup> and PD-L1<sup>-</sup>. Some PD-L1<sup>+</sup>/PAX5<sup>-</sup> are macrophages (CD68, blue)

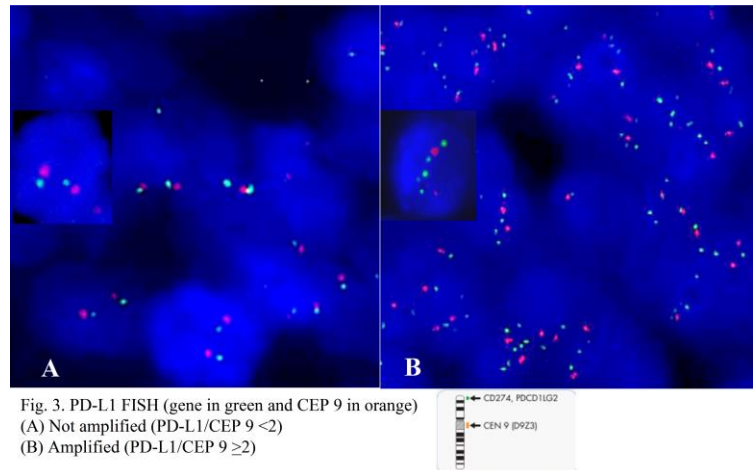


Fig. 3. PD-L1 FISH (gene in green and CEP 9 in orange)

(A) Not amplified (PD-L1/CEP 9 <2)

(B) Amplified (PD-L1/CEP 9 ≥2)

Moreover, we found that about 13% (14/104) of cases had high tumour cell expression of the ligand without FISH amplification, raising the question if other mechanism may play a role in the high PD-L1 expression without cytogenetic alterations.

### 5.3 Tumour Associated Macrophages (TAM): PD-1/PD-L1 pathway activation and M2 polarization

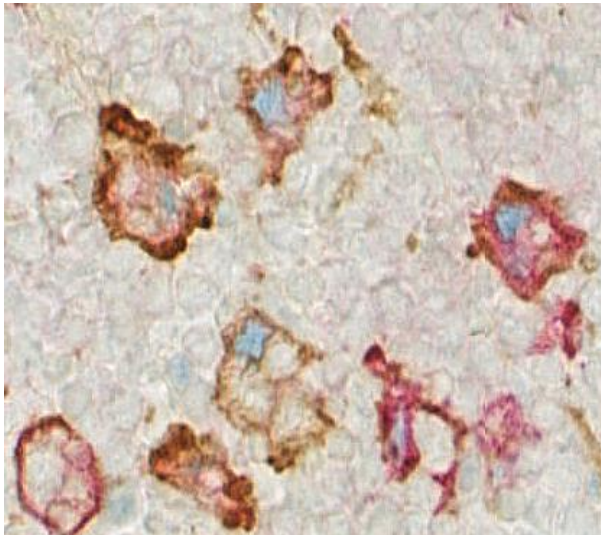


Fig. 4. Representative immunohistochemical analysis of PD-1 expression in PT-DLBCL macrophages using multi-staining technique (CMAF blue, PD-1 brown, CD163 red)

Firstly, we evaluated the immunological background of human testis. In non-neoplastic tissues, the number of myeloid cells is irrelevant and of lymphoid cells is low with a high percentage of T-lymphocytes. In PT-DLBCL the percentage of resident macrophages was 98% (102/104).

The number of TAM (as defined by the expression of CD68/CD163/CMAF) was very high. TAM expressed PD-1 ranging from 20% to 60% in about 10% (11/104) of cases (Fig. 4).

Then, we determined the TAM phenotype (M1 or M2) by means of expression of CD68 or co-expression CD68/CD163/CMAF. We detected a slight predominance of M2 class. Furthermore, we analyzed the association TAM polarization and PD-L1 expression by IHC and IF. PD-L1 expression was predominant on M2 macrophages (Fig.5).

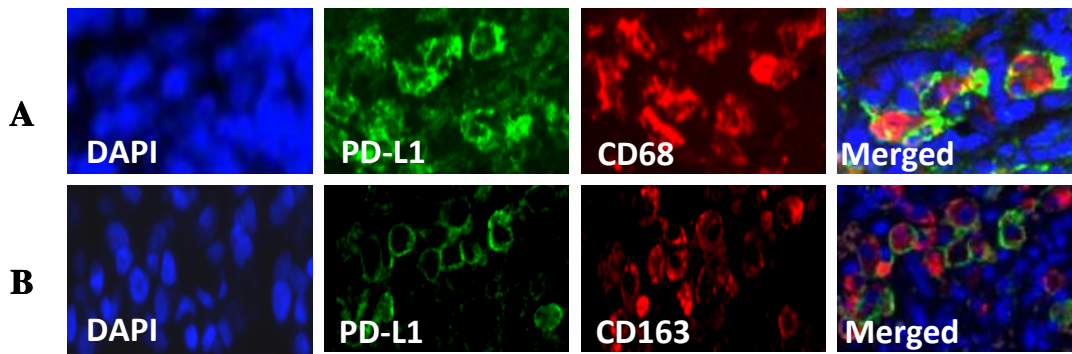


Fig. 5 Macrophages polarization and PD-L1 expression by immunofluorescence (IF).

(A) M1 polarized macrophages (CD68<sup>+</sup>)PD-L1<sup>+</sup>

(B) M2 polarized macrophages (CD163<sup>+</sup>) PD-L1<sup>+</sup>

The analysis of IF data by Vectra system revealed a predominant PD-L1 expression on M2 TAM

#### 5.4 Tumour-Infiltrating Lymphocytes (Tils)

The lymphocytes were predominantly T-lymphocytes using as a T-cells marker CD3. Subpopulations of T cells were then defined by the presence and absence of CD4, CD8 and PD-1.

In our cases the most represented Tils were cytotoxic CD8<sup>+</sup> lymphocytes. Interestingly we found an inverse correlation between the CD8<sup>+</sup> Tils and CD4<sup>+</sup> Tils with the expression of PD-L1 by the neoplastic cells. Higher CD8 (score 3: 16/104 cases) and CD4 (score 3: 8/104) expression were correlated with a better prognosis (1% relapse, average survival ~7y) and a M1/PD-L1<sup>+</sup> TAM phenotype.

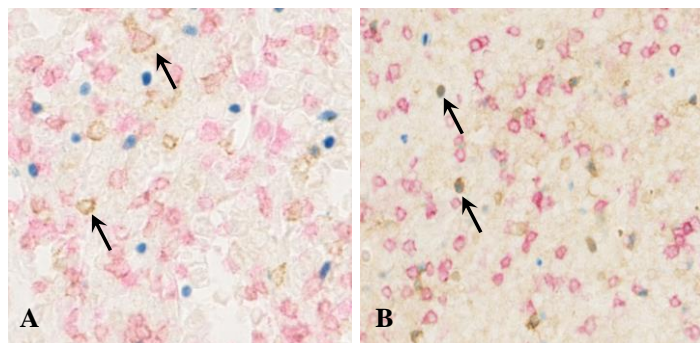


Fig. 6 PT-DLBCL Tils multistaining immunohistochemical analysis

(A) Predominant CD8<sup>+</sup> (red). Some of CD8<sup>+</sup> cells were also PD-1<sup>+</sup> (brown, activated/exhausted T-cells). In blue CD4<sup>+</sup> T-cells.

(B) In this case, the CD4<sup>+</sup> T-cells (brown) coexpressed also FOXP3(blue), revealing a regulatory phenotype.

After we analyzed the activated/exhausted phenotype (CD8 and PD-1 double positive): only few T-exhausted/activated (score 3: 6/104 ; score 2: 11/104 ) cells were observed as also only few T-regulatory cells (score 3: 1/104; score 2: 6/104) (Fi.g. 6)

## **6. Discussion**

Primary testicular lymphoma (PTL) is a rare and aggressive form of extranodal lymphoma. However, the outcomes of PT-DLBCL patients remain poor owing to the high rate of relapse in the CNS and contralateral testis.

The interaction of PD-1, member of the B7 receptor family, with its ligand (PD-L1 and PD-L2) exerts an important checkpoint function in the regulation of T-cell mediated immune responses in the presence of foreign antigens (46). The PD-1/PD-L1 checkpoint is operative in peripheral tissues and essentially downregulates T-cell mediated cytokine production and T-cell receptor driven cell proliferation, helping to control local inflammatory responses and to maintain self-tolerance (47). PD-1 and PD-L1 are mostly expressed in activated T cells, antigen-presenting cells and other immune cells. Importantly, cells of the same lineage can express PD-1 and PD-L1 simultaneously, suggesting substantial cross talk (48). Almost immediately after activation of the T-cell receptor, ligation of PD-1 to PD-L1/PDL2 triggers inhibition of intracellular phosphoinositide-3 kinase activity, downstream Akt activation, and other stimulatory pathways within T-cells, this translates in down regulation of T-cell functions (48).

PD-L1 is highly over-expressed in many solid tumour types and has recurrently been associated with poor disease-related outcomes. This suggests that PD-L1 is a robust prognostic marker across different solid neoplasms and a possible biomarker to personalize PD-1 pathway blockade. In lymphomas, PD-L1 expression is rare and heterogeneous amongst different lymphoid cancers of the same cell lineage, and on reactive cells present at the tumour microenvironment. PD-L1, which is usually expressed in the antigen presenting cells and malignant lymphoid cells, interacts with PD-1 on T cells to suppress an effective antitumor immune response by inhibiting signalling downstream from the T-cell receptor (TCR) (49).

The PD-1 is mainly expressed in follicular germinal center T cells, particularly in CD4<sup>+</sup>/CD25<sup>-</sup> cells. Moreover, it also may be expressed on many CD8<sup>+</sup> Tils, and increased expression of PD-1 is a marker of the activated/exhausted state of these cells. Additionally, it had been hypothesized that Tils were CD8<sup>+</sup> T cells showing that PD-1 expression in Tils significantly correlated with PD-L1 overexpression in tumor B-cells (50).

It has become evident that manipulating the immune system taints to be an advantageous management strategy for many tumours including lymphomas. Through research has elucidated several mechanisms how this is achieved, it has also become clear that both tumour cells and microenvironmental compounds should be considered and modulated in a proper manner. These findings have led to a plethora of new potential treatment options, which have already proven to be beneficiary for patients. However, it has also become evident that there is no uniform treatment response, highlighting the need for individualized analysis of patients' tumours and the

corresponding individual immunological/immunogenetic background in order to decipher on the one hand the specific pathways used by the tumour to hamper the hosts' immune system and the potential responsiveness of the latter. It has also become evident that immunotherapy can and probably should be synthetically combined with the other pillars of cancer therapy (surgery, chemotherapy, and radiotherapy) as this can markedly improve the impact of each therapy approach.

As reported by literature, also in our study the dual expression of MYC and BCL-2 and *BCL-2*, *MYC* translocations were associated with a worse prognosis. The DH and DE status are correlated with a negative impact on prognosis.

We detected the expression of PD-L1 in about 15% of cases; of these just the 31% presented amplification in the neoplastic cells. These result leads to the question if other mechanisms (cytokine signalling such as interferon (INF), infectious aetiologies) are implicated in the over-expression of the PD-L1, with the same result: activation of the JAK/STAT.

Furthermore, our observations showed an association between the expression of PD-L1 by tumour B cells and the expression of PD-1 on macrophages, with a correlation between the presence of a PD1<sup>+</sup> TAM and poor prognosis, also if the literature available data suggest the contrary (51).

Notably, we also found that the M2 macrophages population expressed significantly more PD-1 than the M1 population, with an important association between the PD-1/PD-L1 pathway activation and the M2 macrophage polarization, confirming the literature data that suggest an inhibiting role of PD-1 on tumour microenvironment, including T cells and macrophages suggesting that PD-1 expression is a global mechanism for limiting immunity across the innate and adaptive immune system.

Furthermore, we highlighted that M1 macrophages were more associated with the presence of Tils (CD8<sup>+</sup> or CD4<sup>+</sup>) than with PD-L1 overexpression in neoplastic B-cells. These results correlated with a better prognosis and suggested a possible tumour-mediated T-cell activation mechanism in TME, also if no statistically relevant differences between T-reg and T-ex/act lymphocytes in respect to prognosis were found due to the limited data.

## **7. Conclusion**

Our study has several limitations. The small study population, variable treatment protocols, and relatively short follow-up period made it difficult to identify relevant prognostic factors. Nevertheless, analyzing the results of our work, we could suggest that in PT-DLBCL, as seen in others lymphoma, the PD-1/PD-L1 pathway activation depends more on TME than on PD-L1 expression by neoplastic cells.

With this study, we highlighted that TME could play an important role to activate the PD-1/PD-L1 pathway in PT-DLBCL. Among the different cells constituting TME, the most important one seems to be the macrophages. Despite the heterogeneous PD-1 expression on Tils, macrophages in our work highly correlated with the expression of PD-1 and PD-L1, influencing the prognosis.

Another relevant result is the correlation between the macrophage polarization and prognosis for which further studies are needed.

Our findings suggest that PT-DLBCL is a unique subtype of DLBCL, with a high risk of relapse. Thus, additional research is required to more characterize the gene expression profile to highlight possible differences between PT-DLBCL and DLBCL-NOS, to improve the treatment of these patients, focusing on the PD-1/PD-L1 pathway and its role on microenvironment, in particular on the macrophages, attractive targets for this aggressive lymphoma.

1. Fend F, Quintanilla-Martínez L. Assessing the prognostic impact of immune cell infiltrates in follicular lymphoma. *Haematologica*. 2014.
2. K., Tarte. Role of the microenvironment across histological subtypes of NHL. *Hematol Am Soc Hematol Educ Progr*. 2017
3. Guo B, Cen H, Tan X, Ke Q. Meta-analysis of the prognostic and clinical value of tumor-associated macrophages in adult classical Hodgkin lymphoma. *BMC Med*. 2016.
4. Li Z, Qiu Y, Personett D, Huang P, Edenfield B, Katz J, et al. Pomalidomide shows significant therapeutic activity against CNS lymphoma with a major impact on the tumor microenvironment in murine models. *PLoS ONE*. 2013.
5. Steidl C, Lee T, Shah SP, Farinha P, Han G, Nayar T, et al. Tumor-associated macrophages and survival in classic Hodgkin's lymphoma. *New Engl J Med*. 2010.223
6. Canioni D, Salles G, Mounier N, Brousse N, Keuppens M, Morchhauser F, et al. High numbers of tumor-associated macrophages have an adverse prognostic value that can be circumvented by rituximab in patients with follicular lymphoma enrolled onto the GELA-GOELAMS FL-2000 trial. *J Clin Oncol*. 2008.
7. Wahlin BE, Sander B, Christensson B, Kimby E. CD8+ T-cell content in diagnostic lymph nodes measured by flow cytometry is a predictor of survival in follicular lymphoma. *Clin Cancer Res*. 2007.
8. Carreras J, Lopez-Guillermo A, Roncador G, Villamor N, Colomo L, Martinez A, et al. High numbers of tumor-infiltrating programmed cell death 1-positive regulatory lymphocytes are associated with improved overall survival in follicular lymphoma. *J Clin Oncol*. 2009.
9. Bashey A, Medina B, Corringham S, Pasek M, Carrier E, Vrooman L, et al. CTLA4 blockade with ipilimumab to treat relapse of malignancy after allogeneic hematopoietic cell transplantation. *Blood*. 2009.



10. Grosso JF, Kelleher CC, Harris TJ, Maris CH, Hipkiss EL, De Marzo A, et al. LAG-3 regulates CD8+ T cell accumulation and effector function in murine self- and tumor-tolerance systems. *J Clin Investig.* 2007.
11. Li B, Greene MI. Special regulatory T-cell review: FOXP3 biochemistry in regulatory T cells—how diverse signals regulate suppression. *Immunology.* 2008.224
12. Sage PT, Francisco LM, Carman CV, Sharpe AH. The receptor PD-1 controls follicular regulatory T cells in the lymph nodes and blood. *Nat Immunol.* 2013.
13. Wang J, Ke XY. The four types of Tregs in malignant lymphomas. *J Hematol Oncol.* 2011.
14. Yang ZZ, Novak AJ, Stenson MJ, Witzig TE, Ansell SM. Intratumoral CD4+CD25+ regulatory T-cell mediated suppression of infiltrating CD4+ T cells in B-cell non-Hodgkin lymphoma. *Blood.* 2006.
15. Carreras J, Lopez-Guillermo A, Fox BC, Colomo L, Martinez A, Roncador G, et al. High numbers of tumor-infiltrating FOXP3-positive regulatory T cells are associated with improved overall survival in follicular lymphoma. *Blood.* 2006.
3. Morin, R. D., Mendez-Lago, M., Mungall, A. J., Goya, R., Mungall, K. L., Corbett, R. D., ... Marra, M. A. Frequent mutation of histone-modifying genes in non-Hodgkin lymphoma. *Nature.* 2011.
4. Morin, R. D., Mungall, K., Pleasance, E., Mungall, A. J., Goya, R., Huff, R. D., ... Marra, M. A. Mutational and structural analysis of diffuse large B-cell lymphoma using whole-genome sequencing. *Blood.* 2013.
5. Cheung, K.-J. J., Delaney, A., Ben-Neriah, S., Schein, J., Lee, T., Shah, S. P., ... Horsman, D. E. High resolution analysis of follicular lymphoma genomes reveals somatic recurrent sites of copy-neutral loss of heterozygosity and copy number alterations that target single genes. *Genes, Chromosomes & Cancer.* 2010.
6. d'Amore, F., Chan, E., Iqbal, J., Geng, H., Young, K., Xiao, L., ... Dave, B. J. Clonal evolution in t(14;18)-positive follicular lymphoma, evidence for multiple common pathways, and frequent

parallel clonal evolution. *Clinical Cancer Research : An Official Journal of the American Association for Cancer Research*. 2008.217

7. Höglund, M., Sehn, L., Connors, J. M., Gascoyne, R. D., Siebert, R., Säll, T., ... Horsman, D. E. Identification of cytogenetic subgroups and karyotypic pathways of clonal evolution in follicular lymphomas. *Genes, Chromosomes & Cancer*,. 2004.

8. Oss, C. W., Ouillette, P. D., Saddler, C. M., Shedden, K. A., & Malek, S. N. Comprehensive analysis of copy number and allele status identifies multiple chromosome defects underlying follicular lymphoma pathogenesis. *Clinical Cancer Research : An Official Journal of the American Association for Cancer Research*. 2007.

9. Bouska, A., McKeithan, T. W., Deffenbacher, K. E., Lachel, C., Wright, G. W., Iqbal, J., ... Chan, W.-C. Genome-wide copy-number analyses reveal genomic abnormalities involved in transformation of follicular lymphoma. *Blood*. 2014.

10. Kerr JF, Wyllie AH, Currie AR. Apoptosis: a basic biological phenomenon with wide-ranging implications in tissue kinetics. *Br J Cancer*. 1972.

11. Rosenquist R, Beà S, Du MQ, Nadel B, Pan-Hammarström Q. Genetic landscape and deregulated pathways in B-cell lymphoid malignancies. *J Intern Med*. 2017.

12. Masir N, Jones M, Marafioti T, Mason DY. Heterogeneous expression of B cell-associated markers in follicular lymphoma. *Histopathology*. 2011.

13. Schmidt-Hansen M, Berendse S, Marafioti T, McNamara C. Does cell-of-origin or MYC, BCL2 or BCL6 translocation status provide prognostic information beyond the International Prognostic Index score in patients with diffuse large B-cell lymphoma treated with rituximab and chemotherapy? A systematic review. *Leuk Lymphoma*. 2017.

14. Adams JM, Cory S. Myc oncogene activation in B and T lymphoid tumours. *Proc R Soc Lond B Biol Sci*. 1985.

15. Bretones G, Delgado MD, León J. Myc and cell cycle control. *Biochim Biophys Acta*. 2015.

16. Cheah CY, Wirth A, Seymour JF. Primary testicular lymphoma. *Blood*. 2014; 123:486–93.





17. Coiffier B, Lepage E, Briere J, Herbrecht R, Tilly H, Bouabdallah R, Morel P, Van Den Neste E, Salles G, Gaulard P, Reyes F, Lederlin P, Gisselbrecht C. CHOP chemotherapy plus rituximab compared with CHOP alone in elderly patients with diffuse large-B-cell lymphoma. *N Engl J Med*. 2002; 346:235–42.
18. Vitolo U., Seymour J.F., Martelli M., Illerhaus G., Illidge T., Zucca E., Campo E. and Ladetto M. Extranodal diffuse large B-cell lymphoma (DLBCL) and primary mediastinal B-cell lymphoma: ESMO Clinical Practice Guidelines for diagnosis, treatment and follow-up, ESMO Guidelines Committee
19. Zucca E, Conconi A, Mughal TI, et al. Patterns of outcome and prognostic factors in primary large-cell lymphoma of the testis in a survey by the international extranodal lymphoma study group. *J Clin Oncol* 2003;21(1):20 –7.
20. Gundrum JD, Mathiason MA, Moore DB, Go RS. Primary testicular diffuse large B-cell lymphoma: a population-based study on the incidence, natural history, and survival comparison with primary nodal counterpart before and after the introduction of rituximab. *J Clin Oncol* 2009;27(31):5227 –32.
21. Vitolo U, Chiappella A, Ferreri AJ, et al. First-line treatment for primary testicular diffuse large B-cell lymphoma with rituximab-CHOP, CNS prophylaxis, and contralateral testis irradiation: final results of an international phase II trial. *J Clin Oncol* 2011;29(20):2766 –72.
22. Meyer PN, Fu K, Greiner TC, et al. Immunohistochemical methods for predicting cell of origin and survival in patients with diffuse large B-cell lymphoma treated with rituximab. *J Clin Oncol* 2011;29(2):200 –7.
23. Bernasconi B, Uccella S, Martin V, et al. Gene translocations in testicular lymphomas. *Leuk Lymphoma* 2014;55(6):1410 –2.
24. Deng L, Xu-Monette ZY, Loghavi S, et al. Primary testicular diffuse large B-cell

- lymphoma displays distinct clinical and biological features for treatment failure in rituximab era: a report from the international PTL consortium. *Leukemia* 2016; 30(2):361 –72.
25. Chapuy B, Roemer MG, Stewart C, et al. Targetable genetic features of primary testicular and primary central nervous system lymphomas. *Blood* 2016; 127(7):869 –81.
26. Chong LC, Twa DD, Mottok A, et al. Comprehensive characterization of programmed death ligand structural rearrangements in B-cell non-Hodgkin lymphomas. *Blood* 2016;128(9):1206 –13.
27. Twa DD, Chan FC, Ben-Neriah S, et al. Genomic rearrangements involving programmed death ligands are recurrent in primary mediastinal large B-cell lymphoma. *Blood* 2014; 123(13):2062–5.
28. Twa DD, Mottok A, Chan FC, et al. Recurrent genomic rearrangements in primary testicular lymphoma. *J. Pathol.* 2015;236(2):136 –41.
29. Magnoli F, Ricotti I, Novario M, et al. Primary testicular diffuse large B-cell lymphoma: morphological and immunophenotypical study with characterization of the T-cell component of the tumor microenvironment. *Leuk Lymphoma* 2015:1 –3.
30. Brown PJ, Wong KK, Felce SL, et al. FOXP1 suppresses immune response signatures and MHC class II expression in activated B-cell-like diffuse large B-cell lymphomas. *Leukemia* 2016;30(3):605 –16.
31. Ruminy P, Etancelin P, Couronne L, et al. The isotype of the BCR as a surrogate for the GCB and ABC molecular subtypes in diffuse large B-cell lymphoma. *Leukemia* 2011;25(4):681 –8.
32. Hans CP, Weisenburger DD, Greiner TC, et al. Confirmation of the molecular classification of diffuse large B-cell lymphoma by immunohistochemistry using a tissue microarray. *Blood* 2004; 103 (1):275 –82.

33. Booman M, Douwes J, Glas AM, de Jong D, Schuurin E, Kluin PM. Primary testicular diffuse large B-cell lymphomas have activated B-cell-like subtype characteristics. *J Pathol* 2006; 210 (2):163 –71.
34. Kraan W, van Keimpema M, Horlings HM, et al. High prevalence of oncogenic MYD88 and CD79B mutations in primary testicular diffuse large B-cell lymphoma. *Leukemia* 2014; 28 (3):719 –20.
35. Wang JQ, Jeelall YS, Horikawa K. Emerging targets in human lymphoma: targeting the MYD88 mutation. *Blood and Lymphatic Cancer: Targets and Therapy* 2013; 3:53 –61.
36. Menter T, Ernst M, Drachneris J, et al. Phenotype profiling of primary testicular diffuse large B-cell lymphomas. *Hematol Oncol* 2014; 32(2):72 –81.
37. Oishi N, Kondo T, Nakazawa T, et al. High prevalence of the MYD88 mutation in testicular lymphoma: Immunohistochemical and genetic analyses. *Pathol Int* 2015; 65(10):528 –35.
38. Dong Z, Ren L, Lin L, Li J, Huang Y. Effect of microRNA-21 on multidrug resistance reversal in A549/DDP human lung cancer cells. *Mol Med Rep* 2015; 11(1):682 –90.
39. Go H, Jang JY, Kim PJ, et al. MicroRNA-21 plays an oncogenic role by targeting FOXO1 and activating the PI3K/AKT pathway in diffuse large B-cell lymphoma. *Oncotarget* 2015; 6(17):15035 –49.
40. Robertus JL, Harms G, Blokzijl T, et al. Specific expression of miR-17-5p and miR-127 in testicular and central nervous system diffuse large B-cell lymphoma. *Mod Pathol* 2009; 22(4):547 –55.
41. Kridel R, Telio D, Villa D, et al. Diffuse large B-cell lymphoma with testicular involvement: outcome and risk of CNS relapse in the rituximab era. *Br J Haematol* 2017; 176(2):210 –21.
42. Wilson WH, Young RM, Schmitz R, et al. Targeting B cell receptor signaling with Ibrutinib in diffuse large B cell lymphoma. *Nat Med* 2015; 21(8):922 –6.
43. Grommes C, Pastore A, Palaskas N, et al. Ibrutinib unmasks critical role of Bruton tyrosine kinase in primary CNS lymphoma. *Cancer Discov* 2017; 7(9):1018 –29.

44. Bernard S, Goldwirt L, Amorim S, et al. Activity of ibrutinib in mantle cell lymphoma patients with central nervous system relapse. *Blood* 2015; 126(14):1695–8.
45. David D.W. Twa, Anja Mottoka, Kerry J. Savage and Christian Steidl, The pathobiology of primary testicular diffuse large B-cell lymphoma: Implications for novel therapies. *Blood Reviews* 32 (2018) 249–255.
46. Blank, C., Kuball, J., Voelkl, S., et al., 2006. Blockade of PD-L1 (B7-H1) augments human tumor-specific T cell responses in vitro. *Int. J. Cancer* 119, 317–327.; Freeman, G.J., Long, A.J., Iwai, Y., et al., 2000. Engagement of the PD-1 immunoinhibitory receptor by a novel B7 family member leads to negative regulation of lymphocyte activation. *J. Exp. Med.* 192, 1027– 1034.).
47. Bryan, L.J., Gordon, L.I., 2015. Blocking tumor escape in hematologic malignancies: the anti-PD-1 strategy. *Blood Rev.* 29 (1), 25– 32.)
48. Hawkes, E., Grigg, A., Chong, G., 2015. Programmed cell death-1 inhibition in lymphoma. *Lancet* 16 (5), e234–45.
49. Batlevi, C., Matsuki, E., Brentjens, R., Younes, A., 2016. Novel immunotherapies in lymphoid malignancies. *Nat. Rev. Clin. Oncol.* 13, 25–40.
50. Four M, Cacheux V, Tempier A, et al. PD-1 and PD-L1 expression in primary central nervous system diffuse large B-cell lymphoma are frequent and expression of PD-1 predicts poor survival. *Hematological Oncology.* 2017;35:487–496
51. Kiyasu, J., Miyoshi, H., Hirata, A., 2015. Expression of programmed cell death ligand 1 is associated with poor overall survival in patients with diffuse large B-cell lymphoma. *Blood* 126 (19), 2193–2201.

# Burkitt lymphoma with a granulomatous reaction: an M1/Th1-polarised microenvironment is associated with controlled growth and spontaneous regression

Massimo Granai,<sup>1,2</sup> Stefano Lazzi,<sup>1</sup> Virginia Mancini,<sup>1</sup> Ayse Akarca,<sup>3</sup> Raffaella Santi,<sup>4</sup> Federica Vergoni,<sup>4</sup> Ester Sorrentino,<sup>1</sup> Raffaella Guazzo,<sup>1</sup> Lucia Mundo,<sup>1,5</sup> Gabriele Cevenini,<sup>1</sup> Claudio Tripodo,<sup>6</sup> Gioia Di Stefano,<sup>4</sup> Benedetta Puccini,<sup>7</sup> Maurilio Ponzoni,<sup>8</sup> Elena Sabattini,<sup>9</sup>  Claudio Agostinelli,<sup>9</sup>  Nuray Bassüllü,<sup>10</sup> Tülay Tecimer,<sup>11</sup> Ahu Senem Demiroz,<sup>12</sup> Leah Mnango,<sup>13</sup> Stephan Dirnhofer,<sup>14</sup> Leticia Quintanilla-Martinez,<sup>2</sup>  Teresa Marafioti,<sup>3</sup> Falko Fend<sup>1</sup> & Lorenzo Leoncini<sup>1</sup> 

<sup>1</sup>Department of Medical Biotechnologies, University of Siena, Siena, Italy, <sup>2</sup>Institute of Pathology, University of Tübingen, Tübingen, Germany, <sup>3</sup>Department of Cellular Pathology, University College London, London, UK, <sup>4</sup>Department of Pathology, University of Florence, Florence, Italy, <sup>5</sup>Health Research Institute, University of Limerick, Limerick, Ireland, <sup>6</sup>Department of Human Pathology, University of Palermo, Palermo, <sup>7</sup>Department of Haematology, University of Florence, Florence, <sup>8</sup>Department of Pathology, University Vita-Salute San Raffaele, Milano, <sup>9</sup>Haemolymphopathology Unit - IRCCS - Azienda Ospedaliero-Universitaria di Bologna, Bologna, Italy, <sup>10</sup>Department of Pathology, Bilim University, İstanbul, <sup>11</sup>Department of Pathology, Acibadem University, İstanbul, <sup>12</sup>Department of Pathology, İstanbul University Cerrahpaşa, İstanbul, Turkey, <sup>13</sup>Department of Pathology, Muhimbili National Hospital and University for Healthcare and Allied Sciences, Dar-es-Salaam, Tanzania, and <sup>14</sup>Institute of Pathology, University Hospital Basel, Basel, Switzerland

Date of submission 12 September 2020  
Accepted for publication 15 April 2021  
Published online Article Accepted 5 May 2021

Granai M, Lazzi S, Mancini V, Akarca A, Santi R, Vergoni F, Sorrentino E, Guazzo R, Mundo L, Cevenini G, Tripodo C, Di Stefano G, Puccini B, Ponzoni M, Sabattini E, Agostinelli C, Bassüllü N, Tecimer T, Demiroz A S, Mnango L, Dirnhofer S, Quintanilla-Martinez L, Marafioti T, Fend F & Leoncini L (2022) *Histopathology* 80, 430–442. <https://doi.org/10.1111/his.14391>

## Burkitt lymphoma with a granulomatous reaction: an M1/Th1-polarised microenvironment is associated with controlled growth and spontaneous regression

**Aims:** Burkitt lymphoma (BL) is an aggressive B-cell lymphoma that, in some instances, may show a granulomatous reaction associated with a favourable prognosis and occasional spontaneous regression. In the present study, we aimed to define the tumour microenvironment (TME) in four such cases, two of which regressed spontaneously.

**Methods and results:** All cases showed aggregates of tumour cells with the typical morphology, molecular cytogenetics and immunophenotype of BL surrounded by a florid epithelioid granulomatous reaction. All four cases were Epstein–Barr virus (EBV)-positive with type I latency. Investigation of the TME showed

similar features in all four cases. The analysis revealed a proinflammatory response triggered by Th1 lymphocytes and M1 polarised macrophages encircling the neoplastic cells with a peculiar topographic distribution.

**Conclusions:** Our data provide an *in-vivo* picture of the role that specific immune cell subsets might play during the early phase of BL, which may be capable of maintaining the tumour in a self-limited state or inducing its regression. These novel results may provide insights into new potential therapeutic avenues in EBV-positive BL patients in the era of cellular immunotherapy.

Address for correspondence: Professor Lorenzo Leoncini, Department of Medical Biotechnologies, Strada delle Scotte, 6 University of Siena, Siena, Italy. e-mail: [Lorenzo.leoncini@dbm.unisi.it](mailto:Lorenzo.leoncini@dbm.unisi.it)

L. Q.-M, T. M., F. F. and L. L. contributed equally to this work.

© 2021 The Authors. *Histopathology* published by John Wiley & Sons Ltd.

This is an open access article under the terms of the Creative Commons Attribution License, which permits use, distribution and reproduction in any medium, provided the original work is properly cited.

Keywords: Burkitt lymphoma, EBV, granulomatous reaction, *in-situ* lymphoid neoplasia, microenvironment, M1 polarised macrophages, Th1 T cells

## Introduction

Burkitt lymphoma (BL) is an aggressive B-cell lymphoma characterised by diffuse proliferation of medium-sized monomorphic lymphoid cells with basophilic cytoplasm and cohesive growth. A so-called starry sky pattern is usually present, owing to the presence of numerous macrophages with tangible apoptotic bodies. However, some cases show a florid granulomatous reaction and are characterised by a favourable outcome and, in rare instances, spontaneous regression.<sup>1–6</sup> More recently, this issue was discussed in the Lymphoma Workshop (LYWS) of the 18th meeting of the European Association for Haematopathology (EAHP) in 2016 in Basel. BL cases with a granulomatous reaction were presented, two of which showed spontaneous remission without further therapy after needle core biopsy or lymph node excision.<sup>7</sup> The almost identical morphological features of these cases may provide a link between the excellent prognosis of these patients and the peculiar immune reaction of the host, highlighting the need for further investigations with comprehensive characterisation of the tumour microenvironment (TME). In fact, none of the previous studies has characterised the nature of the inflammatory infiltrate and its polarisation towards an activated (proinflammatory) or tolerant (protumoral) state.

Only in the last decade has the cellular background in which lymphoma cells thrive become an important target of inquiry. The functions of what used to be considered passive bystanders are quickly becoming elucidated, in order to provide potential targets for immunotherapy. In recent years, a model has been developed to describe the complex mechanism of macrophage activation as polarisation towards two opposite states, namely M1 and M2, with proinflammatory and protumoral properties respectively. The M1/M2 nomenclature has been inspired by the Th1 versus Th2 concept.<sup>8</sup>

Th1 lymphocytes and M1 macrophages are the primary sources of proinflammatory cytokines, which also promote cancer immunosurveillance and cytotoxicity. On the other hand, these effects are counterbalanced by M2 macrophages, Th2 lymphocytes and

regulatory T cells (Tregs) having anti-inflammatory and protumoral effects.<sup>9</sup> In particular, Th1 cells drive the type 1 pathway ('cellular immunity') to fight viruses and eliminate cancerous cells, whereas Th2 cells drive the type 2 pathway ('humoral immunity'), up-regulating antibody production.<sup>9</sup>

Differentiation of CD4<sup>+</sup> T cells into Th1 and Th2 effector cells is controlled by the transcription factors T-box protein expressed in T cells (T-bet; also called TBX21) and GATA-binding protein 3 (GATA3), respectively. T-bet overexpression causes differentiation into the Th1 lineage, whereas loss of T-bet expression induces default commitment to the Th2 and Th17 lineages.<sup>10</sup> T-bet directly activates interferon (IFN)- $\gamma$  gene transcription, and enhances the development of Th1 cells. Therefore, CD4<sup>+</sup>/T-bet<sup>+</sup> cells are considered to be Th1 cells, whereas CD4<sup>+</sup>/GATA3<sup>+</sup> cells are considered to be Th2 cells.

Th1 lymphocytes are well-known IFN- $\gamma$  secretors, being involved in the regulation of macrophage polarisation, promoting and maintaining the formation of granulomas.<sup>9,11</sup> IFN- $\gamma$  activates the IFN regulatory factor–signal transducer and activator (STAT) (via STAT1) pathway, switching macrophage function towards the M1 phenotype.<sup>11</sup>

However, the immunophenotypic features that distinguish M1 and M2 macrophages are still not standardised.<sup>12,13</sup> Given the fact that, in recent studies,<sup>13</sup> the scavenger receptor CD163 alone has not been considered to be a reliable marker of M2 polarisation, the combination of c-Maf, an essential transcription factor for interleukin-10 gene expression in macrophages, and CD68 as a generic macrophage marker may be used to identify M2 macrophages. On the other hand, an antibody against phosphorylated STAT1 (pSTAT1) may be used to identify M1 macrophages and IFN- $\gamma$ -primed dendritic cells.

Epstein–Barr virus (EBV)-specific T-cell responses in BL have not been fully elucidated. Indeed, Epstein–Barr nuclear antigen (EBNA) 1, which is usually the only latent protein expressed in EBV<sup>+</sup> BL, has the ability to inhibit proteasomal processing through its Gly-Ala repeat domain.<sup>14</sup> In addition, studies have shown defects in major histocompatibility complex class I antigen processing in BL.<sup>15</sup> These features are



well-known aspects of BL cells, potentially explaining their escape from immune surveillance.<sup>16</sup> On the other hand, other authors have shown that EBNA1-specific CD4<sup>+</sup> Th1 cells can be isolated from EBV-seropositive healthy adults,<sup>17</sup> and that these cells are cytolytic for BL cell lines constitutively expressing human leukocyte antigen (HLA) class II.<sup>18–21</sup>

Therefore, the aim of this study was to investigate the immune landscape in four cases of EBV<sup>+</sup> BL with a granulomatous reaction, focusing on the quantitative and topographic distribution of the innate immunity [M1/M2 macrophages, plasmacytoid dendritic cells (pDCs), and natural killer (NK) cells] and adaptive immunity (Th1/Th2 lymphocytes and Tregs) cell subsets.

## Materials and methods

A formalin-fixed paraffin-embedded (FFPE) BL case was retrieved from the Department of Medical Biotechnologies, University of Siena, Siena, Italy (case 1), and two cases (case 2 and case 3) were retrieved from the LYWS of the 18th EAHP meeting, in Basel, Switzerland, 2016, and were included in the workshop report.<sup>7</sup> The third case submitted to the LYWS was not included in this study because of lack of available sections. The fourth case (case 4) was retrieved from the 1st Workshop to support the NIHR-RIGHT Aggressive Infection Related-East African Lymphoma (AI-REAL) Study in Dar-es-Salaam (Tanzania), in February 2020.

The diagnosis of BL was issued by expert haematopathologists following the criteria described in the 2017 World Health Organization classification of tumours of haematopoietic and lymphoid tissue.<sup>6</sup> Diagnostic immunohistochemistry was performed on the Bond III Autostainer (Leica Microsystems, Newcastle upon Tyne, UK), according to the manufacturer's instructions. *In-situ* hybridisation for EBV-encoded small RNAs (EBERs) was performed on deparaffinised 4-mm-thick FFPE tissue sections with a Dako Detection Kit for EBER (DakoCytomation, Glostrup, Denmark). The slides were counterstained with haematoxylin and fixed in Faramount (DakoCytomation).

Fluorescence *in-situ* hybridisation for *MYC* rearrangement was performed for each case, with a break-apart probe (BAP) (Vysis *MYC* Dual Colour Break Apart Rearrangement Probe; Abbott, Wiesbaden, Germany) and a dual fusion probe (ZytoVision GmbH, Bremerhaven, Germany), according to the manufacturer's instructions. For each specimen, a 4-

µm-thick tissue section embedded in paraffin was cut. Briefly, the slides were incubated in heat pretreatment solution, washed, digested, dehydrated, and hybridised with probes. At least 100 intact non-overlapping nuclei were analysed manually on a Leica DM 600B (Leica Microsystems, Heerbrugg Switzerland) fluorescence microscope equipped with 4',6-diamidino-2-phenylindole, Spectrum Green and Spectrum Orange filters.

The antibody panels used for multiplex immunohistochemistry (mIHC) consisted of eight different triple and double stains: (i) CD68, CD163, and c-Maf; (ii) programmed death-ligand 1 (PD-L1), CD163, and c-Maf; (iii) CD4, CD25, and forkhead box P3 (FOXP3); (iv) CD8, programmed cell death protein 1 (PD-1), and lymphocyte-activation gene 3 (LAG3); (v) pSTAT1, CD68, and CD123; (vi) CD4 and T-bet; (vii) CD4 and GATA3; and (viii) CD20 and T-bet (see Table S1 for antibody characteristics). CD56 and CD57 were included as single stains. Double staining and triple staining were performed with an automated staining system (DISCOVERY ULTRA IHC/ISH research platform; Roche Diagnostics, Indianapolis, USA) for open procedures, according to the manufacturer's protocols.<sup>22</sup> The detailed protocols for the application of each stain are shown in Doc. S1. The CD68+/pSTAT1+, CD123+/pSTAT1+, CD163+/CD68+/c-Maf+, CD163+/c-Maf+, CD4+/T-bet+, CD4+/GATA3+, CD4+/CD25+/FOXP3+ and CD8+/PD-1+/LAG3+ cells were evaluated manually and independently by three experienced pathologists (M.G., V.M. and T.M.) by counting the individual cell types in 10 high-power fields under a × 40 objective 172 (Nikon Eclipse E400, Nikon Corporation, Tokyo, Japan), and taking into account either nuclear and surface stains, reported as percentages for each cell type in scores rounded up to the nearest 5%.<sup>23,24</sup> Only CD163+/CD68+/c-Maf+ and CD163+/CD68-/c-Maf+ cells were considered to be M2 macrophages; CD163-/CD68+/c-Maf- and CD68+/pSTAT1+ cells were considered to be M1 macrophages, and CD123+/pSTAT1+ cells were considered to be IFN-γ-primed pDCs.<sup>25</sup> The interobserver reproducibility of each cell count was assessed according to the coefficient of variation as a percentage (CV%), which is the ratio of the standard deviation to the mean of the three percentage observations. For each variable, percentage agreement across the four cases analysed was then expressed as the mean of 100 – CV% and its 95% confidence interval, estimated with the bias-corrected and accelerated bootstrap technique. The percentages of each cell type for each observer and the level of interobserver reproducibility for each variable are shown in Table S2.

Tissue sections from the same set of cases and without antibody/chromogens were used as negative controls. Three tonsils, three reactive lymph nodes and three cases of conventional BL with the typical starry sky pattern were used as positive controls.

## Results

### CLINICAL HISTORY

Case 1 was a 65-year-old female with an isolated right axillary lymphadenopathy and no signs of systemic infection. She underwent excision of the enlarged lymph node, and a diagnosis of focal involvement by EBV-positive B cells with features of BL was made, associated with reactive lymphadenitis, and a granulomatous reaction. The computed tomography–positron emission tomography (CT-PET) scan showed no evidence of other hypermetabolic lymph nodes. Bone marrow biopsy showed normal haematopoiesis, and flow cytometry analysis showed a normal phenotype. Therefore, the patient was followed closely, and a ‘watch and wait’ strategy was used, without any chemotherapy. The patient was well and in good condition 30 months after the initial diagnosis.

Case 2 was a 16-year-old male who presented with recurrent swelling on the left side of the neck. First, he was treated with antibiotic therapy for an upper respiratory tract infection. After 7 months, a diagnosis of viral infection was made, without specific treatment. Because of persistent lymph node enlargement, an excisional lymph node biopsy was performed. The lymph node was 60 mm in diameter, and a diagnosis of BL with a granulomatous reaction was made. The patient had no signs of other lymphadenopathies, splenomegaly, or hepatomegaly. The levels of lactate dehydrogenase (LDH) and  $\beta$ 2-microglobulin were normal. A CT-PET scan showed no evidence of disease, and the bone marrow biopsy was also negative. The patient refused multi-agent chemotherapy. After 4 years, he was in complete remission without any treatment.

Case 3 was a 47-year-old female who presented with cervical swelling for 1 month without B symptoms. A computed tomography (CT) scan showed a 33 × 24-mm lymphadenopathy next to the left parotid. Peripheral blood and biochemical parameters were normal, except for LDH: 512 U/l (range, 225–450 U/l). The left submandibular lymph node was excised for further investigation, and a diagnosis of BL with granulomatous reaction was proposed. Multi-agent chemotherapy was initiated. After three cycles of chemotherapy, the patient was in complete

remission, and after 2 years of follow-up he showed no evidence of disease.

Case 4 was a 12-year-old male from Kigoma, Tanzania. He was admitted to the local hospital for a swelling in the right lower jaw region that had persisted for >2 months. Prior to the swelling, there was a history of trauma followed by mobility of the lower jaw and regional pain. After tooth extraction, there was no reduction in the symptoms and there was a further increase in the swelling. The patient was sent to a reference centre for further management. The CT scan of the head showed features suggestive of BL in the right lower jaw region, mild right maxillary sinusitis, no evidence of cervical or mediastinal lymphadenopathy, and no evidence of brain involvement. Surgical enucleation and curettage of the tumour was performed. After six cycles of chemotherapy with rituximab, cyclophosphamide, oncovin (vincristine), doxorubicin, and methotrexate, the patient showed no residual disease and was discharged. After 16 months of follow-up, the patient was asymptomatic.

### MICROSCOPIC AND IMMUNOHISTOCHEMICAL FINDINGS

The morphological and immunophenotypic features of all four cases are summarised in Table 1. The common features of all the cases in the study were the presence of focal or diffuse infiltration by BL cells, and a prominent granulomatous reaction. All cases were EBV-positive with latency I.

In particular, in case 1, morphological examination of the surgical specimens revealed an overall preserved lymph node architecture characterised by follicular hyperplasia with reactive germinal centres (GCs), and prominent perisinusoidal and perifollicular clear areas composed of monocytoid B-lymphoid cells. Exclusively within the monocytoid B-lymphoid cell areas, nests of dark-appearing, atypical cells were occasionally present (Figure 1A). Some nests appeared to coalesce focally, forming wider ill-defined aggregates composed of medium-sized lymphoid cells with round nuclei, finely clumped chromatin, multiple small peripheral nucleoli, and small to moderate amounts of basophilic cytoplasm, morphologically consistent with BL cells (Figure 1B). Mitotic figures and apoptotic bodies were seen within the nests and focal ill-defined aggregates. In addition, a florid granulomatous reaction, sometimes encircling the neoplastic clusters of cells, was present (Figure 1B; haematoxylin and eosin- HE). The immunophenotype (CD20, CD10, bcl-6 and IgM positivity, bcl-2

**Table 1.** Clinical and immunophenotypic features

Case	Age (years)/sex	Location	Stage	Treatment	Prognosis	EBV	MYC protein expression	MYC translocation
Case 1	65/F	Right axillary lymph node	I	None	Healthy after 30 months of follow-up	IHC: EBNA1+ (LMP1-, LMP2-, EBNA2-, BZLF1-)	Yes (100%)	t(8;14) break-apart and fusion probes
Case 2: LYWS-353	26/M	Mandibular lymph node	I	None	Healthy after 48 months of follow-up	IHC: EBNA1+/BZLF1-	Yes (100%)	t(8;14) break-apart and fusion probes
Case 3: LYWS-360	47/F	Cervical lymph node	I	Three cycles of chemotherapy*	Healthy after 24 months of follow-up	IHC: EBNA1+/BZLF1-	Yes (100%)	t(8;14) break-apart and fusion probes
Case 4	12/M	Mandibular mass	I	Six cycles of chemotherapy*	Healthy after 16 months of follow-up	IHC: EBNA1+ (LMP1-, LMP2-, EBNA2-, BZLF1-)	Yes (100%)	t(8;14) break-apart and fusion probes

EBNA, Epstein-Barr nuclear antigen; EBV, Epstein-Barr virus; F, female; IHC, immunohistochemistry; LMP, latent membrane protein; LYWS, Lymphoma Workshop; M, male.

\*Rituximab plus hyperfractionated cyclophosphamide, vincristine, doxorubicin, and dexamethasone, followed by methotrexate and cytarabine.

negativity, a high Ki67 proliferative index of >95%) (Figure 2A–D; Table 1), MYC protein expression (Figure 2E), and cytogenetics (MYC translocation as shown with both dual fusion and a BAP; Figure 2E, inset) were consistent with BL (Table 1). The tumour cells were also EBV-positive as shown by EBER *in-situ* hybridisation (Figure 2F). Immunohistochemistry (IHC) revealed only the expression of EBNA1 among EBV latency proteins, whereas latent membrane protein 1 (LMP1), latent membrane protein (LMP2), EBNA2 and BZLF1 were negative (Table 1). Therefore, the diagnosis of focal involvement by EBV+ BL in a background of reactive lymphadenitis was made.

Cases 2, 3 and 4 (Figure 3) showed a clearly effaced lymph node architecture with the presence of an overt BL with a florid granulomatous reaction, in contrast to the limited and interfollicular pattern found in case 1.

Moreover, case 2 was characterised by the presence of patchy BL cells intermingled with histiocytes, fibroblasts, and abundant collagen deposition. On the other hand, case 3 showed extensive necrotic areas with conspicuous foci of apoptotic debris.

#### TME FEATURES

Analysis of TME in all four cases showed comparable characteristics. Overall, in all four cases, analysis of the macrophages encircling the tumour areas by the use of mIHC showed a prevalence of M1 macrophages, defined as CD68+/CD163-/c-Maf- cells, accounting for 80–95% of the total macrophages, whereas M2 macrophages (CD68+/CD163+/c-Maf+) were scarce (5–20%) (Figure 4A,B; Table 2). In the reactive lymph nodes, the plasticity of M1 and M2 may be more active in controlling the immune responses to different antigens.<sup>26,27</sup> Most of the macrophages in GCs are M2, and this is possibly the reason for the high number of M2 macrophages that we found in reactive lymph nodes (personal communication of C. Tripodo, Human Pathology Section, Department of Health Sciences, University of Palermo; Figure S1).

The pSTAT1/CD68/CD123 triple staining highlighted that macrophages (CD68+) express nuclear pSTAT1, indicating IFN- $\gamma$  priming and confirming an M1 phenotype of the macrophages (Figure 4D,E; Table 2). The proportion of IFN- $\gamma$ -primed macrophages (CD68+/pSTAT1+) ranged from 35% to 75% of the total CD68+ cells, in contrast to the considerably lower proportion detected in the controls (<5%). In addition, pSTAT1 nuclear staining was also found in scattered and small clusters of CD123+ cells, in the

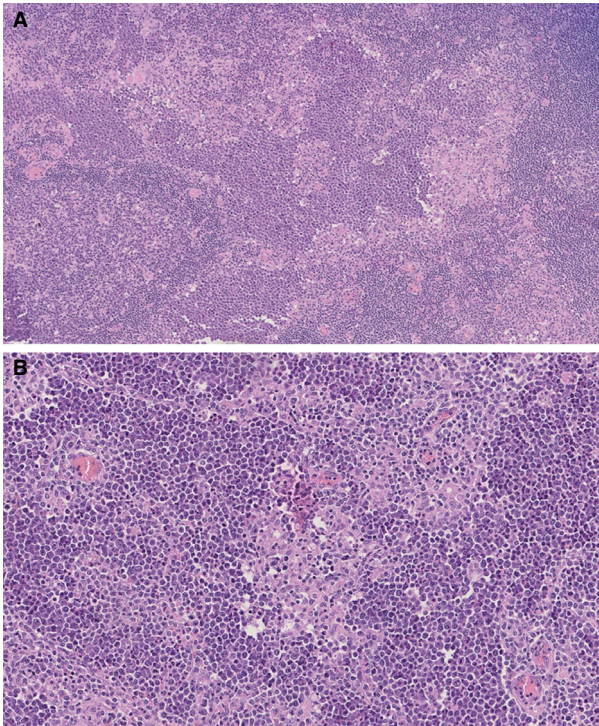


**Figure 1.** Morphology of case 1. **A**, Nests of dark-appearing atypical cells were occasionally present in the marginal zone of the otherwise reactive lymph node. **B**, Small to medium-sized lymphoid cells with round nuclei, finely clumped chromatin, multiple small peripheral nucleoli, surrounded by a granulomatous epithelioid reaction.

proximity of granulomas, possibly representing activated pDCs, and ranging from 15% to 35% (Figure 4A,B; Table 2). On the other hand, only a few CD123+/pSTAT1+ cells were found in the controls (<5%). In addition, the PD-L1/CD163/c-Maf panel showed that epithelioid granulomas were significantly positive for PD-L1, as a secondary effect of IFN- $\gamma$  activation (Figure S2). The dominant reactive lymphoid infiltrate was mostly composed of CD4+ T cells, ranging from 75% to 90% of the total CD4+ T cells. In particular, Th1 cells (CD4+/T-bet+ cells) were consistently represented, ranging from 20% to 35% of the total CD4+ T cells (Figure 5A; Table 2). Interestingly, Th1 lymphocytes were found in the immediate proximity of the granulomas, further underlining the cooperation between innate and adaptive immunity. In contrast, the tumour-free areas and the reactive lymph node control showed a scant or absent Th1 infiltrate (5–10%) (Figure S3A; Table 2). However, CD4/T-bet double staining revealed a subpopulation of CD4-/T-bet+ cells. Double staining with CD20 showed the B-cell origin of such cells, which more

probably represented a subset of monocytoid B cells, as previously reported by Jöhrens *et al.*<sup>26</sup> This finding was particularly evident in case 1, in which BL cells were nested in areas of florid monocytoid B-cell hyperplasia (Figure S4), but was also made in the other cases, maintaining the topographic correlation with the granulomas. Th2 cells (CD4+/GATA3+ cells) were also represented in the tumour areas, ranging from 10% to 25%. However, these values were lower than those in the reactive tissue (Figure S3B; Table 2). A few scattered cytotoxic CD8+ T cells (<5%; Table 2), Tregs (CD4+/CD25+/FOXP3+; <5%; Table 2) and NK cells (CD56+/CD57+; <5%; Table 2) were seen (not shown).

## Discussion

In this article, we report four cases of localised (stage I) EBV-positive BL with a prominent granulomatous reaction and a similar TME consisting of Th1 lymphocytes and M1 macrophages. The TME described above is quite different from that of conventional BL with the typical starry sky pattern, in which the most prominent component of TME is represented by M2 macrophages.<sup>23</sup> Such cases usually present with bulky disease and multiple localisation, and intensive chemotherapy is required. On the other hand, cases of BL with a florid granulomatous reaction typically present at an early stage of disease and have a particularly good prognosis, with some cases showing spontaneous regression.<sup>1–6</sup> Although a proinflammatory immune reaction may be responsible for the favourable outcome, thorough characterisation of the reactive infiltrate in these cases was lacking. Using mIHC, we have now shown that the TME has features of an activated cellular immune response characterised by the prevalence of Th1 lymphocytes and M1 macrophages forming granulomas enclosing neoplastic cells. Th1 lymphocytes are well-known IFN- $\gamma$ -secreting cells that activate inflammatory pathways mainly via macrophage polarisation towards an M1 functional status. In addition, they promote granuloma formation and inhibit Th2 lymphocyte proliferation (Figure 6).<sup>9,11</sup> Accordingly, the vast majority of macrophages were primed by IFN- $\gamma$ , as demonstrated by pSTAT1 nuclear positivity.<sup>9–10</sup> In addition, because of the dichotomous role of IFN- $\gamma$ , which activates both the immune innate response and on the checkpoint inhibitors, the positivity for PD-L1 in the granulomas' epithelioid macrophages may indicate, in our context, strong activation of the innate immune response.<sup>28,29</sup>

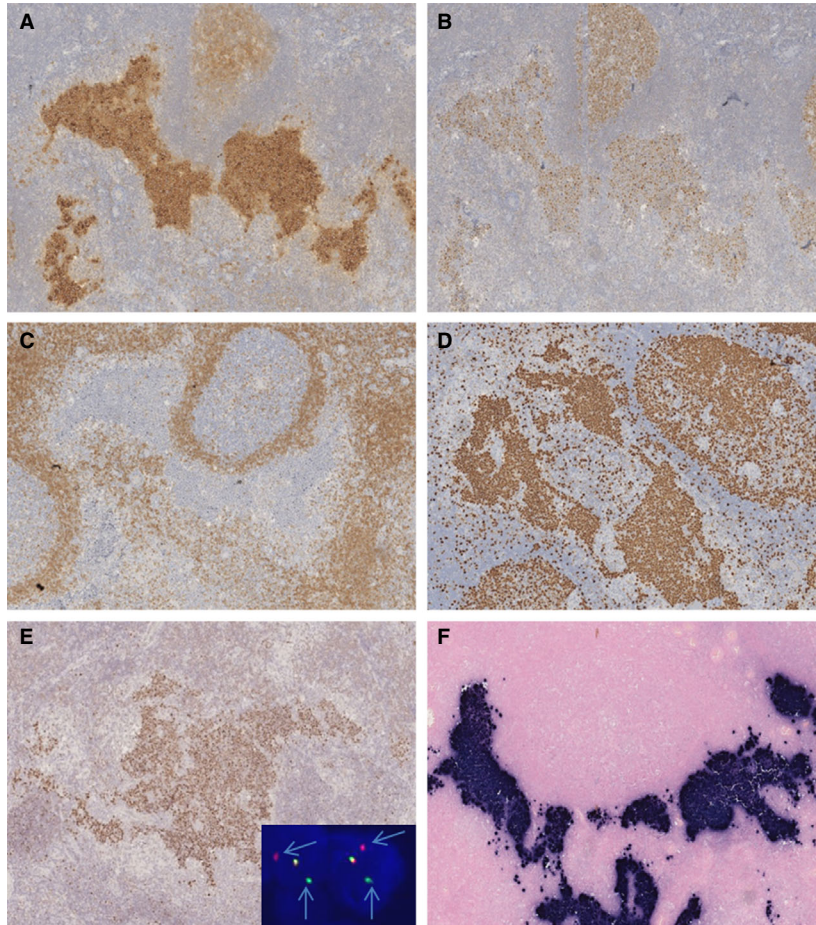


**Figure 2.** Immunophenotype of case 1. The immunophenotype of the atypical cells, i.e. CD10 positivity (A), bcl-6 positivity (B), bcl-2 negativity (C), a high Ki67 proliferation index of >95% (D), and MYC protein expression (E) and cytogenetics (*MYC* rearrangement as determined with break-apart probes; E, inset), was consistent with Burkitt lymphoma. These cells were also EBV-positive as determined with Epstein-Barr virus-encoded small RNA *in-situ* hybridisation (F).

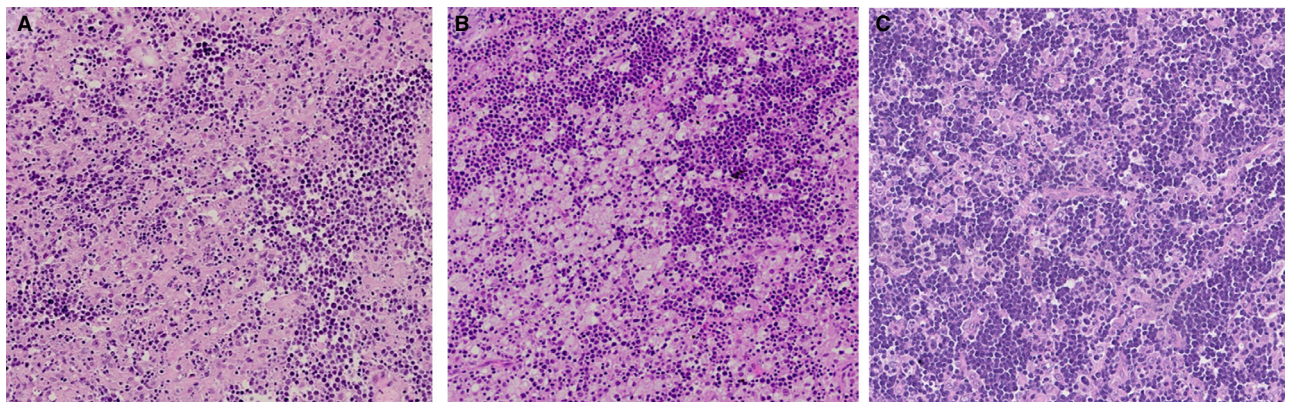


**Figure 3.** Morphological features of case 2, case 3, and case 4. There was a prominent granulomatous reaction, comprising epithelioid histiocytes and fibroblasts surrounding Burkitt lymphoma cells, in case 2 (A), case 3 (B), and case 4 (C). [Colour figure can be viewed at [wileyonlinelibrary.com](http://wileyonlinelibrary.com)]

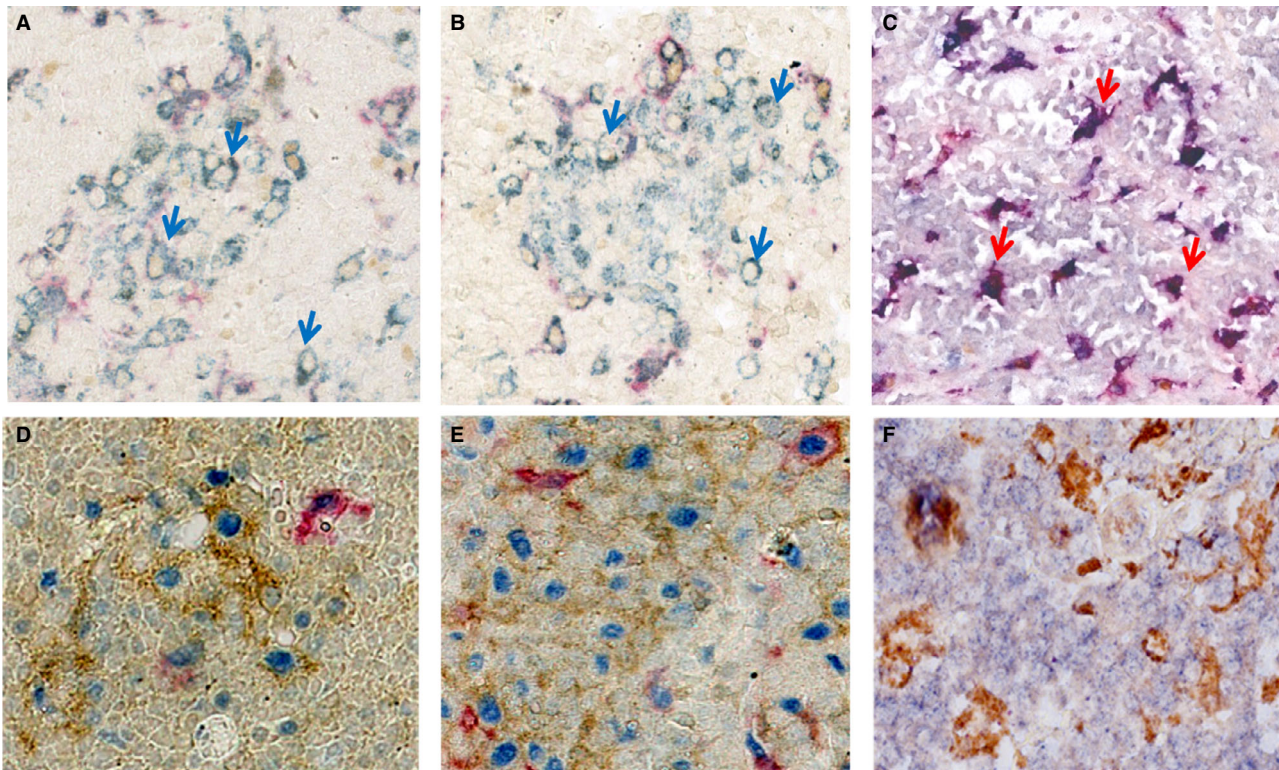


**Figure 4.** Immunohistochemical characterisation of macrophages. Triple staining was performed with c-Maf (brown), CD163 (red), CD68 (blue), phosphorylated signal transducer and activator 1 (pSTAT1) (blue), CD68 (brown), and CD123 (red). A high number of M1 (CD68+/CD163-/c-Maf-) macrophages (blue arrows) were seen in the granulomas surrounding the clusters of Burkitt cells in case 1 (A) and case 2 (B); in contrast, in the conventional Burkitt lymphoma (BL) case control (C), the predominant macrophage population was represented by M2 (CD68+/CD163+/c-Maf+) macrophages (red arrows). Interferon- $\gamma$ -primed macrophages and plasmacytoid dendritic cells expressed nuclear pSTAT1 in case 1 (D) and case 2 (E). On the other hand, only a few CD123+/pSTAT1+ cells were found in the conventional BL case control (F). [Colour figure can be viewed at [wileyonlinelibrary.com](http://wileyonlinelibrary.com)]

Another important observation in this study was the peculiar topographic distribution of the reactive inflammatory cells. In fact, Th1 lymphocytes, pDCs and M1 macrophages were detected in the immediate proximity of the BL cells. Intriguingly, we also observed numerous CD20+/T-bet+ cells, which more probably represented monocytoid B cells, around the clusters of BL cells.<sup>30</sup> There are recent data suggesting that T-bet is a central regulator of antiviral immunity in all lymphocyte lineages, and that T-bet+ B cells may represent an important component of ongoing immune responses during chronic viral infections.<sup>31</sup> Furthermore, our results are in accordance with previous observations that have underlined the role of EBNA1-specific CD4+ T cells in the regulation of the immune response in healthy carriers of EBV.<sup>17–21</sup> Our data may well represent an *in-vivo* picture of a T-bet-mediated immune response fostered by IFN- $\gamma$  and subsequent granuloma formation comprising M1 polarised

macrophages with an activated STAT1 signalling pathway.

We believe that the fractions of cells that we scored in our IHC experiments reflect specific Th states according to the expression of selected Th proteins. However, we need to consider a variety of states and transitions that may form part of the highly dynamic tumour-infiltrating T-cell landscape and that we are not taking into account. Besides Th1 and Th2, in addition Th0, Th17, Th9 and Th22 cells and other potentially relevant Th phenotypes could contribute to the overall Th infiltration of BL, such as bcl-6+ and/or c-Maf+ T follicular helper cells, which are variably represented among CD4+ T cells in lymphomas of the GC phenotype, or variants in regulatory subsets that may be aberrantly expanded in tumours, such as eomesodermin+/granzyme K+/type 1 regulatory-like CD4+ effectors.<sup>32</sup>

Therefore, our findings need to be confirmed in further studies using different methods that allow more

**Table 2.** Tumour microenvironment results

Cell populations	Case 1 (%)	Case 2 (%)	Case 3 (%)	Case 4 (%)	Control (%)
<b>Macrophages</b>					
M1 (CD68+/CD163-/c-Maf-)	95	85	90	80	25–35
M2 (CD68+/CD163+/c-Maf+)	5	15	10	20	55–70
<b>pSTAT1+ DCs</b>					
CD68+/pSTAT1+/CD123–	65	75	40	35	<5
CD68–/pSTAT1+/CD123+	35	20	15	15	<5
<b>T lymphocytes</b>					
CD4+	90	80	85	75	50–70
Th1 (TBX21+/CD4+)	35	20	30	25	5–10
Th2 (GATA3+/CD4+)	10	15	25	15	25–40
Tregs (CD25+/CD4+/FOXP3+)	<5	<5	<5	<5	5–15
Cytotoxic (CD8+)	15	20	15	25	30–40
<b>NK cells</b>					
CD56+/CD57+	<5	<5	<5	<5	<5

DC, dendritic cell; FOXP3, forkhead box P3; GATA3, GATA-binding protein 3; NK, natural killer; pSTAT1, phosphorylated signal transducer and activator 1; TBX21, T-box transcription factor 21.

comprehensive characterisation of the TME (e.g. gene expression analysis).

The interplay with the TME may be a crucial event for the outcome of EBV-related diseases, and the viral interaction with host immune surveillance requires further investigation in correlation with the EBV latency programme. It has been shown that the pattern of viral protein expression determines the immunogenicity of the infected cells.<sup>33,34</sup> The virus encodes eight antigenically distinct latent-cycle proteins, which show a marked hierarchy of immunodominance for the CD8+/CD4+ T-cell response. Epitopes derived from the EBNA3A, EBNA3B and EBNA3C family of proteins tend to induce the strongest responses across a range of different HLA class I alleles. LMP1-specific responses are extremely rare, whereas LMP2 is more frequently immunogenic but almost always induces low-frequency subdominant responses.<sup>35</sup> Although EBNA1 was initially supposed to mount an immunologically weak response, more recent studies demonstrated that healthy EBV carriers had an efficient CD4+ T cell response to this antigen that was mainly Th1 in nature.<sup>36,37</sup> On these grounds, conventional BLs with EBV latency I may show a different immune signature from those with a

heterogeneous latency programme characterised by the expression of LMP1, LMP2, and/or lytic genes (non-canonical latency programme).<sup>23,38,39</sup> Indeed, all of the cases reported here showed a latency I programme, with the sole expression of EBNA1.

A further observation of this study concerned the distinctive morphological features of case 1. In fact, in this case the nests of BL cells were found exclusively within prominent areas of clear cells identified as monocytoid B cells, which might represent a possible niche from which BL cells originate and spread, as has been previously reported for Hodgkin's lymphoma.<sup>40,41</sup> Although there is consensus that BL is related to GC B lymphocytes, it has been hypothesised that EBV-positive BL cases may derive from a later developmental stage of B cells, i.e. post-GC/memory B cells.<sup>42,43</sup> This is in line with the fact that, in healthy carriers, EBV resides in memory B cells that re-enter the GC reaction following antigenic stimulation.<sup>44–46</sup> Only one case with similar features has been recently reported in the literature, in a human immunodeficiency virus (HIV)-positive female,<sup>47</sup> and was reported as 'Burkitt microlymphoma'. We have also observed a similar case in an HIV-positive patient (Figure S5). Both cases developed overt BL with an

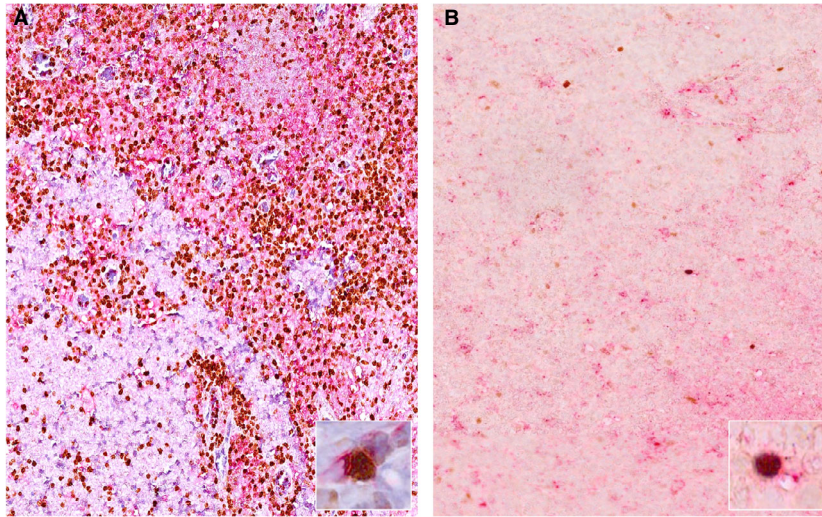


**Figure 5.** Characterisation of a Th1 infiltrate with CD4/T-box protein expressed in T cells (T-bet) double staining (CD4, red; T-bet, brown). A reactive lymphoid infiltrate, mostly composed of CD4+ T cells, in particular Th1 cells (CD4+/T-bet+), is shown; this was found in the immediate proximity of the granulomas in case 1 (A,A inset: higher-magnification double-positive stains); on the other hand, only a few scattered Th1 cells were detected in the conventional Burkitt lymphoma case control (B,B inset). [Colour figure can be viewed at [wileyonlinelibrary.com](http://wileyonlinelibrary.com)]

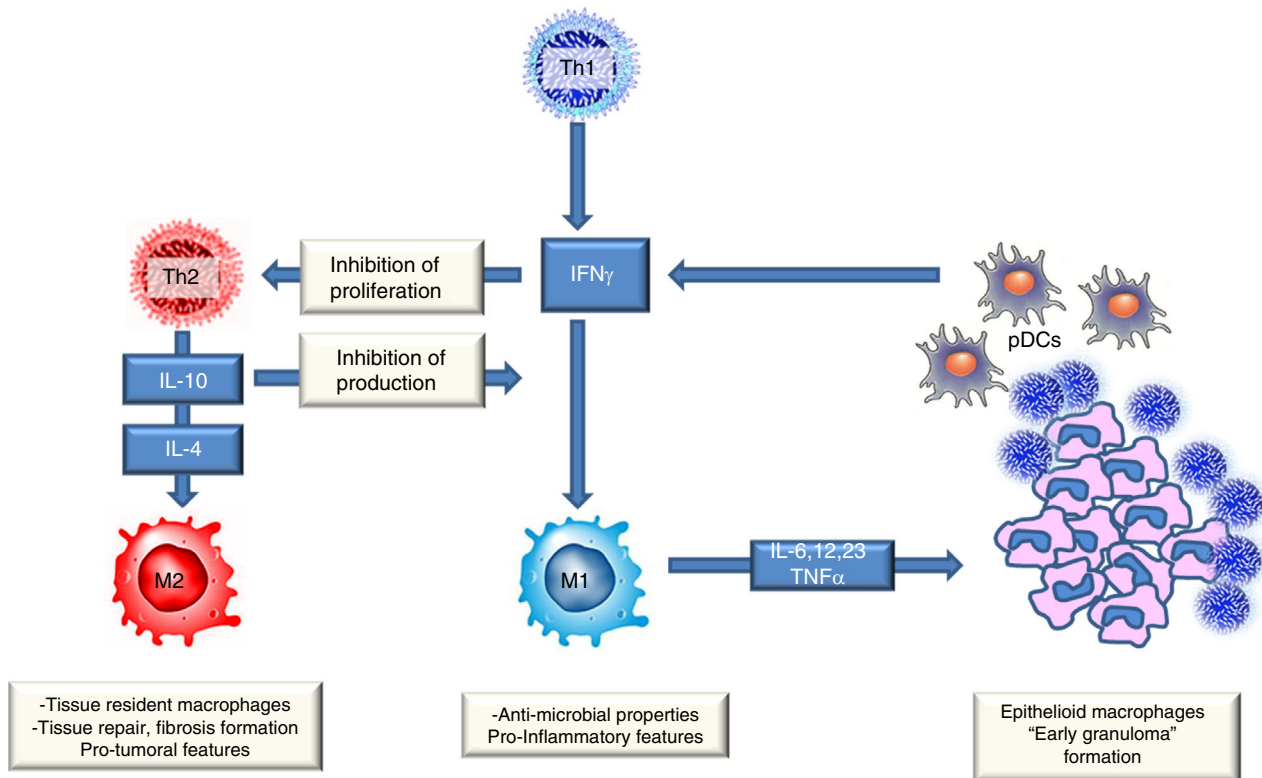


**Figure 6.** The role of Th1 lymphocytes. Th1 lymphocytes are well-known interferon- $\gamma$ -secreting cells that activate inflammatory pathways, mainly via macrophage polarisation towards an M1 functional status. In addition, they promote granuloma formation and inhibit Th2 lymphocyte proliferation. [Colour figure can be viewed at [wileyonlinelibrary.com](http://wileyonlinelibrary.com)]



unfavourable outcome shortly after the diagnosis, whereas the case reported here occurred in an immunocompetent host, and was characterised by a granulomatous reaction and spontaneous regression, possibly representing an early phase of BL.

BL in the setting of a granulomatous reaction and conspicuous monocytoid B-cell hyperplasia might be easily overlooked, and making the correct diagnosis may be challenging.<sup>6</sup> Awareness of these features is important to avoid misdiagnosis. Our study provides, for the first time, an *in-vivo* picture of the immune surveillance of BL with a granulomatous reaction that might explain why an aggressive lymphoma is kept in check and behaves in such a self-limiting way. In contrast to conventional BL, the important role of Th1 and M1 macrophages in the TME is highlighted. In addition, the recognition of TME features of BL may be helpful for identifying a subset of BL patients with a better prognosis, and who are thus suitable for less burdensome therapy. Further studies are warranted to investigate the reason why similar tumour cells trigger different immune responses.

In addition, our data may provide the rationale for new potential therapeutic avenues to explore in EBV-positive BL patients in the era of immunotherapy, and in particular adoptive T-cell therapy with EBNA1-specific Th1 cells.<sup>48,49</sup>

### Conflicts of interest

The authors declare that they have no conflicts of interest.

### Compliance with ethical standards

All procedures performed in studies involving human participants were in accordance with the ethical standards of the institutional research committee and with the 1964 Helsinki declaration and its later amendments or comparable ethical standards. This was a non-interventional study on archived tissue samples.

### Author contributions

R. Santi, F. Vergoni, D. Di Stefano, B. Puccini, E. Sabattini, C. Agostinelli, N. Bassüllü, T. Tecimer, A. S. Demiroz, L. Mnango, and S. Dirnhofer: provided tumour samples and clinical data. A. Akarca, E. Sorrentino, R. Guazzo, and L. Mundo: performed IHC and cytogenetic analysis. M. Granai, S. Lazzi, V.

Mancini, R. Santi, F. Vergoni, G. Cevenini, C. Tripodo, G. Di Stefano, M. Ponzoni, E. Sabattini, C. Agostinelli, S. Dirnhofer, T. Marafioti, L. Quintanilla-Martinez, F. Fend, and L. Leoncini: analysed and interpreted the data. M. Granai, S. Lazzi, T. Marafioti, L. Quintanilla-Martinez, F. Fend, and L. Leoncini: designed and coordinated the study. M. Granai, S. Lazzi, L. Quintanilla-Martinez, F. Fend, and L. Leoncini: interpreted the data and wrote the manuscript.

### References

- Hollingsworth HC, Longo DL, Jaffe ES. Small Non-cleaved cell lymphoma associated with florid epithelioid granulomatous response. A clinicopathologic study of seven patients. *Am. J. Surg. Pathol.* 1993; 17: 51–59.
- Haralambieva E, Rosati S, van Noesel C *et al.* Florid granulomatous reaction in Epstein-Barr virus-positive non-endemic Burkitt lymphomas: report of four cases. *Am. J. Surg. Pathol.* 2004; 28: 379–383.
- Schrager JA, Pittaluga S, Raffeld M *et al.* Granulomatous reaction in Burkitt lymphoma: correlation with EBV positivity and clinical outcome. *Am. J. Surg. Pathol.* 2005; 29: 1115–1116.
- Janegová A, Janega P, Ilencíková D *et al.* Burkitt lymphoma with unusual granulomatous reaction. A case report. *Cesk. Patol.* 2011; 47: 19–22.
- Li JN, Gao LM, Wang WY *et al.* HIV-related Burkitt lymphoma with florid granulomatous reaction: an unusual case with good outcome. *Int. J. Clin. Exp. Pathol.* 2014; 7: 7049–7053.
- Swerdlow SH, Campo E, Harris NL *et al.* eds. *World Health Organization classification of tumours of haematopoietic and lymphoid tissues, 4th edn. revised.* Lyon: IARC Press, 2017.
- Rimsza L, Pittaluga S, Dirnhofer S *et al.* The clinicopathologic spectrum of mature aggressive B cell lymphomas. *Virchows Arch.* 2017; 471: 453–466.
- Mills CD, Kincaid K, Alt JM *et al.* M-1/M-2 macrophages and the Th1/Th2 paradigm. *J. Immunol.* 2000; 164: 6166–6173.
- Kidd P. Th1/Th2 balance: the hypothesis, its limitations, and implications for health and disease. *Altern. Med. Rev.* 2003; 8: 223–246.
- Kanhere A, Hertweck A, Bhatia U *et al.* T-bet and GATA3 orchestrate Th1 and Th2 differentiation through lineage-specific targeting of distal regulatory elements. *Nat. Commun.* 2012; 3: 1268.
- Wang N, Liang H, Zen K. Molecular mechanisms that influence the macrophage M1–M2 polarization balance. *Front. Immunol.* 2014; 5: 614.
- Buechler C, Ritter M, Orsó E *et al.* Regulation of scavenger receptor CD163 expression in human monocytes and macrophages by pro- and antiinflammatory stimuli. *J. Leukoc. Biol.* 2000; 67: 97–103.
- Barros MHM, Hauck F, Dreyer JH *et al.* Macrophage polarization: an immunohistochemical approach for identifying M1 and M2 macrophages. *PLoS One* 2013; 8: e80908.
- Blake N, Lee S, Redchenko I *et al.* Human CD8+ T cell responses to EBV EBNA1: HLA class I presentation of the (Gly-Ala)-containing protein requires exogenous processing. *Immunity* 1997; 7: 791–802.
- Levitaskaya J, Sharipo A, Leonchiks A *et al.* Inhibition of processing by internal repeat region of the Epstein-Barr virus nuclear antigen 1. *Nature* 1995; 375: 685–688.

16. Yi Y, Manoury B, Fahraeus R. Self-inhibition of synthesis and antigen presentation by Epstein-Barr virus-encoded EBNA1. *Science* 2003; **301**: 1371–1374.
17. Bickham K, Münz C, Tsang ML *et al.* EBNA1-specific CD4+ T cells in healthy carriers of Epstein-Barr virus are primarily Th1 in function. *J. Clin. Invest.* 2001; **107**: 121–130.
18. Khanna R, Burrows SR, Thomson SA *et al.* Class I processing-defective Burkitt's lymphoma cells are recognized efficiently by CD4+ EBV-specific CTLs. *J. Immunol.* 1997; **158**: 3619–3625.
19. Münz C, Bickham KL, Subklewe M *et al.* Human CD4+ T lymphocytes consistently respond to the latent Epstein-Barr virus nuclear antigen EBNA1. *J. Exp. Med.* 2000; **191**: 1649–1660.
20. Leen A, Meij P, Redchenko I *et al.* Differential immunogenicity of Epstein-Barr virus latent-cycle proteins for human CD4+ T-helper 1 responses. *J. Virol.* 2001; **75**: 8649–8659.
21. Paludan C, Bickham K, Nikiforow S *et al.* Epstein-Barr nuclear antigen 1-specific CD4(+) Th1 cells kill Burkitt's lymphoma cells. *J. Immunol.* 2002; **169**: 1593–1603.
22. Steele KE, Brown C. Multiplex immunohistochemistry for image analysis of tertiary lymphoid structures in cancer. *Methods Mol. Biol.* 2018; **1845**: 87–98.
23. Granai M, Mundo L, Akarca AU *et al.* Immune landscape in Burkitt lymphoma reveals M2-macrophage polarization and correlation between PD-L1 expression and non-canonical EBV latency program. *Infect. Agents Cancer* 2020; **15**: 28.
24. Granai M, Ambrosio MR, Akarca A *et al.* Role of Epstein-Barr virus in transformation of follicular lymphoma to diffuse large B-cell lymphoma: a case report and review of the literature. *Haematologica* 2019; **104**: e269–e273.
25. Rauch I, Müller M, Decker T. The regulation of inflammation by interferons and their STATs. *JAKSTAT* 2013; **2**: e23820.
26. Shapouri-Moghaddam A, Mohammadian S, Vazini H *et al.* Macrophage plasticity, polarization, and function in health and disease. *J. Cell. Physiol.* 2018; **233**: 6425–6440.
27. Liu Y-C, Zou X-B, Chai Y-F *et al.* Macrophage polarization in inflammatory diseases. *Int. J. Biol. Sci.* 2014; **10**: 520–529.
28. Hu X, Ivashkiv LB. Cross-regulation of signaling pathways by interferon- $\gamma$ : implications for immune responses and autoimmune diseases. *Immunity* 2009; **31**: 539–550.
29. Bellucci R, Martin A, Bommarito D *et al.* Interferon- $\gamma$ -induced activation of JAK1 and JAK2 suppresses tumor cell susceptibility to NK cells through upregulation of PD-L1 expression. *Oncoimmunology* 2015; **4**: e1008824.
30. Jöhrens K, Shimizu Y, Anagnostopoulos I *et al.* T-bet-positive and IRTA1-positive monocytoid B cells differ from marginal zone B cells and epithelial-associated B cells in their antigen profile and topographical distribution. *Haematologica* 2005; **90**: 1070–1077.
31. Barnett BE, Staupe RP, Odorizzi PM *et al.* Cutting edge: B cell-intrinsic T-bet expression is required to control chronic viral infection. *J. Immunol.* 2016; **197**: 1017–1022.
32. Gruarin P, Maglie S, De Simone M *et al.* Eomesodermin controls a unique differentiation program in human IL-10 and IFN- $\gamma$  coproducing regulatory T cells. *Eur. J. Immunol.* 2019; **49**: 96–111.
33. Merlo A, Turrini R, Dolcetti R *et al.* The interplay between Epstein-Barr virus and the immune system: a rationale for adoptive cell therapy of EBV-related disorders. *Haematologica* 2010; **95**: 1769–1777.
34. Parsons E, Otieno JA, Ong'echa JM *et al.* Regulatory T cells in endemic Burkitt lymphoma patients are associated with poor outcomes: a prospective, longitudinal study. *PLoS One* 2016; **11**: e0167841.
35. Woodberry T, Suscovich T, Henry L *et al.* Differential targeting and shifts in the immunodominance of Epstein-Barr virus-specific CD8 and CD4 T cell responses during acute and persistent infection. *J. Infect. Dis.* 2005; **192**: 1513–1524.
36. Wood VHJ, O'Neil JD, Wei W *et al.* Epstein-Barr virus-encoded EBNA1 regulates cellular gene transcription and modulates the STAT1 and TGF $\beta$  signaling pathways. *Oncogene* 2007; **26**: 4135–4147.
37. Heller KN, Upshaw J, Seyoum B *et al.* Distinct memory CD4+ T-cell subsets mediate immune recognition of Epstein Barr virus nuclear antigen 1 in healthy virus carriers. *Blood* 2007; **109**: 1138–1146.
38. Arvey A, Ojesina AI, Pedamallu CS *et al.* The tumor virus landscape of AIDS-related lymphomas. *Blood* 2015; **125**: e14–e22.
39. Abate F, Ambrosio MR, Mundo L *et al.* Distinct viral and mutational spectrum of endemic Burkitt lymphoma. *PLoS Pathog.* 2015; **11**: e1005158.
40. Mohrmann RL, Nathwani BN, Brynes RK *et al.* Hodgkin's disease occurring in monocytoid B-cell clusters. *Am. J. Clin. Pathol.* 1991; **95**: 802–808.
41. Plank L, Hansmann ML, Fischer R. Monocytoid B-cells occurring in Hodgkin's disease. *Virchows Arch.* 1994; **424**: 321–326.
42. Bellan C, Lazzi S, Hummel M *et al.* Immunoglobulin gene analysis reveals 2 distinct cells of origin for EBV-positive and EBV-negative Burkitt lymphomas. *Blood* 2005; **106**: 1031–1036.
43. Amato T, Abate F, Piccaluga P *et al.* Clonality analysis of immunoglobulin gene rearrangement by next-generation sequencing in endemic Burkitt lymphoma suggests antigen drive activation of BCR as opposed to sporadic Burkitt lymphoma. *Am. J. Clin. Pathol.* 2016; **145**: 116–127.
44. Onnis A, Navari M, Antonicelli G *et al.* Epstein-Barr nuclear antigen 1 induces expression of the cellular microRNA hsa-miR-127 and impairing B-cell differentiation in EBV-infected memory B cells. New insights into the pathogenesis of Burkitt lymphoma. *Blood Cancer J.* 2012; **2**: e84.
45. Robbiani D, Deroubaix S, Feldhahn N *et al.* Plasmodium infection promotes genomic instability and AID-dependent B cell lymphoma. *Cell* 2015; **162**: 727–737.
46. Ambrosio MR, Lo Bello G, Amato T *et al.* The cell of origin of Burkitt lymphoma: germinal centre or not germinal centre? *Histopathology* 2016; **69**: 885–886.
47. Park D, Ozkaya N, Hariharan A. Novel insights into the early histopathogenesis of immunodeficiency-associated Burkitt lymphoma: a case report of Burkitt microlymphoma arising within HIV lymphadenitis. *Histopathology* 2016; **69**: 516–521.
48. Feucht J, Opher K, Lang P *et al.* Adoptive T-cell therapy with hexon-specific Th1 cells as a treatment of refractory adenovirus infection after HSCT. *Blood* 2015; **125**: 1986–1994.
49. Icheva V, Kayser S, Wolff D *et al.* Adoptive transfer of Epstein-Barr virus (EBV) nuclear antigen 1-specific T cells as treatment for EBV reactivation and lymphoproliferative disorders after allogeneic stem-cell transplantation. *J. Clin. Oncol.* 2013; **31**: 39–48.

## Supporting Information

Additional Supporting Information may be found in the online version of this article:

**Data S1.** Supplementary materials and methods.

**Figure S1.** High number of M2 macrophages in a reactive lymph node.

**Figure S2.** Dichotomous role of IFN- $\gamma$ .

**Figure S3.** Th1 and Th2 expression in the controls.

**Figure S4.** Expression of T-bet in B cells.

**Figure S5.** Partial lymph node involvement by BL in an HIV-positive patient.

**Table S1.** Antibody characteristics.

**Table S2.** The individual scores of the observers and the agreement for all separate cell types.

RESEARCH ARTICLE

Open Access



# Immune landscape in Burkitt lymphoma reveals M2-macrophage polarization and correlation between PD-L1 expression and non-canonical EBV latency program

Massimo Granai<sup>1,2†</sup>, Lucia Mundo<sup>1†</sup>, Ayse U. Akarca<sup>3</sup>, Maria Chiara Siciliano<sup>1</sup>, Hasan Rizvi<sup>4</sup>, Virginia Mancini<sup>1</sup>, Noel Onyango<sup>5</sup>, Joshua Nyagol<sup>6</sup>, Nicholas Othieno Abinya<sup>5</sup>, Ibrahim Maha<sup>7</sup>, Sandra Margielewska<sup>8</sup>, Wenbin Wi<sup>8</sup>, Michele Bibas<sup>9</sup>, Pier Paolo Piccaluga<sup>10</sup>, Leticia Quintanilla-Martinez<sup>2</sup>, Falko Fend<sup>2</sup>, Stefano Lazzi<sup>1</sup>, Lorenzo Leoncini<sup>1\*</sup> and Teresa Marafioti<sup>11,3</sup>

## Abstract

**Background:** The Tumor Microenvironment (TME) is a complex milieu that is increasingly recognized as a key factor in multiple stages of disease progression and responses to therapy as well as escape from immune surveillance. However, the precise contribution of specific immune effector and immune suppressor components of the TME in Burkitt lymphoma (BL) remains poorly understood.

**Methods:** In this paper, we applied the computational algorithm CIBERSORT to Gene Expression Profiling (GEP) datasets of 40 BL samples to draw a map of immune and stromal components of TME. Furthermore, by multiple immunohistochemistry (IHC) and multispectral immunofluorescence (IF), we investigated the TME of additional series of 40 BL cases to evaluate the role of the Programmed Death-1 and Programmed Death Ligand-1 (PD-1/PD-L1) immune checkpoint axis.

**Results:** Our results indicate that M2 polarized macrophages are the most prominent TME component in BL. In addition, we investigated the correlation between PD-L1 and latent membrane protein-2A (LMP2A) expression on tumour cells, highlighting a subgroup of BL cases characterized by a non-canonical latency program of EBV with an activated PD-L1 pathway.

**Conclusion:** In conclusion, our study analysed the TME in BL and identified a tolerogenic immune signature highlighting new potential therapeutic targets.

**Keywords:** Burkitt lymphoma, Tumour microenvironment, EBV, PD-L1, Immunotherapy, Immune checkpoint

\* Correspondence: [lorenzo.leoncini@dbm.unisi.it](mailto:lorenzo.leoncini@dbm.unisi.it)

†Massimo Granai and Lucia Mundo contributed equally to this work.

<sup>1</sup>Department of Medical Biotechnology, University of Siena, Siena, Italy

Full list of author information is available at the end of the article



© The Author(s). 2020 **Open Access** This article is licensed under a Creative Commons Attribution 4.0 International License, which permits use, sharing, adaptation, distribution and reproduction in any medium or format, as long as you give appropriate credit to the original author(s) and the source, provide a link to the Creative Commons licence, and indicate if changes were made. The images or other third party material in this article are included in the article's Creative Commons licence, unless indicated otherwise in a credit line to the material. If material is not included in the article's Creative Commons licence and your intended use is not permitted by statutory regulation or exceeds the permitted use, you will need to obtain permission directly from the copyright holder. To view a copy of this licence, visit <http://creativecommons.org/licenses/by/4.0/>. The Creative Commons Public Domain Dedication waiver (<http://creativecommons.org/publicdomain/zero/1.0/>) applies to the data made available in this article, unless otherwise stated in a credit line to the data.

## Background

Over recent years, the understanding of the biology of B-cell lymphomas has advanced significantly with the identification of the role played by the tumour micro-environment (TME) in lymphomagenesis [1, 2]. The TME of B-cell lymphomas mainly contains variable numbers of mesenchymal stem cells, immune cells and soluble factors. The complex interplay between tumour cells and TME regulates tumorigenesis and provides novel targets for immunotherapies [3, 4]. In aggressive lymphomas, particularly in BL, due to their high proliferation rate, intensive chemotherapy is required to counteract proliferation and dissemination of neoplastic cells. Unfortunately, these burdensome treatments are not as effective in elderly and immunocompromised patients [5]. Furthermore, in equatorial Africa, where BL is the most common childhood cancer, the prognosis of BL is still poor because the intensive therapeutic regimens often result in a severe neutropenia, with fatal consequences in resource poor settings [6–10]. Shortcomings of current BL therapies make the exploration of new therapeutic avenues a substantial and reasonable aim [7]. Therefore, a proper characterization of the TME in BL might be helpful to identify alternative therapeutic targets.

One of the histological hallmarks of BL is the high content of tumour-associated macrophages (TAMs) involved in apoptotic tumour cell clearance that confer the so-called starry-sky appearance [11]. Although little is known about the functional status of macrophages and their impact on tumour immune response in BL, TAMs may function as potential mediator of tumour progression through secretion of chemokines, cytokines and expression of immune checkpoint-associated proteins as PD-L1 [12, 13].

The expression of PD-L1 in B-cell lymphoma remains controversial, especially in BL. Indeed, PD-L1 has been reported in 80% of BL cases (8 out of 10) by Majzner [14]. However, this result was not reproduced by others [15]. Moreover, the role of the antigenic signature of Epstein Barr virus (EBV) in modulating the tumour microenvironment and the expression of immune-tolerant proteins has not been analysed in any of these studies. These different and somehow discordant results may be due to the diverse latency program of EBV infected cells and thus to different patterns of viral genes expression.

The constitutive association between EBV and BL, especially with endemic Burkitt lymphoma raises questions regarding the role of the virus in altering and actively shaping the tumour microenvironment [16–20]. Indeed, EBV orchestrates a variety of complex mechanism favouring the escape of lymphoma cells from anti-tumour immune responses while promoting the creation

of niches in which tumour cells may find support for their growth and survival [19–22].

Computational methods such as GEP deconvolution allow high sensitivity discrimination of cell subsets within complex tissues, as tumours [23]. These approaches provide quantitative/ functional information also on rare tumour-infiltrating elements, offering the unprecedented opportunity of reanalysing available genomic data and identifying the immune signature. Here, we applied the computational algorithm CIBERSORT to GEP datasets of 40 BL samples previously published by our group [24], including endemic BL (eBL), sporadic BL (sBL) and immunodeficiency associated BL (idBL) cases, to draw a map of immune and stromal components of TME. Finally, in order to validate GEP preliminary data, we applied multiplex immunohistochemistry to an additional cohort of 24 cases. These results were further supported by Vectra analysis of additional 16 BL by immunofluorescence. Thus, a total of 80 BL cases were included in the study.

In addition, we investigated the PD-1/PD-L1 pathway activation status and the contribution of EBV in PD-L1 induction as alternative mechanism responsible for immune evasion.

## Methods

### CIBERSORT and gene set enrichment analyses

A CIBERSORT-based deconvolution of GEP datasets (GSE26673) from 40 BL samples (13 eBLs, 21 sBLs, 6 idBLs; discovery cohort), previously published [24], was carried out using a 547-gene signature matrix customized for characterizing tissue sample immune cell composition, according to CIBERSORT instructions (<https://cibersort.stanford.edu/>) [23]. Briefly, normalized gene expression data were used to infer the relative proportions of 22 types of infiltrating immune cells while gene expression datasets were prepared using standard annotation files and data uploaded to the CIBERSORT web portal (<http://cibersort.stanford.edu/>), with the algorithm run using the default signature matrix at 1000 permutations. Gene set enrichment analysis (GSEA) was run on GSE26673.

### Multiplex immunohistochemistry

Multiplex immunohistochemistry was performed on 24 FFPE BL cases (12 eBL, 8 sBL and 4 idBL; validation cohort 1) which were retrieved from the Departments of Histopathology, University College Hospital, London (UK); Medical Biotechnologies, University of Siena, Siena (Italy); University of Nairobi, Nairobi (Kenya) and Istituto Lazzaro Spallanzani, Rome (Italy). The diagnosis of BL was issued by expert hematopathologists following the criteria described in the revised 4th edition of World Health Organization classification of tumours of

Haematopoietic and Lymphoid Tissue [25]. Single immunohistochemistry for the diagnostic antibodies, for EBV antigens and EBV in situ hybridization was carried out on the Bond III Autostainer (Leica, Microsystems, Newcastle upon Tyne, UK) by following the manufacturer’s instructions.

By applying multiplex immunostaining (IHC), we investigated the simultaneous expression of: a) CD68 (Abcam, ab 955, 1:150) brown, CD-163 (Abcam, Ab87099, 1:100) red and C-Maf (Abcam, Ab243901, 1:150,) blue; b) PD-1 (Abcam, NAT105, 1:100) brown and CD8 (Leica Biosystem,4B1, 1:200) red and Granzyme B (Abcam134933, marker for T- cell activation) blue c) PD-L1 (ab238697, Abcam, 1:100) brown, CD-163 (Abcam, Ab87099, 1:100) red and MYC (Abcam, Ab32072, Y69 clone, 1:150) in blue;. The triple immunostaining was assessed as previously described [26]. The colour assignment and staining location are: a) PD-L1 brown/membranous; CD-163 red/membranous; C-MYC blue/nuclear b) PD-L1, brown/membranous; CD163 red/membranous; C-Maf blue/nuclear; c) PD-1 brown/membranous; CD8 red/membranous and Granzyme B blue/nuclear. Tissue sections from the same set of cases and without antibody/chromogens were used as negative control.

The percentage of each cell population characterized by multiplex immunostaining was calculated by counting the individual cell types in 10 hpf using a 40x objective (NIKON Eclipse E400).

**Multiplex immunofluorescence staining**

Multiplex immunofluorescence (mIF) was carried out on 16 formalin fixed paraffin embedded (FFPE) endemic BL cases (validation cohort 2), belonging to set of samples previously studied and well characterized for EBV latency program [27].

Multiplex IF was applied to simultaneously detect the expression of: a) CD68 (Abcam, ab 955, 1:150) and CD163 (Leica Biosystem, 10D6, 1:200); b) PD-L1 (Dako, clone 22C3, 1:100) and CD163 (Leica Biosystem, 10D6, 1:200); c) PD-L1 and EBV-LMP2A

(Abcam, clone 15F9, ab59028, 1:200). These double stainings use red and green or magenta and green chromogens. The colour assignment and staining location are: a) CD68 red/membranous; CD163 green/membranous; b) PD-L1, green/membranous and CD163, pink/membranous or PD-L1, green/membranous and CD163, red/membranous; c) PD-L1, red; LMP2A green/ membranous. The staining procedure was established according to previously published work [28]. Tissue sections from the same set of cases and without antibody/fluorophore were used as negative control. Multiplex IF staining reaction and image analysis (including quantification of antibodies expression) were performed using the Vectra 2.0 system (PerkinElmer, Waltham, MA) and Tissue FAXSFluo slide scanning system (TissueGnostics, Vienna Austria) based on a Zeiss Axio Imager Z2 upright epifluorescence microscope.

**Results**

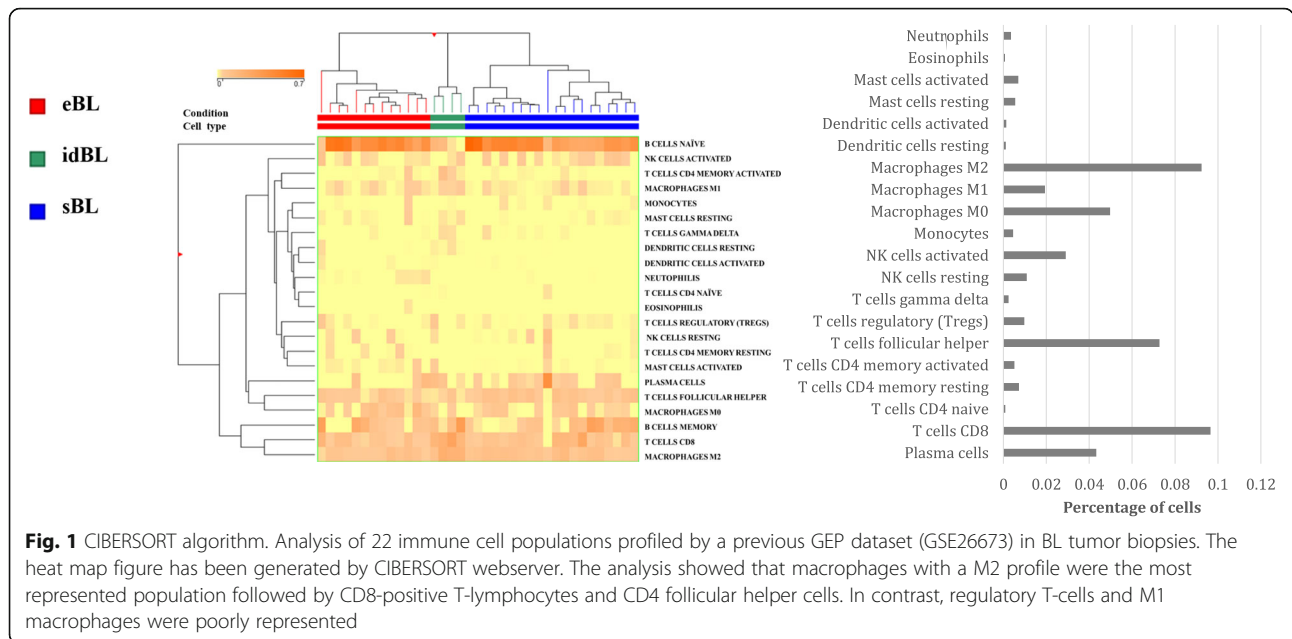
**EBV status**

EBV status and the viral proteins expression in all the study cases are reported in Table 1. In particular, in the discovery cohort EBV was positive in all of the eBL, in 6 out of 21 sBL and in 5 out of 6 idBL.

In the validation cohort 1, all of the eBL cases (12/12) were EBV positive, of which 10 expressed only EBNA1 by IHC while the remaining two were characterized by a non-canonical latency of EBV with the expression of both EBNA1 and LMP2A. Only two out of the 8 sBL cases were EBV positive showing a latency I expression pattern with the sole positivity of EBNA1. All of the idBL cases (4/4) were EBV positive and showed a latency of type I. In the validation cohort 2, all the eBL cases were EBV positive, with 11 out of 16 cases showing an EBV type I latency, while the remaining 5 cases exhibited a non-canonical EBV latency consisting of EBNA1 and LMP1 expression in one case and EBNA1 and LMP2A in the other 4.

**Table 1** EBV status and the viral protein expression. Note: NA stands for not available

		EBER/EBNA1+	EBNA1+/LMP1+	EBNA1+/LMP2A+	EBNA1+/LMP1+/LMP2A+	EBV-	Total
Discovery cohort	<b>eBL</b>	13	NA	NA	NA	–	13
	<b>sBL</b>	6	NA	NA	NA	15	21
	<b>idBL</b>	5	NA	NA	NA	1	6
Validation cohort 1 (mIHC)	<b>eBL</b>	10	–	2	–	–	12
	<b>sBL</b>	2	–	–	–	6	8
	<b>idBL</b>	4	–	–	–	–	4
Validation cohort 2 (mIF)	<b>eBL</b>	11	1	4	–	–	16
		51	1	6	–	22	80



**CIBERSORT identifies M2-polarized macrophages as the most representative TME component in BL**

The computational algorithm CIBERSORT to GEP datasets from BL samples revealed a heterogeneous reactive milieu with slight differences in tumour microenvironment among the three BL subtypes (eBL, sBL and idBL), most likely reflecting their underlying immunological status. The analysis showed that macrophages with a M2 profile were the most represented population followed by CD8-positive T-lymphocytes and CD4 follicular T-helper cells. In contrast, regulatory T-cells and M1 macrophages were poorly represented (Fig. 1).

**Multiplex IHC showed M2 macrophage polarization, cytotoxic T cells exhaustion and PD-L1 expression in Burkitt lymphoma cells**

The analysis confirmed a shift towards M2 phenotype (CD68 + CD163+/c-maf +) in all BL cases of validation cohort 1 ranging from 60 to 80% of total TAMs (Table 2, Fig. 2a). In particular, the evaluation of M1 macrophages, defined by CD68+, CD163-, c-maf- cells showed very similar values among the series ranging from 20 to

40% of total TAMs. CD8/ PD1/ Granzyme B staining highlighted that the vast majority of CD8+ T cells co-expressed PD-1 ranging from 60 to 80 and 50% to 70% of total tumor infiltrating cytotoxic T cells for eBL and idBL respectively (insert Fig. 2a; Table 2). Interestingly, sBL cases, in which EBV was negative to a greater extent (6 out of 8 cases) showed a markedly lower PD1 expression on CD8 positive T cells (from 35 to 50% of total CD8+ cells; Table 2).

The vast majority of TAMs in eBL and idBL cases expressed PD-L1 ranging from 65 to 80% and from 55 to 75% (Fig. 2b, Table 2). Interestingly, PD-L1 expression on TAMs in sBL showed lower values (from 20 to 40%; Table 2). In addition, C-Myc/PD- L1/CD163 triple staining also disclosed clusters of MYC/PD-L1 double positive cells in 2 eBL cases characterized by expression of LMP2A. PD-L1 expression in these cases was focal and heterogeneous with a degree of intensity from weak to strong in 10–30% of the total tumor cells, clustering with TAMs (Fig. 2b). The co-expression of PD-L1 and LMP2A in scattered neoplastic cells was then confirmed by double IF (insert Fig. 2b), identifying a possible

**Table 2** miHC for TAMs and PD-L1 expression on 24 BL samples (validation cohort 2) stained for PD-L1, CD68, CD163 and c-maf; miHC for cytotoxic T cells on 24 BL samples (validation cohort 2) stained for PD1, CD8 and granzyme B

miHC for PD-1/PD-L1 expression and macrophage polarization		eBL (n = 12)	sBL (n = 8)	iBL (n = 4)
TAM	M1 (CD68+/CD163-/c-maf-)	20–40%	30–40%	20–30%
	M2 (CD68+/CD163+/c-maf+)	60–80%	60–70%	70–80%
PD-L1	TAMs (PD-L1+/CD163+)	65–80%	20–40%	55–75%
	BL cells (MYC+/PD-L1+)	10–30%	0–10%	0–10%
Exhausted cytotoxic T cells	CD8+/PD1+/granzyme B-	60–80%	20–40%	60–80%

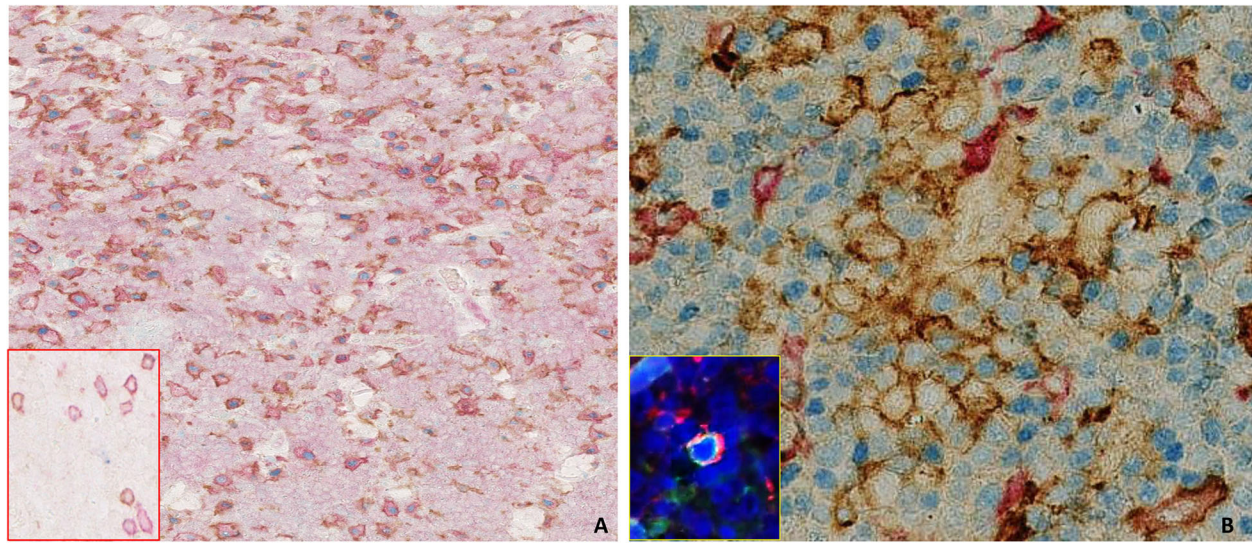


**Fig. 2** Macrophage polarization and PD-L1 expression on TAMs: **(a)** CD68 (brown), CD163 (red), c-maf (blue). The majority of TAMs express M2 phenotype markers (CD163+, c-maf+). (O.M: 10x). Inset: CD8 (red), Granzyme B (blue) and PD-1(brown), pattern of PD1 expression on cytotoxic T cells. **(b)** C-MYC (blue),PD-L1 (brown), CD163 (red); the majority of TAMs in eBL and idBL cases expressed PD-L1, in addition triple staining disclosed clusters of C-MYC/PD-L1 double positive cells in 2 cases characterized by co-expression of LMP2A (Inset double IF) clustering with TAMs (O.M: 40x)

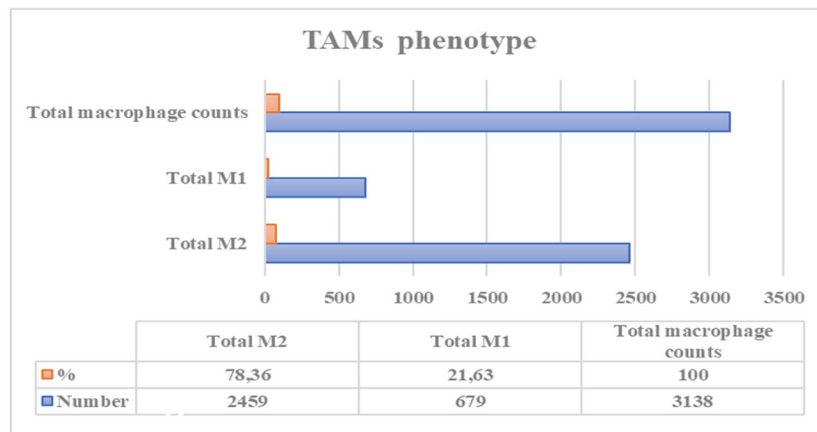
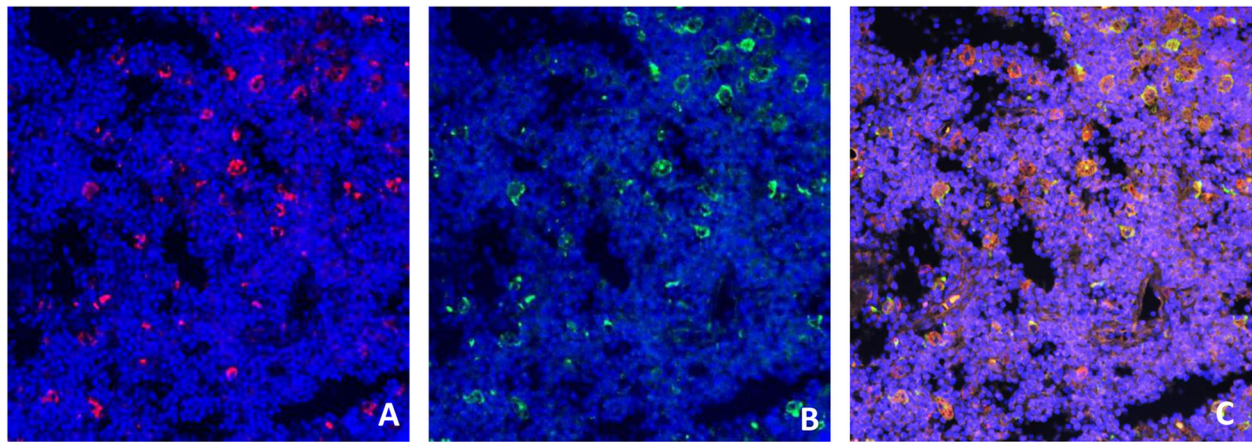


**Fig. 3** Immunofluorescence staining for Tumor-associated Macrophage Polarization in BL. **(a)** CD68 (red) **(b)** CD163 (green). Nuclei were stained with DAPI. **c** shows merge of A,B pictures. **(d)** Example of total macrophage count by Vectra analysis in one case



correlation between EBV and LMP2A in PD-L1 induction. Of note, EBV negative BL (6 out of 24 cases) and conventional BL cases with canonical EBV type I latency characterized by the sole expression of EBNA1 (16 out of 24 cases) showed low or absent PD-L1 positivity ranging from 0 to 10% of total tumor cells. These findings indicate that PD-L1 checkpoint activation is more likely related to an unusual latency program of EBV rather than to the EBV presence itself.

#### Multiplex immunofluorescence confirmed the prevalence of M2 macrophages and revealed a heterogeneous PD-L1 expression

Tissue samples were studied by mIF and analysed by VECTRA to quantify macrophages and PD-L1 expression on 16 BL samples (validation cohort 2) stained for PD-L1, CD68 and CD163.

In all the cases in validation cohort 2 the M2 macrophages were the most represented population ranging from 66 to 78% of total TAMs (Fig. 3), thus confirming the CIBERSORT and mIHC results. In addition, the vast majority of them were positive for PD-L1 with a range of expression from 35 to 70% of total macrophages (Fig. 4; Table 3).

#### Discussion

Although multiple studies have investigated TME and PD-L1 expression in B-cell lymphomas, only limited, small studies have been conducted in BL [14–16].

In the present study, we extensively evaluated the TME composition, activation status and expression of inhibitory immune checkpoints both on the inflammatory infiltrate and neoplastic cells of BL tumors including eBL, sBL and idBL cases. Thus, we investigated PD-L1 expression and the contribution of EBV in fostering the activation of the PD1-PD-L1 axis. The influence of the microenvironment on cell proliferation and destruction varies greatly according to the inherent histotype of the lymphoma cell type [29–31]. In particular, Hodgkin lymphoma (HL) tissue often consists of

relatively few monoclonal cancer cells but at least 90% non-malignant cells (e.g., regulatory T cells), contributing to a rather unique surrounding immune ecosystem. On the other hand, BL seems to be largely devoid of such a supportive cellular environment, although the high content of Tumor-Associated Macrophages (TAMs) might play a distinct, specific, important role in neoplastic progression through secretion of chemokines, cytokines and immune checkpoint-associated proteins as PD-L1 [12, 13].

In the recent decade a model has been developed to describe the complex mechanism of macrophage activation as a polarization towards two opposite states, namely M1 and M2, with pro-inflammatory and protumoral properties respectively [32–36]. TAM density in particular M2-TAMs have been associated with tumor progression and poor prognosis in DLBCL [37, 38].

In the present work, we identified a polarization towards a M2 phenotype of TAMs in all cases by applying three different approaches (CIBERSORT, mIHC and mIF) regardless of the subtype of BL, and thus, of EBV status.

These cells, intimately associated with the neoplastic cells, constituted also the major source of PD-L1, which may inhibit the overall inflammatory response and allow the neoplastic cells to evade antitumor immunity. However, the lower rate of PD-L1 expression on TAMs in sBL, as compared with eBL and idBL, which are frequently associated with EBV, may suggest a role of the virus in inducing PDL1 expression.

PD-L1 is a major regulator of T cell function and, after engaging PD-1, leads to an altered functional state of T-cells, namely T cell exhaustion [39]. In this regard, we found that in eBL and idBL the vast majority of the CD8+ infiltrating T cells expressed PD-1 highlighting an adaptive immune response resistance mechanism in such cases.

However, PD-L1 limits an antitumor immune response by signalling not only through PD-1 but also with another receptor, namely CD80 (also named B7-1), expressed on the surface of activated CD8+ T cells [40–42]. The

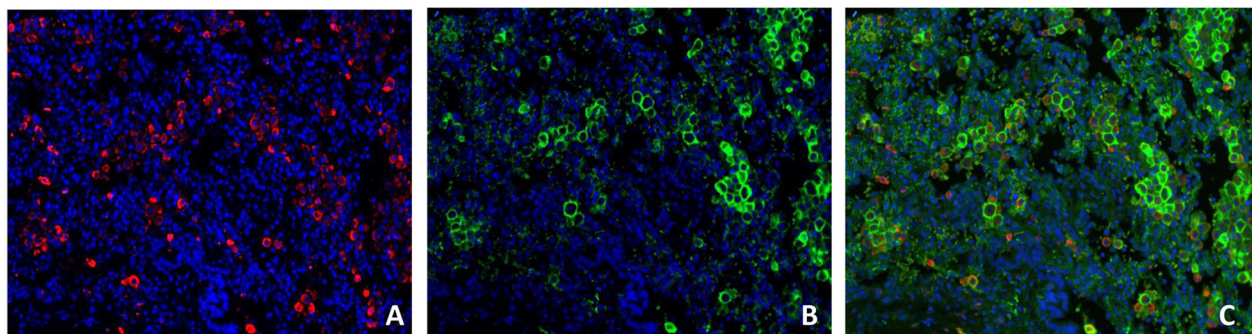


**Fig. 4** Immunofluorescence staining for PD-L1 and TAMs. **a** CD163 (red), **b** PDL-1 (green) merge **(c)**. The vast majority of TAMs exhibited M2 phenotype markers (CD163+) and expressed PD-L1 to a greater extent

**Table 3** mIF and VECTRA analysis of macrophages and PD-L1 expression on 16 BL samples (validation cohort 2) stained for PD-L1, CD68 and CD163

mIF	
Macrophage polarization and PD-L1 expression	n
M1	22–34%
M2	66–78%
n (%) PDL1 (+) CD163(+)	35–70%

influence of the PD-L1/PD-1 interaction on CD8+ T cell function has been extensively characterized and is known to limit CD8+ T cell responses by inhibiting TCR signaling, thus restricting CD8+ T cell survival, proliferation, and cytokine production. On the other hand, the role of the PD-L1/CD80 pathway on CD8+ T cell functions in BL is unknown, and thus, further studies are necessary.

In addition, the role of PD-1 expression in Tumor Infiltrating Lymphocytes (TILs) on both lymphoid and epithelial malignancies is controversial [38]. PD-1 expression in CD8+ cells has been associated with the selective suppression of cytotoxic lymphocytes in EBV positive nasopharyngeal carcinoma [43]. On the other hand, the PD-1+ TILs have also been described to lack Tim-3 expression in papilloma virus positive cancers, and thus possibly representing activated T-cells [44].

Emerging evidence in EBV-related malignancies indicates that the virus possesses the ability to actively shape the tumor microenvironment, and favours its escape from anti-tumor immune responses through a variety of complex mechanisms [18]. EBV may induce a strong up-regulation of PD-L1 expression both directly on the surface of human primary monocytes, or indirectly on neoplastic cells, through its viral proteins LMP-1 which interfere with downstream cellular signalling (i.e. AP1; JAK/STAT) [45, 46] to induce an immune tolerant niche for EBV-related tumors [47–49]. LMP-2 may also exert its tolerogenic effect by affecting crucial cell-cycle regulating pathways such as PI3K/Akt which plays a critical role in PD-L1 expression [50–52].

Although PD-L1 expression has been largely investigated in B cell lymphomas, the distinction of its expression in cellular microenvironment and/or in tumour cells has not been made in most studies [1–4].

Here we showed that EBV in BL might induce PD-L1 expression on tumor cells in a minority of cases characterized by a non-canonical latency with LMP2A positivity. On the other hand, it might influence PD-L1 upregulation on TAMs also in cases with canonical EBV latency I. However, the prevalence of M2 macrophages as primary constituent of the TME in BL is a constant finding in all BL subtypes and thus, macrophage polarization towards a pro-tumoral state seems an event related to the intrinsic characteristics of the tumor.

## Conclusions

In conclusion, although based on a small sample size, our findings may provide insights on BL TME and its underlying mechanisms of immune evasion. The cross-talk between different actors including TAMs, PD-1/PD-L1, T-cells, viral antigens and tumor cells may result in the failure of innate immunity in BL which results in M2 polarization. Despite the good response to conventional therapy of BL, our data may provide a rationale for new immunotherapeutic strategies.

## Abbreviations

TME: Tumor Microenvironment; BL: Burkitt lymphoma; GEP: Gene expression profiling; IHC: immunohistochemistry; IF: immunofluorescence; PD-1: Programmed Death-1; PD-L1: Programmed Death Ligand-1; LMP2A: Latent membrane protein 2A; LMP1: latent membrane protein 1; EBV: Epstein-Barr virus; TAM: Tumour associated macrophage; eBL: endemic Burkitt lymphoma; sBL: sporadic Burkitt lymphoma; idBL: immune deficiency Burkitt lymphoma; GSEA: Gene set enrichment analysis; FFPE: formalin fixed paraffin embedded; HL: Hodgkin lymphoma; DLBCL: Diffuse large B cell lymphoma

## Acknowledgements

Not applicable.

## Authors' contributions

MG, LL, TM, LM designed the study, analyzed the data, and drafted the manuscript. LM, AA, MCS, VM, HR, NJ, NO, NOA, IM, MS, MB provided the samples and performed the experiments, NOA, SL, PP, FF, LQ participated in the study design. FF and LQ revised the manuscript. All authors read and approved the final manuscript.

## Funding

Department of medical biotechnology of the University of Siena.

## Availability of data and materials

All data are available from the corresponding author.

## Ethics approval and consent to participate

All procedures performed in studies involving human participants were in accordance with the ethical standards of the institutional research committee and with the 1964 Helsinki declaration and its later amendments or comparable ethical standards. This was a non-interventional study on archived tissue samples.

## Consent for publication

Not applicable.

## Competing interests

The authors declare that they have no competing interests.

## Author details

- <sup>1</sup>Department of Medical Biotechnology, University of Siena, Siena, Italy.
- <sup>2</sup>University Hospital of Tübingen, Institute of Pathology, Tübingen, Germany.
- <sup>3</sup>Department of Pathology, University College London, London, UK.
- <sup>4</sup>Department of Cellular Pathology, Barts Health NHS Trust, London, UK.
- <sup>5</sup>Department of Clinical Medicine and Therapeutics, University of Nairobi, Nairobi, Kenya.
- <sup>6</sup>Department of Human Pathology, University of Nairobi, Nairobi, Kenya.
- <sup>7</sup>South Egypt Cancer Institute, Assiut University, Assiut, Egypt.
- <sup>8</sup>Institute of Immunology and Immunotherapy, University of Birmingham, Birmingham, UK and Durham University, Durham, UK.
- <sup>9</sup>Clinical Department, National Institute for Infectious Diseases "Lazzaro Spallanzani" I.R.C.C.S, Rome, Italy.
- <sup>10</sup>Department of Experimental, Diagnostic, and Specialty Medicine Bologna University Medical School, S. Orsola Malpighi Hospital, Bologna and Euro-Mediterranean Institute of Science and Technology (IEMEST), Palermo, Italy.
- <sup>11</sup>Department of Cellular Pathology, University College Hospital, London, London, UK.

Received: 10 March 2020 Accepted: 20 April 2020

Published online: 06 May 2020

## References

- Mulders TA, Björn EW. Targeting the immune microenvironment in lymphomas of B-cell origin: from biology to clinical application. *Cancers* (Basel). 2019;11:915.
- Scott DW, Gascoyne RD. The tumour microenvironment in B cell lymphomas. *Nat*. 2014;14:517–34.
- Xu B, Wang T. Intimate cross-talk between cancer cells and the tumor microenvironment of B-cell lymphomas: the key role of exosomes. *Tumor Biol*. 2017;39:1–12.
- Sin Yee Guna SY, Ling Lee SW. Targeting immune cells for cancer therapy. *Redox Biol*. 2019;25:101174.
- Ribrag V, Koscielny S. Rituximab and dose-dense chemotherapy for adults with Burkitt's lymphoma: a randomised, controlled, open-label, phase 3 trial. *Lancet*. 2016;387:2402–11.
- Ngoma T, Adde M. Treatment of Burkitt lymphoma in equatorial Africa using a simple three-drug combination followed by a salvage regimen for patients with persistent or recurrent disease. *Br J Haematol*. 2012;158:749–62.
- God JM, Haque A. Immune evasion by B-cell lymphoma. *J Clin Cell Immunol*. 2011;16:1–3.
- Gopal S, Gross TG. How I treat Burkitt lymphoma in children, adolescents, and young adults in sub-Saharan Africa. *Blood*. 2018;132:254–63.
- Bouda GC, Traorè F. Advanced Burkitt lymphoma in sub-Saharan Africa pediatric units: results of the third prospective multicenter study of the Groupe Franco-Africain d'Oncologie Pédiatrique. *J Glob Oncol*. 2019;5:1–9.
- Silva WFD, Garibaldi PMM. Outcomes of HIV-associated Burkitt lymphoma in Brazil: high treatment toxicity and refractoriness rates - a multicenter cohort study. *Leuk Res*. 2019;10:106287.
- Ford CA, Petrova S. Oncogenic properties of apoptotic tumor cells in aggressive B cell lymphoma. *Curr Biol*. 2015;25:577–88.
- Pham LV, Pogue E. The role of macrophage/B-cell interactions in the pathophysiology of B-cell lymphomas. *Front Oncol*. 2018;8:147.
- Kumar D, Xu ML. Microenvironment cell contribution to lymphoma immunity. *Front Oncol*. 2018;8:288.
- Majzner RG, Simon JS. Assessment of programmed death-ligand 1 expression and tumor-associated immune cells in pediatric cancer tissues. *Cancer*. 2017;123:3807–15.
- Chen BJ, Chapuy B. PD-L1 expression is characteristic of a subset of aggressive B-cell lymphomas and virus-associated malignancies. *Human Cancer Biology*. 2013;19:3462–73.
- Tan GW, Visser L. The microenvironment in Epstein-Barr virus-associated malignancies. *Pathogens*. 2018;7:40.
- Rowe M, Fitzsimmons L. Epstein-Barr virus and Burkitt lymphoma. *Chin J Cancer*. 2014;33:609–19.
- Dolcetti R. Cross-talk between Epstein-Barr virus and microenvironment in the pathogenesis of lymphomas. *Semin Cancer Biol*. 2015;34:58–69.
- Dojcinov, S.D.; Fend, F. EBV-positive Lymphoproliferations of B- T- and NK-cell derivation in non-Immunocompromised hosts. *Pathogens*. 2018;7:2–45.
- Linke-Serinsöz E, Fend F, Quintanilla-Martinez L. Human immunodeficiency virus (HIV) and Epstein-Barr virus (EBV) related lymphomas, pathology view point. *Semin Diagn Pathol*. 2017;34:352–63.
- Granai M, Ambrosio MR. Role of Epstein Barr virus in transformation of follicular lymphoma to diffuse large B-cell lymphoma: a case report and review of the literature. *Haematol*. 2019;104:269–73.
- Rivera-Soto R, Damania B. Modulation of Angiogenic processes by the human Gammaherpesviruses, Epstein-Barr Virus and Kaposi's Sarcoma-Associated Herpesvirus. *Front Microbiol*. 2019;10:1544.
- Chen B, Khodadoust MS. Profiling tumor infiltrating immune cells with CIBERSORT. *Methods Mol Biol*. 2018;1711:243–59.
- Piccaluga PP, De Falco G. Gene expression analysis uncovers similarity and differences among Burkitt lymphoma subtypes. *Blood*. 2011;117:3596–608.
- Swerdlow SH, Campo E. WHO classification of Tumours of Haematopoietic and lymphoid tissues. 4th ed. Lyon: IARC; 2008.
- Marafioti T, Paterson JC. The inducible T-cell co-stimulator molecule is expressed on subsets of T cells and is a new marker of lymphomas of T follicular helper cell-derivation. *Haematol*. 2010;95:432–9.
- Abate F, Ambrosio MR. Distinct viral and mutational Spectrum of endemic Burkitt lymphoma. *PLoS Pathog*. 2015;11.
- Parra ER, Uraoka N. Validation of multiplex immunofluorescence panels using multispectral microscopy for immune-profiling of formalin-fixed and paraffin-embedded human tumor tissues. *Sci Rep*. 2017;7:1–11.
- Fowler NH, Cheah CY. Role of the tumor microenvironment in mature B-cell lymphoid malignancies. *Haematol*. 2016;101:531–40.
- Shain KH, Dalton WS. The tumor microenvironment shapes hallmarks of mature B-cell malignancies. *Oncogene*. 2015;34:4673–82.
- Wang M, Zhao J. Role of tumor microenvironment in tumorigenesis. *J Cancer*. 2017;8:761–73.
- Xue J, Schmidt SV. Transcriptome-based network analysis reveals a Spectrum model of human macrophage activation. *Immunity*. 2014;40:274–88.
- Steidl C, Lee T. Tumor-associated macrophages and survival in classic Hodgkin's lymphoma. *N Engl J Med*. 2010;362:875–85.
- Li YL, Shi ZH. Tumor-associated macrophages predict prognosis in diffuse large B-cell lymphoma and correlation with peripheral absolute monocyte count. *BMC Cancer*. 2019;19:1049.
- Larionova I, Cherdynseva N. Interaction of tumor-associated macrophages and cancer chemotherapy. *Oncoimmunology*. 2019;8:1596004.
- Komohara Y, Niino D. Clinical significance of CD163+ tumor-associated macrophages in patients with adult T-cell leukemia / lymphoma. *Cancer Sci*. 2013;104:945–51.
- Bingle L, Brown NJ. The role of tumour associated macrophages in tumour progression: implications for new anticancer therapies. *J Pathol*. 2002;196:254–65.
- Nam SJ, Go H. An increase of M2 macrophages predicts poor prognosis in patients with diffuse large B-cell lymphoma treated with rituximab, cyclophosphamide, doxorubicin, vincristine and prednisone. *Leuk Lymphoma*. 2014;55:2466–76.
- Jiang Y, Li Y. T-cell exhaustion in the tumour microenvironment. *Cell Death Dis*. 2015;6:1–9.
- Butte MJ, Keir ME. Programmed death-1 ligand 1 interacts specifically with the B7-1 costimulatory molecule to inhibit T cell responses. *Immunity*. 2007; 27(1):111–22.
- Rollins MR, Gibbons Johnson RM. CD80 expressed by CD8(+) T cells contributes to PD-L1-induced apoptosis of activated CD8(+) T cells. *J Immunol Res*. 2017;2017:1–6.
- Cirone M, Lucania G. Human Herpesvirus 8 (HHV-8) inhibits monocyte differentiation into dendritic cells and impairs their Immunostimulatory activity. *Immunol Lett*. 2007;113(1):40–6.
- Larcharoensub N, Mahaprom K. Characterization of PD-L1 and PD-1 expression and CD8+ tumor-infiltrating lymphocyte in Epstein-Barr virus-associated nasopharyngeal carcinoma. *Am J Clin Oncol*. 2018;41:1204–10.
- Shayan G, Ferris RL. PD-1 blockade upregulate TIM-3 expression as a compensatory regulation of immune check point receptors in HNSCC TIL. *J Immunother Cancer*. 2015;3:196.
- Bi X, Wang H. PD-L1 is upregulated by EBV- driven LMP1 through NF-kB pathway and correlates with poor prognosis in natural killer /T-cell. *J Hematol Oncol*. 2016;9:109–21.
- Hudnall SD, Küppers R. Precision molecular pathology of Hodgkin lymphoma. 1st ed. PLOS Pathogens; 2018.
- Wasil LR, Tomaszewski MJ. The effect of Epstein-Barr virus latent membrane protein 2 expression on the kinetics of early B cell infection. *PLoS One*. 2013;8:1–14.
- Deb Pal A, Banerjee S. Epstein-Barr virus latent membrane protein 2A mediated activation of sonic hedgehog pathway induces HLA class Ia downregulation in gastric cancer cells. *Virology*. 2015;484:22–32.
- Rancan C, Schirmann L. Latent membrane protein LMP2A impairs recognition of EBV- infected cells by CD8+ T cells. *PLoS Pathog*. 2015;11:1–23.
- Yang L, Huang F. Posttranscriptional control of PD-L1 expression by 17β-estradiol via PI3K/Akt signaling pathway in ERα-positive Cancer cell LinesInternational journal of gynecologic. *Cancer*. 2017;27:196–205.
- Kristin J. Lastwika, Willie Wilson III, Control of PD-L1 Expression by Oncogenic Activation of the AKT-mTOR Pathway in Non-Small Cell Lung Cancer *Cancer Res* January 15 2016 (76) (2) 227–238;
- Gao Y, Yang J. IFN-γ-mediated inhibition of lung cancer correlates with PD-L1 expression and is regulated by PI3K-AKT signaling. *Int J Cancer*. 2018;143:931–43.

## Publisher's Note

Springer Nature remains neutral with regard to jurisdictional claims in published maps and institutional affiliations.

## Original Article

# Prognostic impact of tumor-associated macrophages, lymphocyte-to-monocyte and neutrophil-to-lymphocyte ratio in diffuse large B-cell lymphoma

Emanuele Cencini<sup>1</sup>, Alberto Fabbri<sup>1</sup>, Luana Schiattone<sup>1</sup>, Anna Sicuranza<sup>1</sup>, Bianca Mecacci<sup>1</sup>, Massimo Granai<sup>2</sup>, Virginia Mancini<sup>2</sup>, Stefano Lazzi<sup>2</sup>, Monica Bocchia<sup>1</sup>, Lorenzo Leoncini<sup>2</sup>

<sup>1</sup>Unit of Hematology, Azienda Ospedaliera Universitaria Senese & University of Siena, Siena, Italy; <sup>2</sup>Unit of Pathology, Department of Medical Biotechnologies, University of Siena, Siena, Italy

Received May 4, 2020; Accepted June 23, 2020; Epub August 25, 2020; Published August 30, 2020

**Abstract:** Introduction: Microenvironment has a prognostic influence in diffuse large B-cell lymphoma (DLBCL); among its components, tumor-associated macrophages (TAM) play a leading role. TAM can be classified into M1 (anti-tumor) and M2 (pro-tumor). Another prognostic factor could be represented by lymphocyte-to-monocyte and neutrophil-to-lymphocyte ratio (LMR and NLR). Objective: The aim of the study is to evaluate the prognostic impact of M1 and M2 TAM subtypes, LMR and NLR in DLBCL. Methods: We analyzed 37 consecutive patients between 2009 and 2013. Out of 37 patients, 28/37 (75.6%) received R-CHOP/CHOP-like regimens, 9/37 (24.4%) less intensive therapies. Immunohistochemistry was performed with antibodies against CD68 and CD163. We divided our cohort into 2 categories according to the Steidl score. TAM who coexpressed CD68 and CD163 were considered as M2. For LMR and NLR we used previously published cut-offs of 2.71 and 2.81. Results: CR rate was 70.3%; we did not record a significant correlation between CD68+ TAM, CD163+ TAM, CD68+/CD163+ TAM, LMR, NLR and CR. We observed a reduced PFS in patients with IPI  $\geq 2$  and high M2 TAM expression and a trend between higher expression of CD68+ TAM and improved PFS. Conclusion: M2 TAM could have a prognostic role for IPI  $\geq 2$  DLBCL patients receiving R-CHOP, which thus warrants further investigation.

**Keywords:** Diffuse large B-cell lymphoma, TAM, prognosis

## Introduction

Diffuse large B-cell lymphoma (DLBCL) is the most common subtype of non-Hodgkin lymphoma (NHL), characterized by aggressive behavior [1]. Anthracycline-based chemoimmunotherapy, such as rituximab, cyclophosphamide, doxorubicin, vincristine and prednisone (R-CHOP), can be curative in most cases; however, 20-40% of patients experience relapse or have refractory disease [1, 2]. International Prognostic Index (IPI) has been validated in the rituximab era, but it includes only clinical variables and it does not consider the well-known biological heterogeneity of the disease [3]. Cell-of-origin (COO), based on gene expression profiling (GEP) is relevant, dividing patients into 2 categories: germinal center B-cell-like (GCB, better prognosis) and activated B-cell-like (ABC, poor prognosis) [4]. Unfortunately, GEP is not

always available and the use of immunohistochemistry (IHC) algorithms, even if acceptable, has reproducibility issues and is not uniformly reported to have prognostic utility [4-6].

Previous GEP-based studies showed that the microenvironment has a prognostic influence in DLBCL. Stromal-1 signature, characterized by an elevated number of macrophages and genes expressed by components of extracellular matrix, is associated with good prognosis, while stromal-2 signature is characterized by increased angiogenesis and dismal outcome [7].

Tumor microenvironment includes macrophages, dendritic cells, T-helper, T-cytotoxic and reactive B-lymphoid cells; it could promote neoplastic cell survival and could be associated with drug resistance [8]. Among its cellular components, tumor-associated macrophages

(TAM) surely play a leading role. TAM are characterized by remarkable plasticity; depending on the stimuli that trigger their activation, they are polarized towards form M1, leading to antitumor responses, or M2, leading to tumor growth and progression [8-10].

The role of TAM in lymphoproliferative malignancies, such as Hodgkin lymphoma (HL) and DLBCL, has been analyzed with conflicting results, owing to a wide heterogeneity in the choice of TAM-associated markers, antibodies used for IHC and best cut-offs [11-14]. Some studies demonstrated that the content of TAM CD68+ was associated with improved survival in DLBCL, while an alteration of CD163/CD68 ratio, due to an increase in TAM CD163+ cell number, suggestive of M2 polarization, was correlated with poor prognosis [15-25].

Another prognostic tool should be represented by lymphopenia and increased neutrophils count (ANC), a surrogate marker of immunological dysfunction and chronic inflammation, respectively [26, 27]. It has been hypothesized that an absolute low lymphocyte count (ALC), together with neutrophilia, could correlate with an impaired immunological response against lymphoid malignancies [26-31]. Some studies observed a prognostic role of ALC, lymphocyte/monocyte ratio (LMR) and neutrophils/lymphocytes ratio (NLR) in DLBCL patients receiving R-CHOP [23, 32, 33]. According to this background, in this study we would like to evaluate the prognostic influence of M1 and M2 TAM subtypes, LMR and NLR in newly diagnosed DLBCL patients.

### Patients and methods

#### Patients

This retrospective study was based on a series of 37 newly diagnosed DLBCL patients managed at the divisions of Hematology and Pathology in Siena and requiring first-line treatment. The patients were recruited from March 2009 to August 2013. Inclusion criteria were: histopathological diagnosis made according to the WHO 2008 classification [34]; at least one evaluable lesion at baseline CT scan; adequate tumor tissues for IHC analysis; available follow-up records. Exclusion criteria were: HIV infection, transformed DLBCL, primary mediastinal DLBCL, primary central nervous system DLBCL,

primary cutaneous DLBCL. All procedures performed in studies were in accordance with the ethical standards of the institutional review board. All patients gave their written informed consent in accordance with the Declaration of Helsinki. At pre-treatment evaluation, medical history, physical examination, complete blood cell count (CBC), a biochemistry panel including lactate dehydrogenase and beta2-microglobulin, HBV, HCV, HIV evaluation, echocardiogram, CT scan, PET scan and bone marrow biopsy were performed. Ann Arbor staging system was applied before starting treatment. In the study, we included DLBCL cases with sufficient diagnostic paraffin-embedded material to perform IHC analysis and with available clinical follow-up information after therapy to perform survival analysis.

#### Treatment regimen and concomitant medications

Treatment regimen consisted of standard dose R-CHOP (rituximab 375 mg/m<sup>2</sup> intravenously on day 1, cyclophosphamide 750 mg/m<sup>2</sup>, doxorubicin 50 mg/m<sup>2</sup>, vincristine 1.4 mg/m<sup>2</sup> with a maximum dose of 2 mg on day 2, prednisone 40 mg/m<sup>2</sup> on days 2-6) or CHOP-like (doxorubicin substituted by a non-pegylated liposomal formulation or mitoxantrone because of cardiac comorbidity or high cardiovascular risk) every 21 days for up to 6 cycles, providing that hematological recovery had occurred. Frail patients according to a comprehensive geriatric assessment (CGA) received less intensive regimens such as rituximab in association with cyclophosphamide, mitoxantrone, vincristine, etoposide, bleomycin and prednisone (VNCOP-B) or bendamustine [35-38]. Involved-field radiotherapy (IF-RT) was administered as consolidation in localized disease. Intravenous hydrocortisone (200 mg), intravenous chlorpheniramine (10 mg) and oral paracetamol (500 mg) were given before the first rituximab administration; if no adverse reactions occurred, hydrocortisone was not given before subsequent courses.

Concomitant medications included antimicrobial prophylaxis of *Pneumocystis jirovecii* with trimethoprim-sulfamethoxazole from beginning to at least 6 months after treatment and granulocyte colony-stimulating factor to patients who developed grade 3-4 neutropenia. HBV-positive

patients received lamivudine prophylaxis until 12 months after therapy. Treatment was discontinued if intermediate evaluation showed unsatisfactory response and at any time in case of unacceptable toxicity.

### *Assessment of response*

Response to treatment was assessed after 4<sup>th</sup> cycle (R-CHOP) or 8<sup>th</sup> week (R-VNCOP-B) and at least 4 weeks after end of treatment according to 2007 Cheson's criteria [39]. All patients received CT scan and PET, while bone marrow biopsy was repeated only if positive before treatment. Patients not achieving CR were considered as treatment failures. During the follow-up period, CT scans were performed at 6, 12 and 24 months; gastric DLBCL cases also received endoscopy. Clinical follow-up was continued every 6 months until the 5<sup>th</sup> year and annually thereafter.

### *Immunohistochemistry and blood sample analysis*

Formalin-fixed, paraffin embedded diagnostic specimens including tumor cells from each patient were selected for IHC analysis. Subsequently, 4- $\mu$ m-thick paraffin sections were performed; one section was stained with hematoxylin and eosin, the other was stained with monoclonal antibodies against human CD68 (clone PG-M1, 1:50; Dako) and CD163 (1:200; Novocastra-Leica). IHC was then performed using an automatic staining system (Benchmark Ultra; Dako). The antibody used for CD163 was stained brown with 3,3' diaminobenzidine (DAB); CD68, on the other hand, was stained red with Permanent Red.

All cases were then evaluated in double blind by 2 professional pathologists, who did not know the clinical data. At least 3 high magnification fields were observed, firstly evaluating in the area with the most intensive expression the total amount of CD68-positive and CD163-positive macrophages and afterwards analyzing the various groups (CD163 or CD68 single-positive, CD163/CD68 double-positive), finally giving a score based on the percentage of their expression, as published by Steidl and colleagues [11]. Based on this percentage, patients were divided into three groups: < 5% (low expression, score 1), 5-25% (intermediate expression, score 2) and > 25% (high expression,

score 3). With the aim of dividing our cohort into only 2 different categories, patient with score 1-2 were considered together. The Steidl score, although designed for HL, was chosen because it represents the best validated and reproducible score to date.

Remarkably, in our analysis CD68/CD163 double-positive macrophages were considered as M2 [15, 16].

For LMR and NLR evaluation, we used the discriminative cut-off values of 2.71 and 2.81, respectively, as previously published [23]. Patients were categorized as high-LMR ( $\geq 2.71$ ) and low-LMR ( $< 2.71$ ) or high LNR ( $\geq 2.81$ ) and low-LNR ( $< 2.81$ ).

### *Statistical analysis*

This was a single arm, single-center study, patients' characteristics were analyzed with descriptive statistics. Categorical variables were analyzed using Chi-square or Fisher's exact test; Fisher's exact test was preferred for small sample size, when the expected frequency was less than 5. Partial remission (PR) was not considered a satisfactory result and grouped together with stable or progressive disease (SD/PD). For survival analysis, primary endpoint was progression-free survival (PFS), defined as the time from the first day of treatment until disease progression, relapse, death for any cause or last follow-up (censored); patients that did not achieve CR after induction therapy were censored at that point for the progression [39]. Overall survival (OS) was defined as the time from the first day of treatment until death for any cause. Survival curves were estimated using the method of Kaplan and Meier and log rank test for significant associations; a  $p$  value  $< 0.05$  was considered statistically significant. All statistical analyses were made using software MedCalc, version 2.0.

## **Results**

### *Characteristics of the patients*

Clinical characteristics of patients are represented in **Table 1**. Median age at diagnosis was 61 years (range 22-89 years), male/female distribution was 16/21. Among them, 21/37 (56.7%) patients had early-stage disease (Ann-Arbor stage I-II), while 16/37 (43.3%)

**Table 1.** Patient's characteristics

Characteristic	Number of patients (%)
Age: median [range]	61 years [22-89]
Men	16/37 (43.2%)
Women	21/37 (56.8%)
Early-stage disease	21/37 (56.7%)
Advanced-stage disease	16/37 (43.3%)
B symptoms	10/37 (27%)
Bulky disease ( $\geq 7$ cm)	4/37 (10.8%)
GCB-type	19/37 (51.3%)
ABC-type	18/37 (48.7%)
LDH elevated	27/37 (73%)
IPI score 0-1	15/37 (40.6%)
IPI score 2	11/37 (29.7%)
IPI score 3-5	11/37 (29.7%)
ECOG performance status 0-1	32/37 (81%)
CD68 expression low	19/37 (51.3%)
CD68 expression high	18/37 (48.7%)
CD163 expression low	12/37 (32.4%)
CD163 expression high	25/37 (67.6%)
M2 TAM CD68/CD163 low	16/37 (43.2%)
M2 TAM CD68/CD163 high	21/37 (56.8%)
LMR $< 2.71$	21/37 (56.8%)
LMR $\geq 2.71$	16/37 (43.2%)
NLR $< 2.81$	11/37 (29.7%)
NLR $\geq 2.81$	26/37 (70.3%)

Abbreviations: GCB, germinal center B-cell; ABC, activated B-cell; LDH, lactate dehydrogenase; IPI, international prognostic index; TAM, tumor associated macrophages; LMR, lymphocyte-to-monocyte ratio; NLR, neutrophil-to-lymphocyte ratio.

patients had advanced-stage disease (stage III-IV); 4/37 patients (10.8%) presented with bulky disease (diameter  $\geq 7$  cm). COO was retrospectively determined by IHC using Hans algorithm, 19/37 (51.3%) and 18/37 (48.7%) cases were GCB and ABC-type, respectively. IPI was low (0-1), intermediate (2) and high (3-4) in 15/37 (40.6%), 11/37 (29.7%) and 11/37 (29.7%) cases, respectively. Out of 37 patients, 28/37 (75.6%) received R-CHOP or CHOP-like regimens, while 9/37 (24.4%) were treated with less intensive regimens such as R-VNCOP-B (7 cases) or R-bendamustine (2 cases).

Overall, the number of CD163-positive cells exceeded that of CD68-positive cells, as previously reported by Nam and colleagues [16]. CD68 expression was low in 19/37 patients

(51.3%) and high in 18/37 (48.7%), while CD163 expression was low in 12/37 patients (32.4%) and high in 25/37 (67.6%). CD68/CD163 double-positive M2 TAM expression was low and high in 16/37 (43.2%) and 21/37 (56.8%) cases, respectively. NLR was  $<$  and  $\geq 2.81$  in 11/37 (29.7%) and 26/37 cases (70.3%); LMR was  $<$  and  $\geq 2.71$  in 21/37 (56.8%) and 16/37 cases (43.2%), respectively. Characteristics of patients were well balanced in the different subgroups, as reported in **Table 2**.

#### Response to treatment

Responses to treatment are summarized in **Table 3**. Out of 37 patients, 26/37 (70.3%) achieved a CR, while 11/37 patients (29.7%) were considered as a treatment failure; in this group, 5/11, 4/11 and 2/11 patients achieved a PR, SD and PD, respectively. Two patients in PR received platinum-containing 2<sup>nd</sup> line therapy, all patients achieved a CR, 1/2 received autologous stem-cell transplantation (ABMT) as consolidation therapy; 1 patient with localized disease was successfully treated with IF-RT; 2 patients did not receive other therapies because of poor clinical conditions and pancreatic neoplasm (1 case each). Two patients in PD received platinum-containing 2<sup>nd</sup> line therapy, 1/2 achieved a CR and received ABMT as consolidation therapy, while the other was chemo-refractory. Out of 4 elderly patients with SD, 3/4 received gemcitabine and the other received palliative RT, none of them responded to treatment.

In responders, CD68 was high in 14/26 (53.8%) cases and low in 12/26 (46.2%); in patients who had treatment failure CD68 was high in 4/11 (36.4%) cases and low in 7/11 (63.6%) ( $P=0.47$ ). CD163 was high in 17/26 (65.4%) patients in CR and low in 9/26 (34.6%); in patients who had treatment failure CD163 was high in 8/11 (72.7%) cases and low in 3/11 (27.3%). CD68/CD163 M2 TAM expression in responders was high in 13/26 (50%) cases and low in 13/26 (50%) cases; in patients who experienced treatment failure was high in 8/11 (72.7%) and low in 3/11 (27.3%) cases ( $P=0.49$ ).

LMR was  $\geq 2.71$  in 12/26 (46.1%) responders and  $< 2.71$  in 14/26 (53.9%), while it was  $\geq 2.71$  in 4/11 (36.3%) non-responders and  $<$

## TAM, LMR, NLR and DLBCL prognosis

**Table 2.** Characteristics of patients according to the CD68 and CD163 expression

Characteristic	CD68			CD163			CD68/CD163		
	Low	High	P	Low	High	p	Low	High	P
Age < 60	6/19	7/18	0.9	5/12	8/25	0.83	7/16	6/21	0.54
Men	8/19	8/18	0.88	6/12	10/25	0.82	8/16	8/21	0.69
Women	11/19	10/18		6/12	15/25		8/16	13/21	
Early-stage	12/19	9/18	0.63	7/12	14/25	0.89	10/16	11/21	0.77
Advanced-stage	7/19	9/18		5/12	11/25		6/16	10/21	
B symptoms	7/19	4/18	0.47	4/12	6/25	0.69	3/16	7/21	0.53
GCB-type	11/19	8/18	0.62	7/12	12/25	0.81	9/16	10/21	0.85
ABC-type	8/19	10/18		5/12	13/25		7/16	11/21	
LDH elevated	12/19	15/18	0.26	8/12	19/25	0.69	10/16	17/21	0.27
IPI score 0-1	9/19	6/18		4/12	11/25		6/16	9/21	
IPI score 2	6/19	5/18	0.47	4/12	7/25	0.82	6/16	5/21	0.7
IPI score 3-5	4/19	7/18		4/12	7/25		4/16	7/21	
ECOG PS 0-1	15/19	17/18	0.33	9/12	24/25	0.09	13/16	19/21	0.63
LMR < 2.71	12/19	9/18	0.63	6/12	15/25	0.82	9/16	12/21	0.95
LMR ≥ 2.71	7/19	9/18		6/12	10/25		7/16	9/21	
NLR < 2.81	7/19	4/18	0.47	3/12	8/25	1.0	5/16	6/21	0.85
NLR ≥ 2.81	12/19	14/18		9/12	17/25		11/16	15/21	

Abbreviations: GCB, germinal center B-cell; ABC, activated B-cell; LDH, lactate dehydrogenase; IPI, international prognostic index; PS, performance status; LMR, lymphocyte-to-monocyte ratio; NLR, neutrophil-to-lymphocyte ratio.

2.71 in 7/11 (63.7%) (P=0.72); NLR was ≥ 2.81 in 19/26 responders (73.1%) and < 2.81 in 7/26 (26.9%), while it was ≥ 2.81 in 7/11 (63.6%) non-responders and low in 4/11 (36.4%) (P=0.69).

### Survival analysis

After a median follow-up of 60 months, 23/37 (62.2%) patients were alive while 14 patients died (37.8%), 7 because of PD, 2 because of secondary malignancies, 3 because of infectious complications and 2 because of cardiac failure in CR. IPI maintained its prognostic value and was associated with both PFS and OS (Figures S1, S2, available on request). There was a trend between high CD68, low M2 TAM expression and increased PFS, while CD163, LMR and NLR were not associated with PFS (Figure 1A-E). Comparable results were obtained with OS analysis (Figure 2A-E). Median PFS and OS were not reached in the entire cohort; 5-y PFS and OS were 61% and 64%, respectively (Figure 3A, 3B). Interestingly, when we tried to separately analyze patients with IPI ≥ 2, we observed a significant association between high M2 TAM and inferior PFS (Figure 4, P=0.04), while there was no association between CD68, CD163, LMR, NLR

and PFS. Moreover, there was a trend between high M2 TAM and inferior OS, even if it did not reach statistical significance (Figure 5), while there was no association between CD68, CD163, LMR, NLR and OS.

### Discussion

In this analysis we observed that i) there was no correlation between TAM CD68+, TAM CD163+, TAM M2, LMR, NLR and the attainment of CR, ii) for patients with IPI ≥ 2, there is a significant association between high M2 TAM and inferior PFS, iii) there was no association between CD68, CD163, LMR, NLR and outcome, while IPI maintained its prognostic value in our cohort of patients treated in the rituximab era.

Prognostic factors in DLBCL are still a matter of debate and treatment strategy is principally determined by IPI [3]. COO assessment with nanostring is not yet available in the majority of laboratories and IHC analysis produced conflicting results [4, 5].

TAM could reflect tumor-associated inflammation and could represent the most important component of microenvironment; its prognos-



## TAM, LMR, NLR and DLBCL prognosis

**Table 3.** Response to treatment

	Number of patients	%	P
CR	26/37	70.3%	
PR	5/37	13.5%	
SD	4/37	10.8%	
PD	2/37	5.4%	
Responders (CR)			
CD68 high	14/18	77.7%	0.47
CD68 low	12/19	63.1%	
CD163 high	17/25	68%	1.0
CD163 low	9/12	75%	
CD68/CD163 M2 high	13/21	61.9%	0.28
CD68/CD163 M2 low	13/16	81.2%	
LMR $\geq$ 2.71	12/16	75%	0.72
LMR $<$ 2.71	14/21	66.6%	
NLR $\geq$ 2.81	19/26	73.1%	0.69
NLR $<$ 2.81	7/11	63.6%	
Treatment failure (PR+SD+PD)			
CD68 high	4/18	22.2%	0.47
CD68 low	7/19	36.8%	
CD163 high	8/25	32%	1.0
CD163 low	3/12	25%	
CD68/CD163 M2 high	8/21	38.1%	0.28
CD68/CD163 M2 low	3/16	18.8%	
LMR $\geq$ 2.71	4/16	25%	0.72
LMR $<$ 2.71	7/21	33.3%	
NLR $\geq$ 2.81	7/26	26.9%	0.69
NLR $<$ 2.81	4/11	36.4%	

Abbreviations: CR, complete remission; PR, partial response; SD, stable disease; PD, progressive disease; LMR, lymphocyte-to-monocyte ratio; NLR, neutrophil-to-lymphocyte ratio.

tic relevance was demonstrated in both solid and hematological malignancies [8]. In our opinion, the comprehension of the contribution of tumor microenvironment to treatment failure in DLBCL could represent a critical hurdle to overcome with the aim to design a targeted-therapy and to finally improve survival.

Riihjarvi and colleagues described the association between CD68 mRNA levels assessed with GEP, CD68 protein expression in IHC and DLBCL outcome. The study was conducted on 59 cases, using the anti-CD68 KP1 antibody and the positive cells were counted manually [18]. With the limitations related to the arbitrary choice of cut-off, CD68 was associated with favorable prognosis in patients treated with rituximab plus chemotherapy, while it was related to an unfavorable outcome in patients

receiving only chemotherapy. Moreover, CD163 expression in GEP and IHC did not show any prognostic relevance [18]. Nam and colleagues analyzed 165 patients receiving R-CHOP and demonstrated that high CD68 expression was associated with OS improvement, while PFS and OS were reduced in cases with an increased CD163/CD68 ratio [17]. Conversely, Cai and colleagues showed that CD68 was a marker of poor prognosis, while the studies by Hasselblom and colleagues and Coutinho and colleagues did not report any significant correlation between CD68 and survival [19, 24, 25]. Gomez-Gelvez and colleagues enrolled 115 DLBCL patients receiving R-CHOP and designed a prognostic score including ABC subtype, FDX3 > 17%, microvessel density < 800/mm<sup>2</sup> and CD68 < 2%; worse PFS was observed in the high-risk group [22].

These conflicting results could be due to wide heterogeneity in the choice of IHC antibodies (KP1 vs PG-M1), TAM markers, threshold (median vs best cut-off), scoring methods (manual vs automated) and treatment received (with or without rituximab) [14].

According to promising findings reported in non-hematological malignancies, major efforts should be focused on M2-TAMs, characterized by a pro-tumoral phenotype. In our opinion and as previously published, double staining for CD68 and CD163 could better identify a M2 phenotype, that was associated with inferior OS, while M1 phenotype did not show any prognostic relevance [15, 16]. Wang and colleagues retrospectively analyzed 355 DLBCL patients treated with R-CHOP and observed lower LMR, higher NLR and CD163+ M2 TAM  $\geq$  9.5% were related to shorter PFS and OS [23]. A recently published systematic review and meta-analysis confirmed that both CD68 and CD163 high density are associated with poor OS, but the highest hazard ratio is reached when CD163/CD68 TAM ratio is analyzed, further confirming that M2 TAM represent a robust predictor of outcome in NHL, including DLBCL, follicular lymphoma, mantle-cell lymphoma and T-cell lymphomas [40].

NLR demonstrated a prognostic role in lymphoproliferative disorders and we find merit in the attempt to identify a simple and reproducible

## TAM, LMR, NLR and DLBCL prognosis

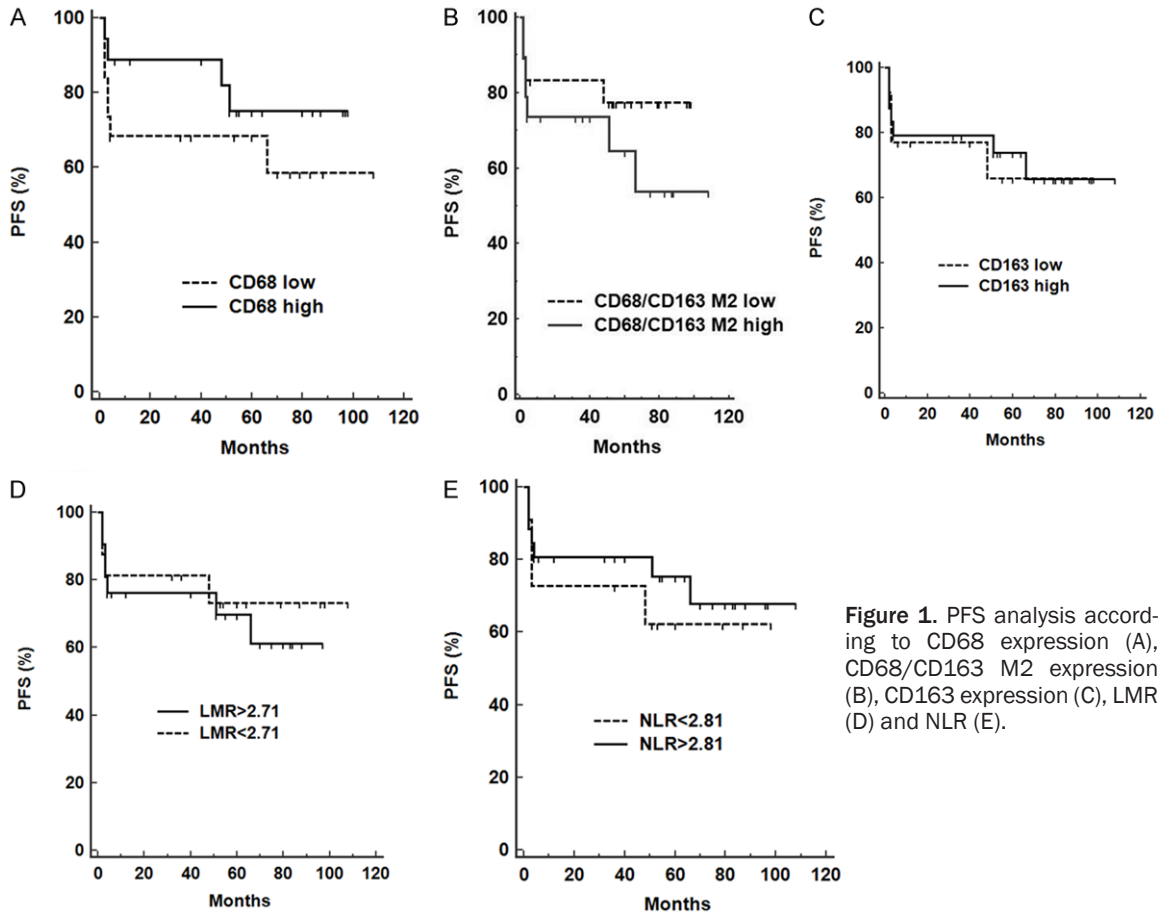


**Figure 1.** PFS analysis according to CD68 expression (A), CD68/CD163 M2 expression (B), CD163 expression (C), LMR (D) and NLR (E).

prognostic tool, that could represent a marker of immunosuppression and systemic inflammation [30, 31, 33]. However, at least 2 relevant biases could be identified, such as the administration of pre-phase steroid and a misdiagnosed infection that could increase ANC. Increased monocytes and decreased lymphocytes count could both promote angiogenesis and immunosuppression, finally favoring tumor growth and progression [23, 32]. Conflicting results have been achieved with regard to LMR and NLR prognostic value and the main issue remains the choice of an optimal cut-off [26-33].

In a recently published study, in 221 DLBCL cases receiving CHOP or R-CHOP, TAM prognostic value persists when patients characterized by different IPI (IPI 0-1, IPI 2-3, IPI 4-5) were further stratified according to CD68 or CD163 expression [41].

In our study, 37 consecutive DLBCL patients were analyzed, all of them received R-containing therapies. Characteristics of patients and

response to treatment are consistent with previously published data, with a CR rate of 70.3%, PFS and OS at 5 years of 61% and 64%, respectively. We observed a trend between low CD68 expression, high M2 TAM expression and reduced PFS and OS, even if a statistical significance was not achieved, while CR rate was not influenced by TAM. LMR and NLR did not influence treatment response and survival. Overall, IPI maintained its prognostic value, patients with IPI 0-1 experienced a more favorable outcome compared to patients with IPI  $\geq 2$ . When we have further stratified cases with IPI  $\geq 2$ , we have observed a significant association between high M2 TAM expression, reduced PFS and a trend to reduced OS. We can argue that patients with intermediate or high IPI could represent a subgroup in which TAM evaluation could increase the prognostic power of IPI.

Our study has some strengths, such as the choice of double CD68/CD163 staining to investigate M2 TAM, the administration of rituximab to all patients and the use of the Steidl

## TAM, LMR, NLR and DLBCL prognosis

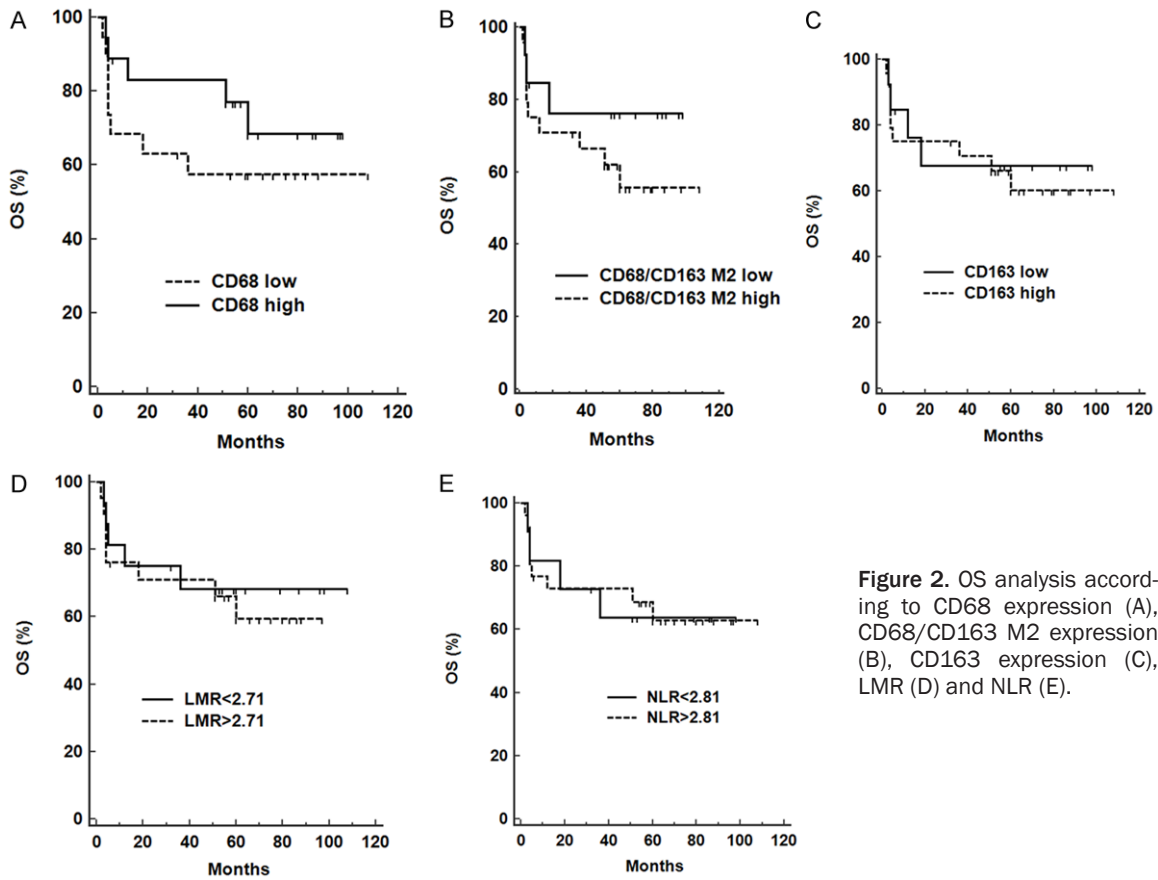


**Figure 2.** OS analysis according to CD68 expression (A), CD68/CD163 M2 expression (B), CD163 expression (C), LMR (D) and NLR (E).

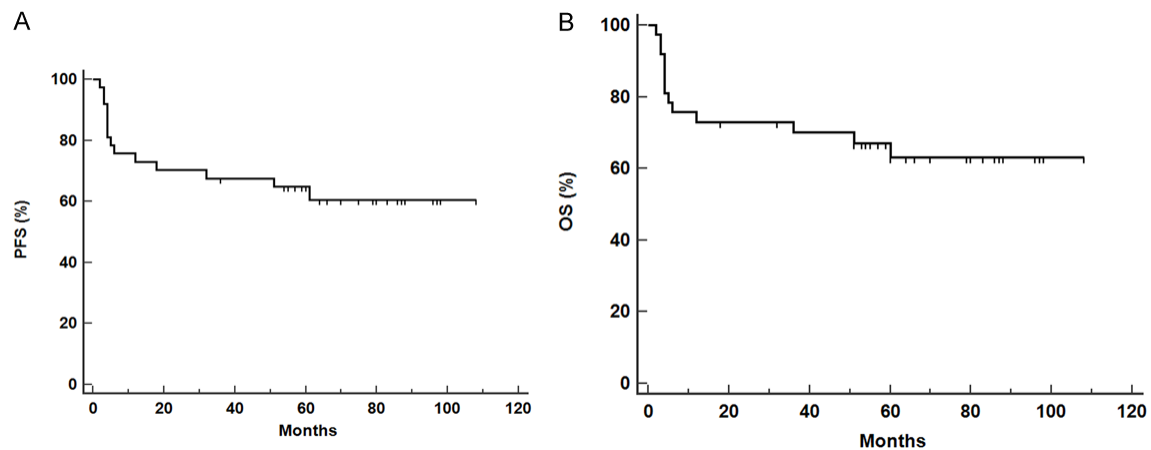


**Figure 3.** PFS (A) and OS (B) analysis in the entire cohort.

score that, even if designed for HL, could guarantee greater reproducibility compared to best cut-off methods used in single-cohort studies. However, our study has some limitations, most notably the retrospective design and small sample size (although comparable to previously published experiences) [20, 42].

In conclusion, we can suggest that high M2 TAM content at diagnosis, especially in association with IPI, could contribute to identify DLBCL patients characterized by poor prognosis. A TAM-targeted strategy could be associated with a COO-targeted strategy in future clinical trials focused on DLBCL with IPI  $\geq 2$ ,

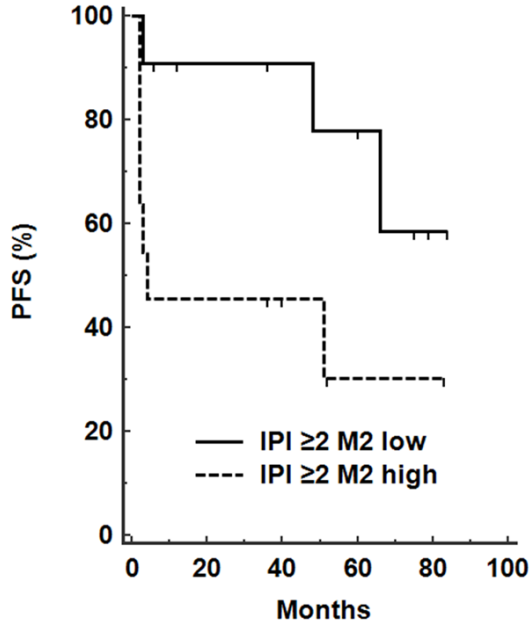


**Figure 4.** PFS analysis in patients with IPI  $\geq$  2, according to the CD68/CD163 M2 expression.

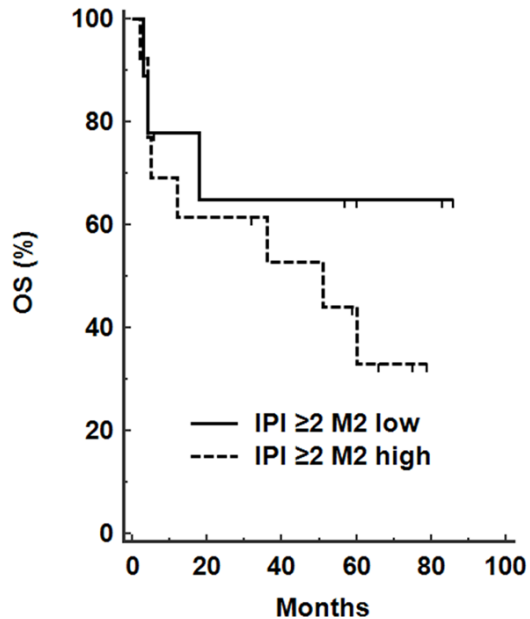


**Figure 5.** OS analysis in patients with IPI  $\geq$  2, according to the CD68/CD163 M2 expression.

with the aim to investigate a novel therapeutic approach for poor-risk patients.

**Disclosure of conflict of interest**

None.

**Address correspondence to:** Emanuele Cencini, Division of Hematology, University Hospital, Viale Bracci - 53100 Siena, Italy. Tel: +39 0577 586798; Fax: +39 0577 586185; E-mail: cencioema@libero.it

**References**

- [1] Tilly H, Gomes da Silva M, Vitolo U, Jack A, Meignan M, Lopez-Guillermo A, Walewski J, André M, Johnson PW, Pfreundschuh M and Ladetto M; ESMO Guidelines Committee. Diffuse large B-cell lymphoma (DLBCL): ESMO Clinical Practice Guidelines for diagnosis, treatment and follow-up. *Ann Oncol* 2015; 26 Suppl 5: v116-25.
- [2] Coiffier B, Thieblemont C, Van Den Neste E, Lepeu G, Plantier I, Castaigne S, Lefort S, Marit G, Macro M, Sebban C, Belhadj K, Bordessoule D, Fermé C and Tilly H. Long-term outcome of patients in the LNH-98.5 trial, the first randomized study comparing rituximab-CHOP to standard CHOP chemotherapy in DLBCL patients: a study by the Groupe d'Etudes des Lymphomes de l'Adulte. *Blood* 2010; 116: 2040-2045.
- [3] Ziepert M, Hasenclever D, Kuhnt E, Glass B, Schmitz N, Pfreundschuh M and Loeffler M. Standard international prognostic index remains a valid predictor of outcome for patients with aggressive CD20+ B-cell lymphoma in the rituximab era. *J Clin Oncol* 2010; 28: 2373-2380.
- [4] Rosenwald A, Wright G, Chan WC, Connors JM, Campo E, Fisher RI, Gascoyne RD, Müller-Hermelink HK, Smeland EB, Giltane JM, Hurt EM, Zhao H, Averett L, Yang L, Wilson WH, Jaffe ES, Simon R, Klausner RD, Powell J, Duffey PL, Longo DL, Greiner TC, Weisenburger DD, Sanger WG, Dave BJ, Lynch JC, Vose J, Armitage JO, Montserrat E, López-Guillermo A, Grogan TM, Miller TP, LeBlanc M, Ott G, Kvaloy S, Delabie J, Holte H, Krajci P, Stokke T and Staudt LM; Lymphoma/Leukemia Molecular Profiling Project. The use of molecular profiling to predict survival after chemotherapy for diffuse large-B-cell lymphoma. *N Engl J Med* 2002; 346: 1937-1947.
- [5] Hans CP, Weisenburger DD, Greiner TC, Gascoyne RD, Delabie J, Ott G, Müller-Hermelink HK, Campo E, Braziel RM, Jaffe ES, Pan Z, Farinha P, Smith LM, Falini B, Banham AH, Rosenwald A, Staudt LM, Connors JM, Armitage JO and Chan WC. Confirmation of the molecular classification of diffuse large B-cell lymphoma by immunohistochemistry using a tissue microarray. *Blood* 2004; 103: 275-282.
- [6] Swerdlow SH, Campo E, Pileri SA, Harris NL, Stein H, Siebert R, Advani R, Ghielmini M, Salles GA, Zelenetz AD and Jaffe ES. The 2016

- revision of the World Health Organization classification of lymphoid neoplasms. *Blood* 2016; 127: 2375-2390.
- [7] Lenz G, Wright G, Dave SS, Xiao W, Powell J, Zhao H, Xu W, Tan B, Goldschmidt N, Iqbal J, Vose J, Bast M, Fu K, Weisenburger DD, Greiner TC, Armitage JO, Kyle A, May L, Gascoyne RD, Connors JM, Troen G, Holte H, Kvaloy S, Dierickx D, Verhoef G, Delabie J, Smeland EB, Jares P, Martinez A, Lopez-Guillermo A, Montserrat E, Campo E, Braziel RM, Miller TP, Rimsza LM, Cook JR, Pohlman B, Sweetenham J, Tubbs RR, Fisher RI, Hartmann E, Rosenwald A, Ott G, Muller-Hermelink HK, Wrench D, Lister TA, Jaffe ES, Wilson WH, Chan WC and Staudt LM; Lymphoma/Leukemia Molecular Profiling Project. Stromal gene signatures in large-B-cell lymphomas. *N Engl J Med* 2008; 359: 2313-2323.
- [8] Mantovani A, Marchesi F, Malesci A, Laghi L and Allavena P. Tumour-associated macrophages as treatment targets in oncology. *Nat Rev Clin Oncol* 2017; 14: 399-416.
- [9] Scott DW and Gascoyne RD. The tumour microenvironment in B cell lymphomas. *Nat Rev Cancer* 2014; 14: 517-534.
- [10] McCord R, Bolen CR, Koeppen H, Kadel EE 3rd, Oestergaard MZ, Nielsen T, Sehn LH and Venstrom JM. PD-L1 and tumor-associated macrophages in de novo DLBCL. *Blood Adv* 2019; 3: 531-540.
- [11] Steidl C, Lee T, Shah SP, Farinha P, Han G, Nayar T, Delaney A, Jones SJ, Iqbal J, Weisenburger DD, Bast MA, Rosenwald A, Muller-Hermelink HK, Rimsza LM, Campo E, Delabie J, Braziel RM, Cook JR, Tubbs RR, Jaffe ES, Lenz G, Connors JM, Staudt LM, Chan WC and Gascoyne RD. Tumor-associated macrophages and survival in classic Hodgkin's lymphoma. *N Engl J Med* 2010; 362: 875-885.
- [12] Cencini E, Fabbri A, Rigacci L, Lazzi S, Gini G, Cox MC, Mancuso S, Abruzzese E, Kovalchuk S, Goteri G, Di Napoli A, Bono R, Fratoni S, Di Lollo S, Bosi A, Leoncini L and Bocchia M. Evaluation of the prognostic role of tumour-associated macrophages in newly diagnosed classical Hodgkin lymphoma and correlation with early FDG-PET assessment. *Hematol Oncol* 2017; 35: 69-78.
- [13] Cencini E, Fabbri A and Bocchia M. Prognostic role of M2 tumour-associated macrophages in lymphoproliferative disorders. *J Pathol* 2017; 242: 511-512.
- [14] Kridel R, Steidl C and Gascoyne RD. Tumor-associated macrophages in diffuse large B-cell lymphoma. *Haematologica* 2015; 100: 143-145.
- [15] Marchesi F, Cirillo M, Bianchi A, Gately M, Olimpieri OM, Cerchiara E, Renzi D, Micera A, Balzamino BO, Bonini S, Onetti Muda A and Avvisati G. High density of CD68+/CD163+ tumour-associated macrophages (M2-TAM) at diagnosis is significantly correlated to unfavorable prognostic factors and to poor clinical outcomes in patients with diffuse large B-cell lymphoma. *Hematol Oncol* 2015; 33: 110-112.
- [16] Wada N, Zaki MA, Hori Y, Hashimoto K, Tsukaguchi M, Tatsumi Y, Ishikawa J, Tominaga N, Sakoda H, Take H, Tsudo M, Kuwayama M, Morii E and Aozasa K; Osaka Lymphoma Study Group. Tumour-associated macrophages in diffuse large B-cell lymphoma: a study of the Osaka Lymphoma Study Group. *Histopathology* 2012; 60: 313-319.
- [17] Nam SJ, Go H, Paik JH, Kim TM, Heo DS, Kim CW and Jeon YK. An increase of M2 macrophages predicts poor prognosis in patients with diffuse large B-cell lymphoma treated with rituximab, cyclophosphamide, doxorubicin, vincristine and prednisone. *Leuk Lymphoma* 2014; 55: 2466-2476.
- [18] Riihijärvi S, Fiskvik I, Taskinen M, Vajavaara H, Tikkala M, Yri O, Karjalainen-Lindsberg ML, Delabie J, Smeland E, Holte H and Leppä S. Prognostic influence of macrophages in patients with diffuse large B-cell lymphoma: a correlative study from a Nordic phase II trial. *Haematologica* 2015; 100: 238-245.
- [19] Hasselblom S, Hansson U, Sigurdardottir M, Nilsson-Ehle H, Ridell B and Andersson PO. Expression of CD68+ tumor-associated macrophages in patients with diffuse large B-cell lymphoma and its relation to prognosis. *Pathol Int* 2008; 58: 529-532.
- [20] Yamamoto W, Nakamura N, Tomita N, Takeuchi K, Ishii Y, Takahashi H, Watanabe R, Takasaki H, Motomura S, Kobayashi S, Yokose T, Ishigatsubo Y and Sakai R. Human leukocyte antigen-DR expression on flow cytometry and tumor-associated macrophages in diffuse large B-cell lymphoma treated by rituximab, cyclophosphamide, doxorubicin, vincristine and prednisone therapy: retrospective cohort study. *Leuk Lymphoma* 2014; 55: 2721-2727.
- [21] Poles WA, Nishi EE, de Oliveira MB, Eugênio AIP, de Andrade TA, Campos AHFM, de Campos RR Jr, Vassallo J, Alves AC, Scapulatempo Neto C, Paes RAP, Landman G, Zerbini MCN and Colleoni GWB. Targeting the polarization of tumor-associated macrophages and modulating miR-155 expression might be a new approach to treat diffuse large B-cell lymphoma of the elderly. *Cancer Immunol Immunother* 2019; 68: 269-282.
- [22] Gomez-Gelvez JC, Salama ME, Perkins SL, Leavitt M and Inamdar KV. Prognostic impact of tumor microenvironment in diffuse large B-cell lymphoma uniformly treated with R-CHOP

- chemotherapy. *Am J Clin Pathol* 2016; 145: 514-523.
- [23] Wang J, Gao K, Lei W, Dong L, Xuan Q, Feng M, Wang J, Ye X, Jin T, Zhang Z and Zhang Q. Lymphocyte-to-monocyte ratio is associated with prognosis of diffuse large B-cell lymphoma: correlation with CD163 positive M2 type tumor-associated macrophages, not PD-1 positive tumor-infiltrating lymphocytes. *Oncotarget* 2017; 8: 5414-5425.
- [24] Cai QC, Liao H, Lin SX, Xia Y, Wang XX, Gao Y, Lin ZX, Lu JB and Huang HQ. High expression of tumor-infiltrating macrophages correlates with poor prognosis in patients with diffuse large B-cell lymphoma. *Med Oncol* 2012; 29: 2317-2322.
- [25] Coutinho R, Clear AJ, Mazzola E, Owen A, Greaves P, Wilson A, Matthews J, Lee A, Alvarez R, da Silva MG, Cabeçadas J, Neuberger D, Calaminici M and Gribben JG. Revisiting the immune microenvironment of diffuse large B-cell lymphoma using a tissue microarray and immunohistochemistry: robust semi-automated analysis reveals CD3 and FoxP3 as potential predictors of response to R-CHOP. *Haematologica* 2015; 100: 363-369.
- [26] Cox MC, Nofroni I, Laverde G, Ferrari A, Amodeo R, Tatarelli C, Saltarelli F, Veggia B, Aloe-Spiriti MA, Ruco L and Monarca B. Absolute lymphocyte count is a prognostic factor in diffuse large B-cell lymphoma. *Br J Haematol* 2008; 141: 265-268.
- [27] Watanabe R, Tomita N, Itabashi M, Ishibashi D, Yamamoto E, Koyama S, Miyashita K, Takahashi H, Nakajima Y, Hattori Y, Motohashi K, Takasaki H, Ohshima R, Hashimoto C, Yamazaki E, Fujimaki K, Sakai R, Fujisawa S, Motomura S and Ishigatsubo Y. Peripheral blood absolute lymphocyte/monocyte ratio as a useful prognostic factor in diffuse large B-cell lymphoma in the rituximab era. *Eur J Haematol* 2014; 92: 204-210.
- [28] Matsuki E, Bohn OL, El Jamal S, Pichardo JD, Zelenetz AD, Younes A and Teruya-Feldstein J. Lymphocyte-to-monocyte ratio may serve as a better prognostic indicator than tumor-associated macrophages in DLBCL treated with rituximab. *Appl Immunohistochem Mol Morphol* 2019; 27: 572-580.
- [29] Keam B, Ha H, Kim TM, Jeon YK, Lee SH, Kim DW, Kim CW and Heo DS. Neutrophil to lymphocyte ratio improves prognostic prediction of International Prognostic Index for patients with diffuse large B-cell lymphoma treated with rituximab, cyclophosphamide, doxorubicin, vincristine and prednisone. *Leuk Lymphoma* 2015; 56: 2032-2038.
- [30] Cencini E, Fabbri A, Sicuranza A and Bocchia M. Prognostic significance of lymphocyte/monocyte count and neutrophil/lymphocyte count in peripheral T cell lymphoma. *Leuk Res* 2019; 77: 5-7.
- [31] Romano A, Parrinello NL, Vetro C, Chiarenza A, Cerchione C, Ippolito M, Palumbo GA and Di Raimondo F. Prognostic meaning of neutrophil to lymphocyte ratio (NLR) and lymphocyte to monocyte ration (LMR) in newly diagnosed Hodgkin lymphoma patients treated upfront with a PET-2 based strategy. *Ann Hematol* 2018; 97: 1009-1018.
- [32] Lin B, Chen C, Qian Y and Feng J. Prognostic role of peripheral blood lymphocyte/monocyte ratio at diagnosis in diffuse large B-cell lymphoma: a meta-analysis. *Leuk Lymphoma* 2015; 56: 2563-2568.
- [33] Azuma Y, Nakaya A, Fujita S, Satake A, Nakaniishi T, Tsubokura Y, Saito R, Konishi A, Hotta M, Yoshimura H, Ishii K, Ito T and Nomura S. Neutrophil-to-lymphocyte ratio (NLR) fails to predict outcome of diffuse large B cell lymphoma. *Leuk Res Rep* 2019; 12: 100173.
- [34] Swerdlow S, Campo E, Harris N, Jaffe E, Pileri S, Stein H, Thiele J and Vardiman J. WHO classification of tumors of haematopoietic and lymphoid tissues. IARC Press: Lyon; 2008.
- [35] Fabbri A, Cencini E and Bocchia M. Treatment decisions and outcome in very elderly patients with diffuse large B-cell lymphoma. *Cancer* 2015; 121: 3746-3747.
- [36] Cencini E, Fabbri A, Schiattone L, Gentili F, Mazzei MA and Bocchia M. Durable response after VNCOP-B and rituximab in an elderly patient with high-grade B-cell lymphoma. *Acta Clin Belg* 2018; 73: 408-412.
- [37] Storti S, Spina M, Pesce EA, Salvi F, Merli M, Ruffini A, Cabras G, Chiappella A, Angelucci E, Fabbri A, Liberati AM, Tani M, Musuraca G, Molinari A, Petrilli MP, Palladino C, Ciancia R, Ferrario A, Gasbarrino C, Monaco F, Fraticelli V, De Vellis A, Merli F and Luminari S. Rituximab plus bendamustine as front-line treatment in frail elderly (> 70 years) patients with diffuse large B-cell non-Hodgkin lymphoma: a phase II multicenter study of the Fondazione Italiana Linfomi. *Haematologica* 2018; 103: 1345-1350.
- [38] Tucci A, Martelli M, Rigacci L, Riccomagno P, Cabras MG, Salvi F, Stelitano C, Fabbri A, Storti S, Fogazzi S, Mancuso S, Brugiattelli M, Fama A, Paesano P, Puccini B, Bottelli C, Dalceglio D, Bertagna F, Rossi G and Spina M; Italian Lymphoma Foundation (FIL). Comprehensive geriatric assessment is an essential tool to support treatment decisions in elderly patients with diffuse large B-cell lymphoma: a prospective multicenter evaluation in 173 patients by the Lymphoma Italian Foundation (FIL). *Leuk Lymphoma* 2015; 56: 921-926.
- [39] Cheson BD, Pfistner B, Juweid ME, Gascoyne RD, Specht L, Horning SJ, Coiffier B, Fisher RI, Hagenbeek A, Zucca E, Rosen ST, Stroobants

## TAM, LMR, NLR and DLBCL prognosis

- S, Lister TA, Hoppe RT, Dreyling M, Tobinai K, Vose JM, Connors JM, Federico M and Diehl V; International Harmonization Project on Lymphoma. Revised response criteria for malignant lymphoma. *J Clin Oncol* 2007; 25: 579-586.
- [40] Xu X, Li Z, Liu J, Zhu F, Wang Z, Wang J, Zhang J, Wang H and Zhai Z. The prognostic value of tumour-associated macrophages in Non-Hodgkin's lymphoma: a systematic review and meta-analysis. *Scand J Immunol* 2020; 91: e12814.
- [41] Li YL, Shi ZH, Wang X, Gu KS and Zhai ZM. Tumour-associated macrophages predict prognosis in diffuse large B-cell lymphoma and correlation with peripheral absolute monocyte count. *BMC Cancer* 2019; 19: 1049.
- [42] Marinaccio C, Ingravallo G, Gaudio F, Perrone T, Nico B, Maoirano E, Specchia G and Ribatti D. Microvascular density, CD68 and tryptase expression in human diffuse large B-cell lymphoma. *Leuk Res* 2014; 38: 1374-1377.

# TAM, LMR, NLR and DLBCL prognosis

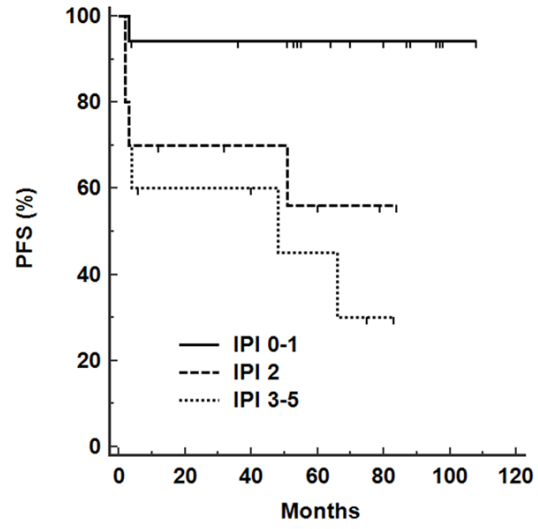


Figure S1. PFS analysis according to IPI.

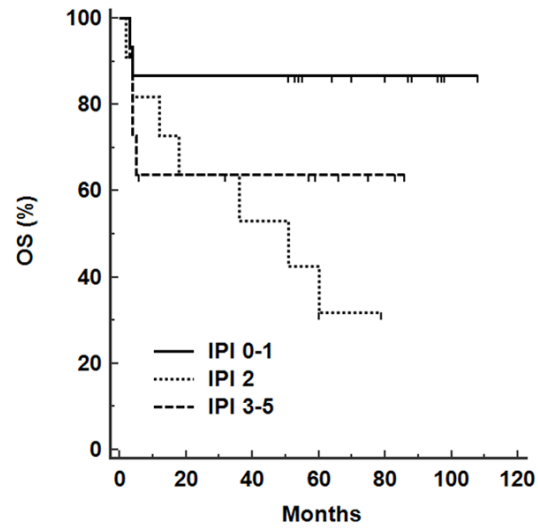


Figure S2. OS analysis according to IPI.